IEEE Access
Multidisciplinary : Rapid Review : Open Access Journal

Received 1 March 2024, accepted 19 March 2024, date of publication 8 April 2024, date of current version 15 April 2024.

Digital Object Identifier 10.1109/ACCESS.2024.3385429

TOPICAL REVIEW

Emerging Trends and Challenges in Thermal Management of Power Electronic Converters: A State of the Art Review

S. M. IMRAT RAHMAN[1], (Graduate Student Member, IEEE), ALI MOGHASSEMI[1], (Graduate Student Member, IEEE), ALI ARSALAN[1,2], (Graduate Student Member, IEEE), LAXMAN TIMILSINA[1], (Graduate Student Member, IEEE), PHANI KUMAR CHAMARTHI[1], (Member, IEEE), BEHNAZ PAPARI[1,2], (Senior Member, IEEE), GOKHAN OZKAN[1,3], (Senior Member, IEEE), AND CHRISTOPHER S. EDRINGTON[1], (Senior Member, IEEE)

[1]Holcombe Department of Electrical and Computer Engineering, Clemson University, Clemson, SC 29634, USA
[2]Department of Automotive Engineering, Clemson University, Greenville, SC 29607, USA
[3]Energy Innovation Center, Clemson University, Clemson, SC 29634, USA

Corresponding author: S. M. Imrat Rahman (smimrar@clemson.edu)

This work was supported by Clemson University's Virtual Prototyping of Autonomy Enabled Ground Systems (VIPR-GS) through the U.S. Army DEVCOM Ground Vehicle Systems Center (GVSC), under Grant W56HZV-21-2-0001.

ABSTRACT Recently, the thermal management of power electronic converters has gained significant attention due to the continuous trend of developing very compact power electronic converters with high power density. With the evolution of power semiconductor devices, high operating temperatures and large thermal cycles have become possible, necessitating a significant improvement in thermal system designs. Researchers have made significant efforts to develop effective thermal management systems to improve the reliability and lifetime of power electronic converters. This article intends to present a thorough review of thermal management systems employed in power electronics cooling. The applied thermal management techniques have been reviewed from the perspective of electrical parameter regulation and heat dissipation control. Regulation of electrical parameters involves active thermal control, which is a method for controlling junction temperature and thermal cycling of power semiconductor devices. The active thermal control implementation processes reviewed in this article consist of increasing overload capacity, manipulating switching and conduction losses, employing modified modulation processes, balancing thermal stress at the converter level, and controlling thermal stress at the system level. Control of heat dissipation can be achieved through direct and indirect cooling of power electronic converters with air or liquid as the coolant. The effectiveness and implementation methods of these cooling techniques, such as channel cooling, phase change material-based cooling, immersion cooling, jet impingement and spray cooling, are reviewed in this paper. Moreover, performance-enhancing ideas and challenges for these techniques are discussed. The primary objective of this review paper is to bridge the existing gap in the literature by offering a comprehensive comparison of commonly employed thermal management techniques.

The associate editor coordinating the review of this manuscript and approving it for publication was Zhilei Yao.

INDEX TERMS Active thermal control (ATC), power semiconductor device (PSD), microchannel, spray cooling, jet impingement, immersion cooling, phase change material (PCM), active cooling.

NOMENCLATURE

ALT-60° DPWM	Alternative 60° Discontinuous Pulse Width Modulation.
ATC	Active Thermal Control.
ANPC	Active Neutral-Point-Clamped.
CHB	Cascaded H-Bridge.
CHF	Critical Heat Flux.
CONV-60° DPWM	Conventional 60° Discontinuous Pulse Width Modulation.
CTE	Coefficients of Thermal Expansion.
DAB	Dual Active Bridge.
DPWM	Discontinuous Pulse Width Modulation.
EV	Electric Vehicle.
FACTS	Flexible Alternating Current Transmission System.
FCS-MPC	Finite Control Set Model Predictive Control.
FCC	Flying Capacitor.
GaN	Gallium Nitride.
HTC	Heat Transfer Coefficient.
HVDC	High-Voltage Direct Current.
IGBT	Insulated-Gate Bipolar Transistor.
LVDC	Low-Voltage Direct Current.
LVRT	Low-Voltage Ride-Through.
MCM	Multi Chip Modules.
MEA	More Electric Aircraft.
MLC	Multi Level Converter.
MMC	Modular Multilevel Converter.
MWCNT	Multiwall Carbon Nanotubes.
MOSFET	Metal–Oxide–Semiconductor Field-Effect Transistor.
MVAC	Medium-Voltage Alternating Current.
NPC	Neutral-Point-Clamped.
NPS	Neutral-Point-Shift.
OPT-ZSSPWM	Optimal Zero Sequence Injection Pulse Width Modulation.
OHP	Oscillating Heat Pipe.
PCM	Phase Change Material.
PEC	Power Electronic Converter.
PI	Proportional-Integral.
PSD	Power Semiconductor Device.
PWM	Pulse Width Modulation.
QAB	Quadruple Active Bridge.
RUL	Remaining Useful Life.
Si	Silicon.
SiC	Silicon Carbide.
SPWM	Sinusoidal Pulse Width Modulation.
SoH	State of Health.
SVC	Static VAR Compensation.
SVM	Space Vector Modulation.
SVPWM	Space Vector Pulse Width Modulation.
ST	Smart Transformer.
TE	Thermo Electric.
THD	Total Harmonic Distortion.
THIPWM	Third Harmonic Injected Pulse Width Modulation.
TMS	Thermal Management System.
WBG	Wide Bandgap.

I. INTRODUCTION

A. BACKGROUND

The application of power electronic converters (PEC) in transportation systems and electrical grids has increased immensely as they provide better controllability and flexibility for these systems [1]. Moreover, the efficiency and power density of power electronic-based systems have risen due to the recent developments in circuit configuration, novel control strategies, novel semiconductor materials, DSPs, and system integration technologies [2]. These latest advancements in power electronics have contributed to the development of sustainable and affordable renewable energy-based sources [3], robust, reliable, and high-quality distributed electrical grid [4], [5], [6], [7], efficient and low-cost electric vehicles (EV) [8], [9], low-fuel-consumption cargo ships, more electric aircraft (MEA) [10], electric motorbikes, electric cars [11], [12], robust high-speed trains, efficient subways with regenerative breaking, public electric buses, and so on [13]. In recent years, the transportation sector, aerospace industries, and energy sectors have extended the requirements regarding the reliability of power electronic systems. Accordingly, the interest in developing innovative and sustainable technologies to ensure the safe and reliable operation of PECs has also grown. The stringent reliability demands have initiated additional challenges due to the following factors [14]:

- Demand for high power density in power electronic converters.
- Strict cost and resource constraints as well as safety compliance.
- Added complexity of power electronic systems due to increased components and sophisticated control algorithms.
- Unpredictable performance of new materials and technologies such as Silicon Carbide (SiC) and Gallium Nitride (GaN) devices.

Therefore, the continuous growth of critical applications such as aerospace, medical centers, data centers, automotive, etc., is a significant instigator for reliable power electronics.

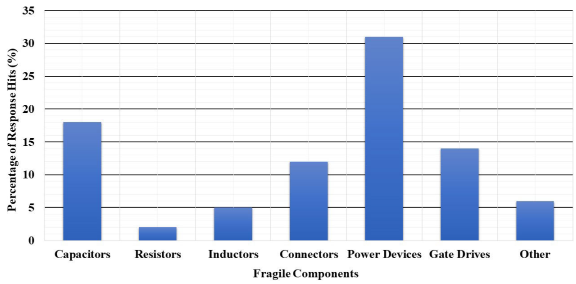

FIGURE 1. Fragile elements.

Moreover, performance enhancement of emerging applications such as wind turbines and PV systems is also an essential factor behind the drive for reliable and affordable power electronic systems [15], [16]. PECs include multiple components, of which power semiconductor devices (PSD) have been identified as having the highest possibility of breakdown, according to a survey conducted in [17]. The findings from this survey are summarized in Figure 1, which demonstrates the strong relationship between the reliability of PSDs and PECs.

B. MOTIVATION

The reliable operation of PSDs must be ensured to improve the reliability of PECs as a whole. The most susceptible points of failure in a PSD have been found at the interconnections inside the device and the bond wires, as shown in Figure 2 [18].

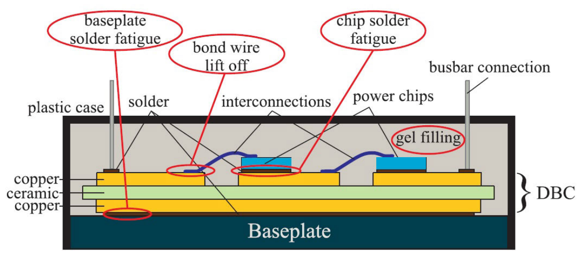

FIGURE 2. Structure of power semiconductor device [18].

Aluminum bond wires are generally used for electrical connections between chips and terminals. During operation, the PSDs are subjected to stress due to alterations in temperature and power, which lead to periodic cooling and heating cycles within the PSDs. The occurrence of periodic heating and cooling cycles due to the fluctuation of temperature and power is referred to as thermal cycling [13]. Mechanical stress between different layers within a PSD develops when temperature changes occur. This is due to the differences in thermal expansion coefficients (CTE) between copper and ceramic [19]. While every intersection within a PSD has to endure stress because of CTE mismatch, the effect of this stress is more prominent for aluminum bond wire and solder between substrate and baseplate [20]. Thus, periodic thermal cycles lead to severe fatigue in bond wire and solder joints, which are significant causes of device aging and breakdown [21]. The influence of increased thermal cycling on the device's lifetime is significantly greater than the average temperature increase [22]. The impact of average temperature and thermal cycling on the reliability of a standard Semikron Insulated-Gate Bipolar Transistor (IGBT) module is depicted in Figure 3, where it can be observed that the effect of thermal cycle amplitude is considerably more significant.

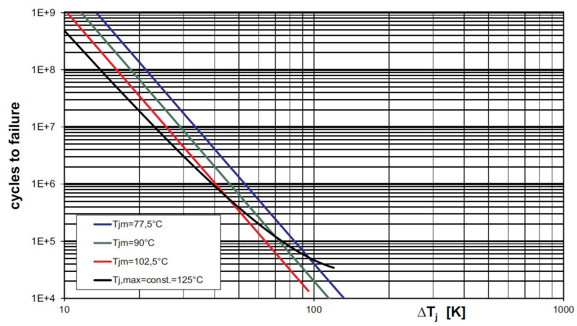

FIGURE 3. Standard IGBT modules Power cycling lifetime as a function of ΔTj and Tjm [23].

Therefore, it is especially crucial to apprehend the impact of temperature on power semiconductor devices, as the reliability, lifetime, efficiency, and robustness of these devices depend significantly on the junction temperature [24]. Recent developments in semiconductor technology have contributed to the rapid increase in the power density and peak junction temperature of PSDs. Although Wide band gap (WBG) devices such as SiC and GaN can operate at very high temperatures, existing packaging techniques, solder components, reliability issues, and expenditure have limited the maximum operating junction temperature to 175°C [25]. Furthermore, the heat dissipation area of these devices has been reduced significantly [26]. Failure to remove the generated heat from these devices can lead to reduced performance and breakdown. Moreover, according to US Air Force Avionics Integrity Program research, high temperature is responsible for over 50% of electronic equipment failures [27]. The causes of failures identified in this study are presented in Figure 4.

Moreover, Black's equation [28] establishes the correlation between device temperature and failure rate as expressed in (1) where A, J, E_A, K_B, and T represent a constant, current density, active energy, Boltzmann constant, and absolute operating temperature, respectively. This equation indicates the failure rate of PSDs escalates considerably when the operating temperature increases.

$$MTF = \frac{1}{\mathrm{AJ}^2} exp\left(\frac{E_A}{K_B T}\right) \tag{1}$$

The most difficult challenges experienced while developing reliable PECs are related to designing proper thermal management systems (TMS) to keep the semiconductor

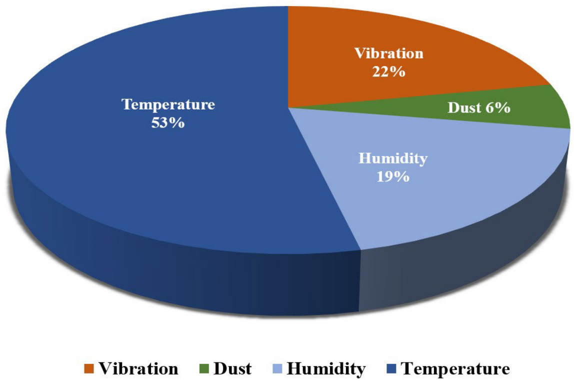

FIGURE 4. Causes of electronic equipment failures [27].

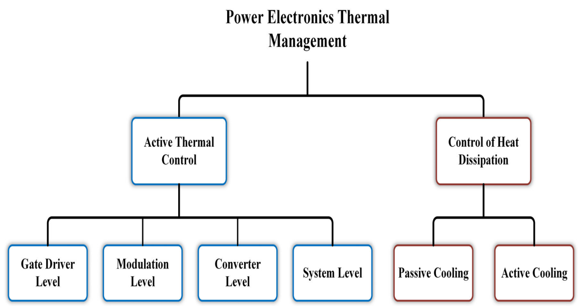

FIGURE 5. Thermal management approaches.

device temperature within limits. TMS regulates the degradation rate of power semiconductors by reducing the thermal stress due to overtemperature and power cycling [29], [30]. These systems can be implemented considering two approaches. The first approach is to control the electrical parameters by active thermal control (ATC), which is a procedure for controlling the junction temperature and reducing the thermal cycling of a power semiconductor. ATC scales down short and medium-term thermal cycles using temperature-related control parameters to regulate the junction temperatures in real time. Thermal control aims to regulate the junction temperatures by adjusting the losses in the targeted devices through specific temperature-related control parameters [31]. These parameters include the switching frequency [32], [33], modulation technique [34], DC-link voltage [35], gate voltage [36], or distributing reactive power [37]. For instance, a short-term temperature drop can be averted or decreased when losses are escalated temporarily by increasing the switching frequency. Additionally, an electrothermal model can be utilized to derive real-time estimations of junction temperatures through electrical measurements, enabling more accurate thermal stress management. The second approach for thermal management is to control the devices' heat dissipation by various active and passive cooling methods. Several cooling methods have been presented in [38], [39], [40], and [41]. In this approach, a fluid is normally applied as the coolant, and based on the working fluid's type, a fan or a pump is used to produce the coolant flow and forced convection. For passive techniques, which are called traditional cooling methods, heat sinks and fins are employed where free convection is the dominant heat transfer mechanism [42]. The general classification of TMSs is depicted in Figure 5.

C. STATE OF CONTRIBUTIONS

Numerous researchers have conducted research on the thermal management of PECs considering ATC. Their research focuses primarily on approaches that regulate the electrical parameters of the cooling system without considering active and passive cooling techniques. Independent studies on PEC cooling can be found in literature that overlooks the ATC aspect. The main focus of this research is to provide a comprehensive overview of both ATC and control of heat dissipation through active and passive cooling techniques. Furthermore, the scope of future work for power electronic cooling is proposed. This work will serve as a comprehensive and valuable reference for ATC techniques at various levels of PECs, direct contact, and indirect contact cooling methods, as well as performance-enhancing ideas for cooling system design.

D. STRUCTURE OF PAPER

The remaining sections of the paper are structured in the following manner. Section II introduces various ATC methods categorized by implementation technique. An overview of several ATC strategies is also provided. Section III provides an overview of several thermal management frameworks found in literature and introduces several active and passive cooling techniques. A review of several categories of active cooling techniques is also provided in this section. Section IV presents challenges and recommendations for future work in TMSs. Moreover, discussions related to multilevel converter configuration, thermal management during fault conditions, the impact of the environment on TMSs and financial considerations are provided. Finally, Section V concludes the paper.

II. ACTIVE THERMAL CONTROL TECHNIQUES

Several categories of ATC techniques have been investigated in literature, which are summarized below.

A. INCREASING OVERLOAD CAPACITY OF POWER MODULES

This approach aims to operate the semiconductor modules near their thermal limit and reduce power losses. It has been shown in [33] that switching frequency and output current influence power loss in IGBT modules. Thus, it is possible to regulate the junction temperature by controlling these two variables. An ATC method for field-oriented control (FOC) based electric cars is presented in [43]. This method reduces the maximum junction temperature by controlling

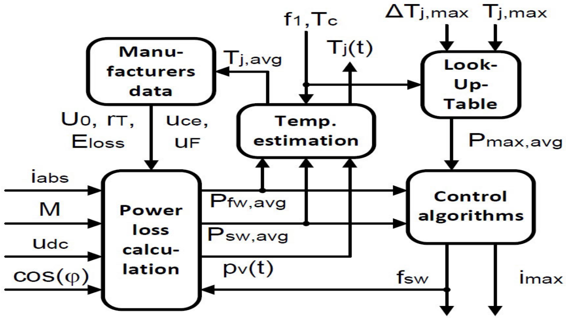

FIGURE 6. **Thermal management framework [43].**

the switching frequency and load current. Figure 6 shows the thermal management framework presented in this work.

Here, the power loss calculation and temperature estimation are completed based on the semiconductor device's datasheet. Then, the control algorithm compares the estimated temperature with a look-up table to determine the converter's switching frequency and maximum current. In [44], an ATC has been proposed for IGBT-based 3-phase inverters that estimate maximum peak operating current and operate the inverters at this current rating. Here, the maximum safe converter current has been determined as a function of the excitation frequency and coolant temperature.

B. REGULATING SWITCHING AND CONDUCTION LOSSES

This ATC approach focuses on the reduction of thermal cycles through the manipulation of losses. A method for accomplishing ATC through a loss manipulation unit is proposed in [45]. Here, the loss manipulation unit regulates the gate resistance and PWM frequency. Figure 7 shows that by applying the proposed method, thermal cycling has been reduced by 38% by varying the switching frequency and gate resistance.

The design of a gate driver for controlling power dissipation across grid-connected PV inverters has been proposed in [36]. As the gate drive parameters (V_{GS} and R_G) affect the conduction and switching losses, they can be manipulated to reduce thermal cycling. Figure 8 shows the main gate driver parameters for regulating the PV inverter lifetime. The study demonstrated that For V_G = 20 V, the variation of R_G significantly reduces the device lifetime. The lifetime reduction is 20 and 9.85 years for R_G = 7 Ω and 70 Ω, respectively. For low V_G, the variation of R_G has very little impact. A temperature-dependent gate driver for power MOSFETs has been proposed in [46]. Here, the gate drive voltage amplitude has been varied to counteract the effect of temperature variation in power semiconductors and accomplish constant power dissipation. The gate-source voltage was regulated to maintain a specific on-state resistance and subsequently control the device temperature.

A gate-driving strategy has been implemented in [47], which reduces thermal cycling in GaN-based DC/DC buck

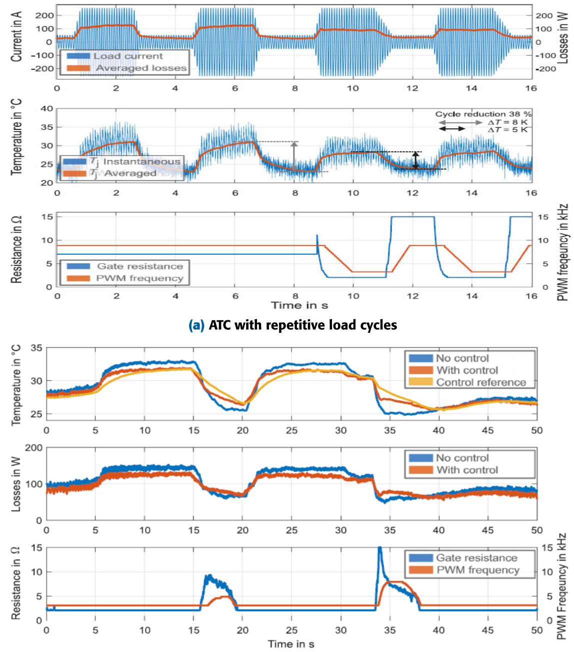

(a) **ATC with repetitive load cycles**

(b) **ATC with realistic load cycles**

FIGURE 7. **Active thermal control by manipulating gate resistance and PWM frequency [45].**

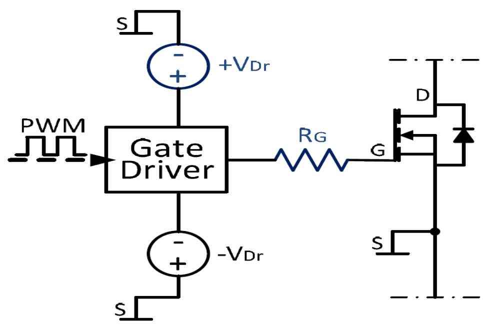

FIGURE 8. **Impact of gate-driver parameter variation on the lifetime of PV inverter [36].**

converters by varying the device losses. A two-step gate driver circuit has been developed that can adjust the shape of the gate voltage by controlling T_{on}, T_{off}, V_{on} and V_{off}. The proposed gate driving circuit can control the device switching and conduction losses and thus achieve active thermal control. Figure 9 shows the variation in the junction temperature of a single GaN device of a bidirectional single-phase DC/DC converter with and without the proposed ATC strategy.

Another ATC method is presented in [48] that manipulates the switching frequency and output power of an inverter to drive the induction motor of an EV. The result from the proposed ATC is presented in Figure 10. At t = 0.2s, the drive system torque becomes maximum, and the junction temperature attains its maximum value of 150 °C. Then, the ATC is activated, reducing the switching frequency from 16 kHz to a set limit of 4 kHz. This reduces power loss and the

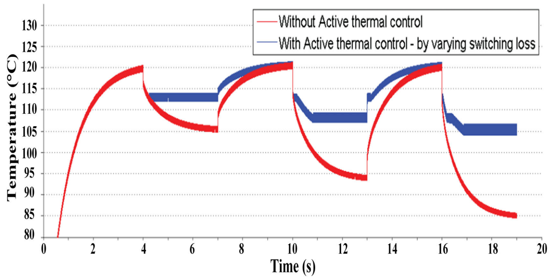

(a) Effect of varying switching losses

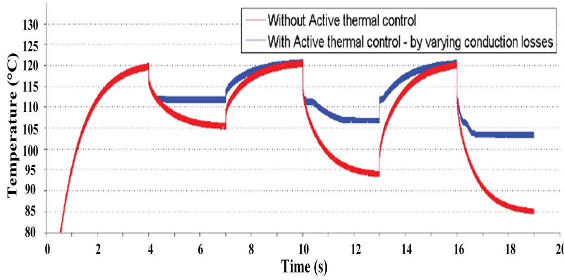

(b) Effect of varying conduction losses

FIGURE 9. **Effect of active thermal control strategies on the junction temperature of a GaN device [47].**

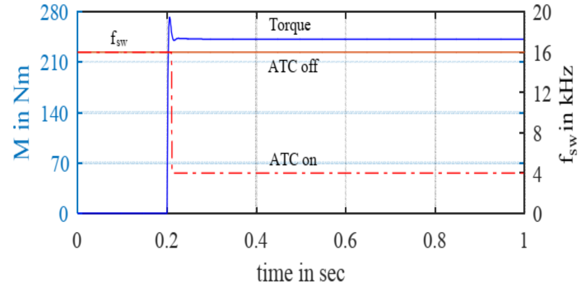

(a) Torque

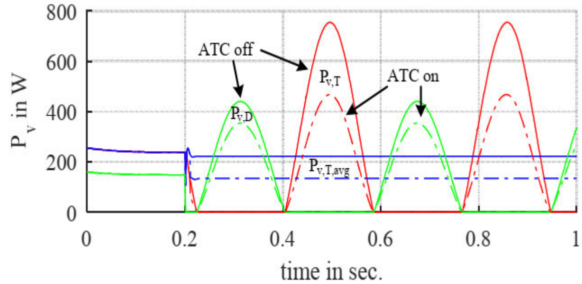

(b) Power loss

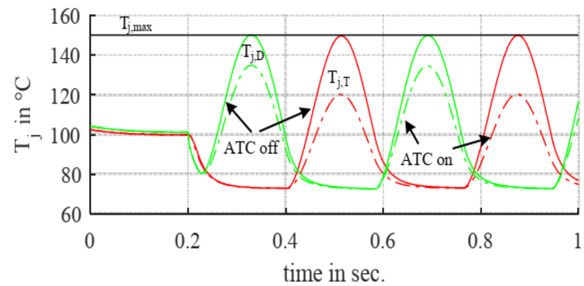

(c) Junction temperature

FIGURE 10. **Simulation results of junction temperature and power losses with and without ATC [48].**

junction temperature of the diode and IGBT modules inside the inverter.

C. OPTIMIZATION OF THE MODULATION PROCESS

Optimized modulation methods can reduce thermal cycling and high junction temperature in PECs. In [49], a method is proposed to minimize thermal stress on semiconductor modules using discontinuous pulse-width modulation (DPWM). This method clamps the output voltage to the positive or negative DC link voltage during a specific interval to reduce the switching loss, resulting in total loss reduction during the clamping period. As a result, the average junction temperature and thermal cycling are reduced. Figure 11 depicts the results of this method. It can be observed that thermal cycling has been reduced between $P_a < P_{load} < P_{nominal}$ when ATC is applied.

A finite set model predictive control (FS-MPC) [50] based approach for regulating the junction temperature of a 2 level 3 phase active rectifier is presented in [51]. This control technique minimizes a cost function based on the predicted outcome of a physical system. For each sampling time, this algorithm checks all possible output states and selects an optimum switching sequence for the rectifier with the objectives of controlling the DC link voltage and regulating the junction temperature of the semiconductor devices. A general framework of the proposed FS-MPC is presented in Figure 12. The results obtained from this study demonstrated that the junction temperature can be controlled between 67°C and 79°C while applying ATC. In [52], another FS-MPC based thermal controller is presented that generates an optimal switching sequence to control thermal stress in an IGBT-based 3-phase inverter. The proposed model is depicted in Figure 13.

Here, the FS-MPC is applied to control the junction temperature of the semiconductor modules and to control the motor current. The controller utilizes information from a system model to generate appropriate control signals for the inverter. A field-oriented control (FOC) strategy controls the machine speed and rotor flux using Proportional-Integral (PI) controllers. Another method has been proposed in [53], where the duty cycle of a DC/DC converter in a photovoltaic system is varied to achieve thermal management. The results from this method are presented in Figure 14. It can be seen that the maximum junction temperature derivative is reduced by restricting the variation of the duty cycle. Moreover, the standard MPPT algorithm embedded in the converters has also been modified.

In [54], a study on the thermal performance of a 3-level back-to-back neutral point clamped (NPC) converter for a wind turbine is presented. The configuration of the converter is depicted in Figure 15. The grid and generator side

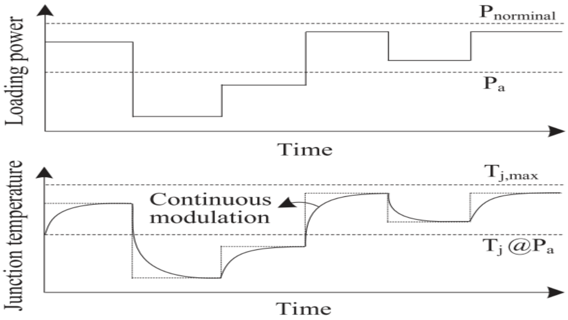

(a) Thermal Cycling with conventional continuous modulation

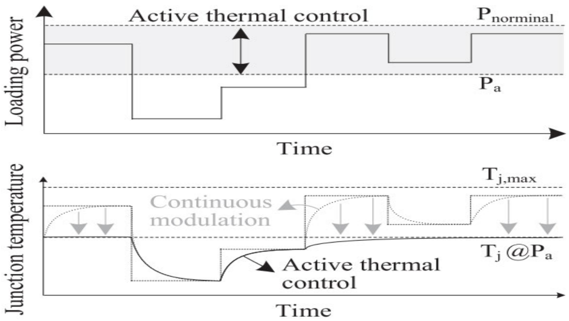

(b) Thermal Cycling with proposed discontinuous modulation

FIGURE 11. Junction temperature variation under fluctuating load [49].

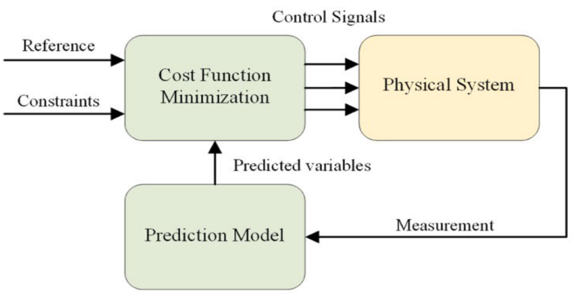

FIGURE 12. General structure of FCS-MPC [51].

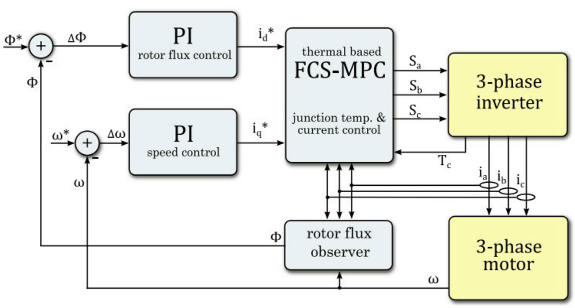

FIGURE 13. Thermal control framework based on FS-MPC [52].

converter can be controlled separately due to the back-to-back configuration. In this study, the following modulation techniques are considered to investigate the thermal performance of the converters: 1) Sinusoidal PWM (SPWM) [55]; 2) Optimal zero sequence injection (Opt-ZSSPWM)

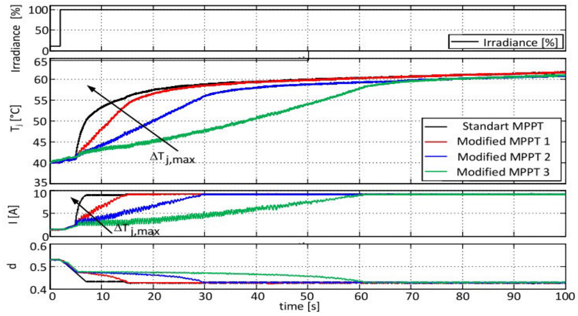

FIGURE 14. Reduction of temperature gradients by varying duty cycle in one IGBT module [53].

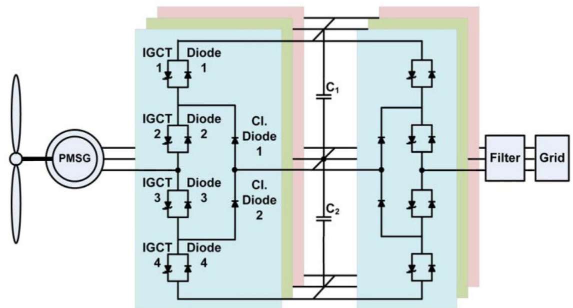

FIGURE 15. 3-level back-to-back NPC configuration for wind turbines [54].

[56]; 3) Alternative zero sequence injection (ALT-ZSSPWM) [57]; 4) Conventional 60° discontinuous PWM (CONV-60° DPWM) [58]; 5) Alternative 60° discontinuous PWM (ALT-60° DPWM) [58]. It is concluded that Conventional 60° discontinuous PWM provides the best thermal performance for both the grid side and generator side converter.

D. BALANCING THERMAL STRESS OF PARALLEL SEMICONDUCTOR DEVICES

The distribution of thermal stress on paralleled converter components might be unevenly balanced due to the connection of nonidentical conductors from the converter to the load, unequal tolerance of the components, physical positioning, etc. In different literature, ATC methods have been proposed to adjust the thermal stress of parallel power devices inside a system. A temperature-based load-sharing method for two parallel buck converters is presented in [59]. Here, the current of the individual converters is adjusted to ensure equal thermal sharing between the converters. In [60], a selective soft switching (SS) technique is presented that can manipulate the device turn-off losses to overcome the thermal imbalance in a multichip system. Multichip systems are a combination of multiple parallel semiconductors used in high-power converters. In the presented method, hotter devices are turned off earlier, and the total current is redistributed to flow through the rest of the devices, reducing their turn-off time. Hence, thermal balance is achieved without affecting the performance of the system. The result from this method is depicted in Figure 16, where there is a

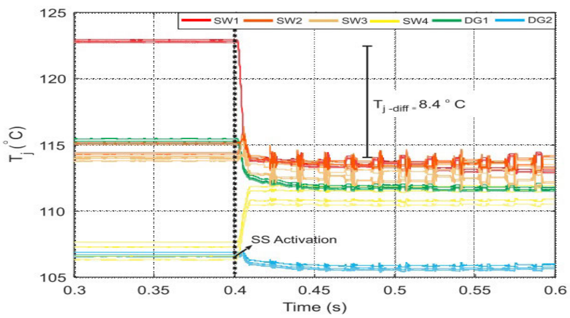

FIGURE 16. Reduction of thermal stress with selective switching [60].

temperature reduction of 8.4°C in the most thermally stressed device.

In [61], the impact of a pulse processing strategy on the junction temperature of multichip modules (MCM) is investigated. Here, thermal balancing is accomplished by switching off the hottest devices during specific periods to redistribute the losses among them. The impact of this strategy is presented in Figure 17, which shows a maximum temperature difference of 7.61°C between the transistors. The temperature difference is reduced to 4.2°C by applying thermal control at t = 3s.

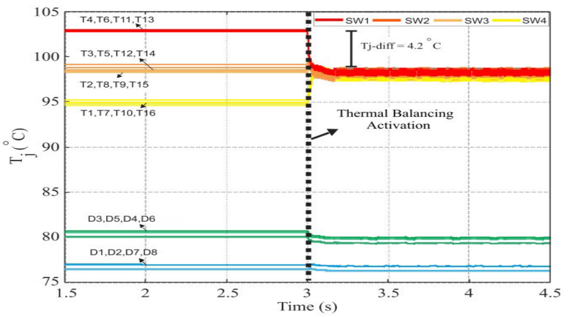

FIGURE 17. Thermal balancing with pulse processing strategy [61].

A gate driver-based method is presented in [62] that regulates the temperature of individual devices to increase the reliability of a power converter. The results from this method are depicted in Figure 18, showing the temperature distribution across six parallel devices. Applying thermal management reduces the temperature difference between the hottest and coldest device to less than 0.5°C.

E. THERMAL STRESS CONTROL AT THE SYSTEM LEVEL

ATC strategies can also facilitate appropriate load-sharing between modular converters to maintain thermal balance among the converters. This way, thermal cycling can be reduced, and the converters can be operated near their thermal limits. In [63], an ATC strategy for hybrid modular multilevel converters (MMC) based high-voltage direct current (HVDC) transmission system is presented. The hybrid MMC is a combination of half-bridge and full-bridge submodules (HBSM and FBSM), with each submodule consisting of

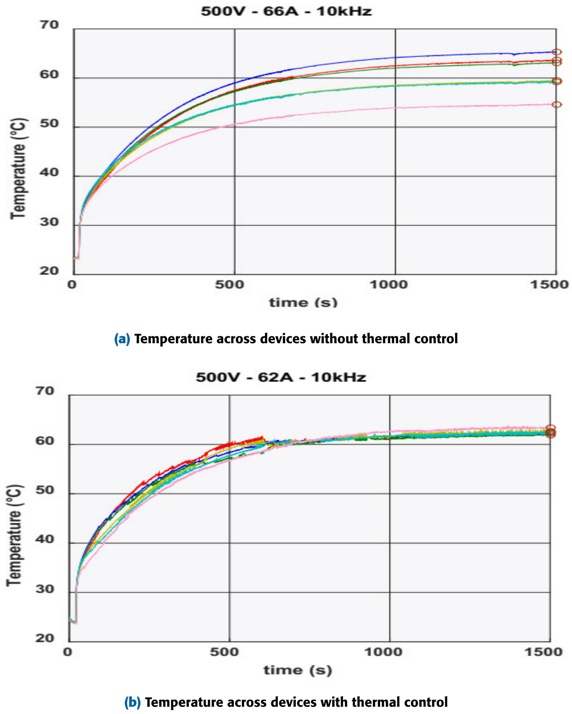

FIGURE 18. Temperature distribution across six parallel devices under load [62].

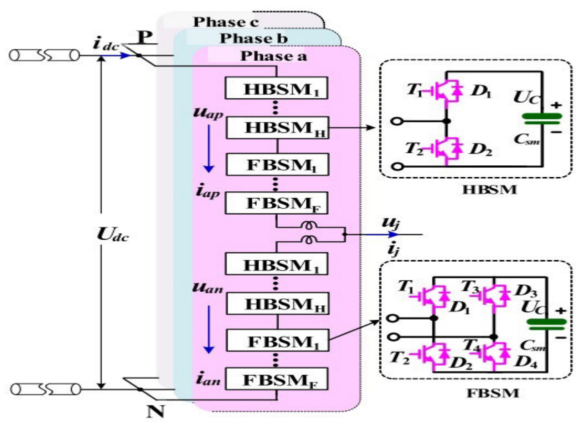

FIGURE 19. MMC framework [63].

multiple IGBTs and diodes. The hybrid MMC framework is presented in Figure 19.

The results from this ATC strategy are presented in Figure 20. Here, ATC is activated at t = 0.2s, and the temperature of T_2 in HBSM is reduced by 20%. In the case of FBSM, the thermal distribution becomes more balanced. In [64], a thermal balancing approach is presented for the submodules of an MMC for HVDC application. A modified space vector PWM (SVPWM) based method is presented in [65] for reducing the junction temperature of thermally stressed devices in multilevel inverters. Multilevel inverters have redundant switching states, which can be employed to control the junction temperature of semiconductor switches.

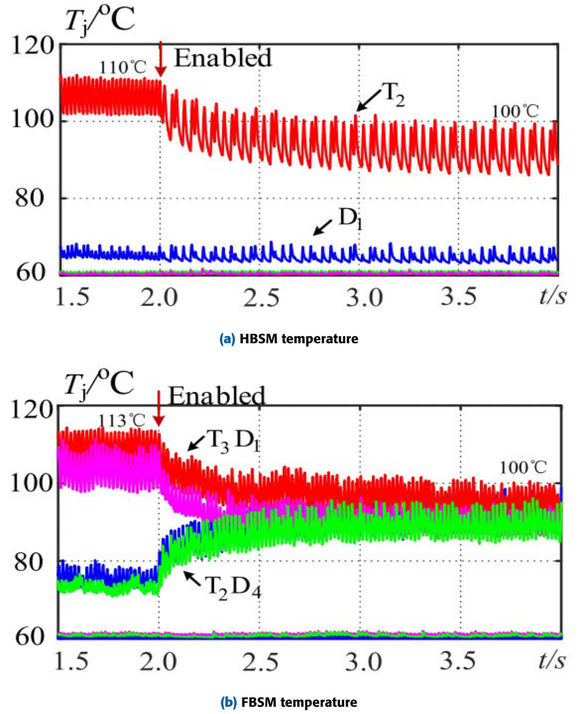

FIGURE 20. Junction temperature of MMC [63].

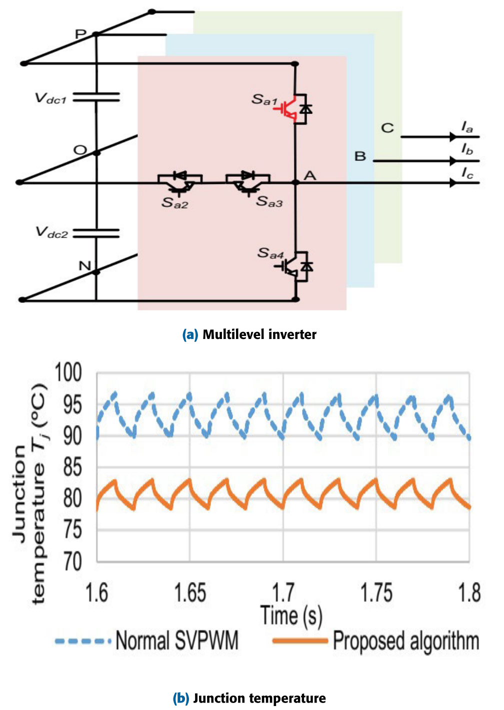

FIGURE 21. Junction temperature across switch S_{a1} of modular inverter [65].

When the proposed algorithm detects thermal overloading in any switch, it estimates the thermal behavior of that switch for various switching sequences. Then, the switching sequence that produces the best thermal performance is applied across that switch. Figure 21a shows the multilevel inverter where switch S_{a1} is under the most thermal stress. Figure 21b shows the junction temperature across S_{a1} with conventional SVPWM and proposed modified SVPWM.

One innovative method for implementing ATC involves utilizing the power routing technique [30]. This technique efficiently distributes the thermal load across various segments of a modular converter, thereby minimizing thermal stress on the most susceptible components and extending the remaining useful life (RUL) of these components. With this approach, each module within a modular PEC handles a specific amount of power to mitigate the thermal stress resulting from temperature variations. The primary objective of this technique is to prolong the lifespan of the most vulnerable modules within the converter. This is accomplished by operating these modules under variable load conditions and reducing stress on the modules that have deteriorated more significantly by shifting their load to less vulnerable counterparts. Figure 22a shows a modular converter with three modules where modules 1, 2, and 3 handle power P_1, P_2, and P_3, respectively. The total power $P_T = P_1 + P_2 + P_3$ where $P_1 = P_2 = P_3$ under regular operating conditions. Nevertheless, when operating under conditions where load-sharing is balanced, there is a risk of uneven module aging, potentially resulting in unexpected module failures and the need for unscheduled maintenance. By employing the power routing technique, each module handles a varying amount of power based on its aging status by employing the power routing technique, as illustrated in Figure 22b. This application of power routing allows for the optimization of maintenance schedules and the extension of the lifespan of modular power converters.

In a modular converter, the cells can be configured in series, parallel, or a combination of both [66]. In the case of series-connected modules, the output power of each cell can be managed by controlling the output voltage of each cell. Likewise, for modules connected in parallel, the output power of each cell can be regulated by controlling the output current of each cell. In the scenario of a combined series and parallel configuration, it is possible to control either the current, voltage, or both to regulate the power output of each cell. The primary goal of implementing power routing is to enhance the operational lifespan of a converter by optimizing its maintenance schedule. To effectively employ power routing methods, it is essential to estimate the remaining useful life (RUL) and state of health (SOH) of the converters, as discussed in [29]. With this information in hand, maintenance activities can be coordinated across all the modules within a PEC, considering each module's RUL. This concept is visually represented in Figure 23, where RUL equalization is achieved between two Power Electronic Building Blocks (PEBBs). The red bars in the diagram indicate the anticipated failure times of the two PEBBs, while P_1 and P_2 represent the power each PEBB processes. By applying the power routing method, the power handled

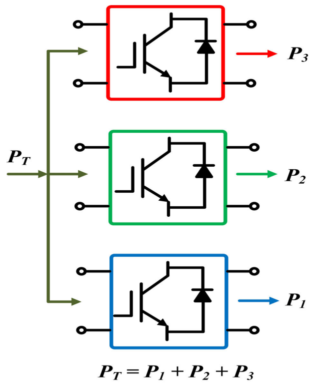

(a) power routing in a modular system

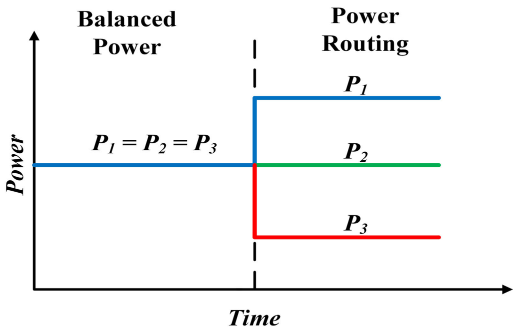

(b) balancing the power between modules

FIGURE 22. Power routing concept.

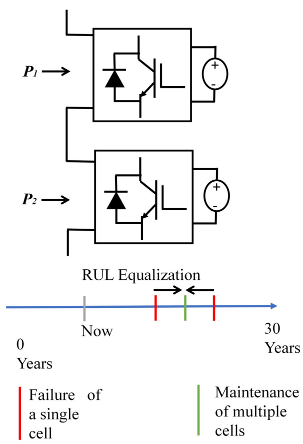

FIGURE 23. RUL management via power routing [30].

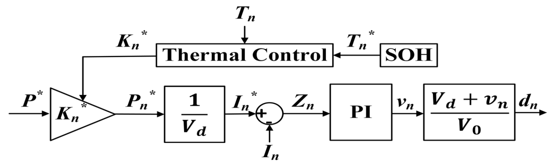

(a) Control strategy

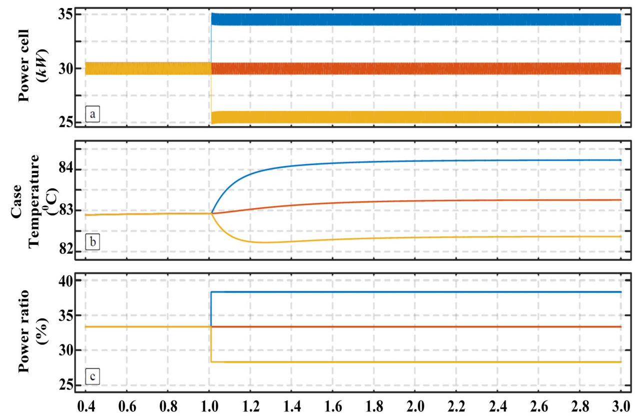

(b) Power ratio and temperature distribution

FIGURE 24. Power routing in three-cell DC/DC boost converter [67].

by each PEBB can be adjusted, ensuring that maintenance for both PEBBs is scheduled simultaneously. The green bar symbolizes the unified maintenance schedule for both PEBBs

Several approaches have been investigated in literature for implementing power routing techniques with series and parallel connected converters. A closed-loop controller has been presented in [67] to reduce the maintenance cost of a parallel-connected three-cell DC-DC converter by considering the State of Health (SOH) of each cell. Figure 24 illustrates the control scheme for this converter along with the simulated results. Within this control scheme, the SOH block estimates the aging level of each cell. It accomplishes this by using information about the power system's usage and real-time electrical measurements. Subsequently, the SOH block provides a temperature reference denoted as (T_n^*) to the thermal controller block. This thermal controller block determines the appropriate power-sharing factor (k_n^*) for the parallel cells. Then, the reference power for each cell, denoted as (P_n^*), is calculated by dividing the total instantaneous reference power (P^*) by the control factor (k_n^*). With the reference power values determined, it becomes possible to calculate the reference current (I_n^*) for each cell. This reference current is then employed to compute the voltage (v_n) that needs to be modulated by each cell. A proportional-integral (PI) controller is employed to determine v_n. The overall effect of this proposed algorithm is the successful redistribution of power among the cells, thereby achieving effective thermal management.

Another study by Marquez et al. [68] proposed a power routing mechanism to mitigate aging imbalances in an interleaved boost converter consisting of three modules. Through the implementation of the proposed power routing technique, the study demonstrated that the lifespan of the most vulnerable power module could be extended by 24 months, as depicted in Figure 25.

Andresen et al. [69] introduced a novel power routing technique based on virtual resistors for parallel converters within the low voltage stage of a smart transformer. This technique is activated during partial load conditions and involves the adjustment of virtual resistors based on condition monitoring data, effectively optimizing power distribution among the converters to enhance overall system performance and extend its operational lifespan. The proposed control

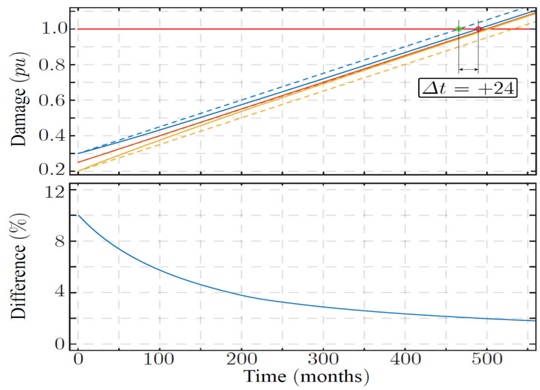

FIGURE 25. Lifetime extension through power routing.

framework for implementing the power routing method is depicted in Figure 26a. Here, three virtual resistors (R_{v1}, R_{v2}, and R_{v3}) are tuned based on information received from the condition monitor and are expressed as a function of accumulated damage as shown in (2).

$$R_{vi} = f(D_{acc}) \tag{2}$$

The reference current for any specific converter (i^*_{cn}) can be calculated by using (3).

$$[i^*_{c1}, i^*_{c2}, i^*_{c3}] = \left(\frac{i^*_{ref}}{R_{v2}R_{v3} + R_{v1}R_{v2} + R_{v1}R_{v3}}\right) .[R_{v2}R_{v3}, R_{v1}R_{v2}, R_{v1}R_{v3}] \tag{3}$$

Figure 26b depicts how the virtual resistor-based power routing technique can extend the Estimated Lifetime (ELT) of converters with different initial damage levels.

Further power routing algorithms designed for MEA with four parallel dual active bridges (DAB) are presented in [70] and [71]. These algorithms aim to increase the system's overall lifetime by estimating the Remaining Useful Life (RUL) of the converters based on their junction temperature profiles, as determined by the mission profile. The total damage for each converter is calculated using 4, allowing for optimized power routing and enhanced system reliability.

$$D_i = D_{ini,i} + \Sigma^m_{period=1} \Delta D_i \tag{4}$$

Here, D_i is total accumulated damage and $D_{ini,i}$ is initial damage. The RUL for a specific converter can be calculated using 5, where ΔD_i is the rate of damage change over a particular time interval.

$$LT_{exp,i} = \frac{1 - D_i}{\Delta D_i} \tag{5}$$

Due to thermal cycling, each converter experiences a varying RUL, and it is the controller's task to determine the power each converter should handle to prolong its operational lifespan. It's worth noting that the power routing algorithm is only operational when the system operates under partial load conditions. In contrast, all the converters process equal power during full-load operation. Figure 28a illustrates the

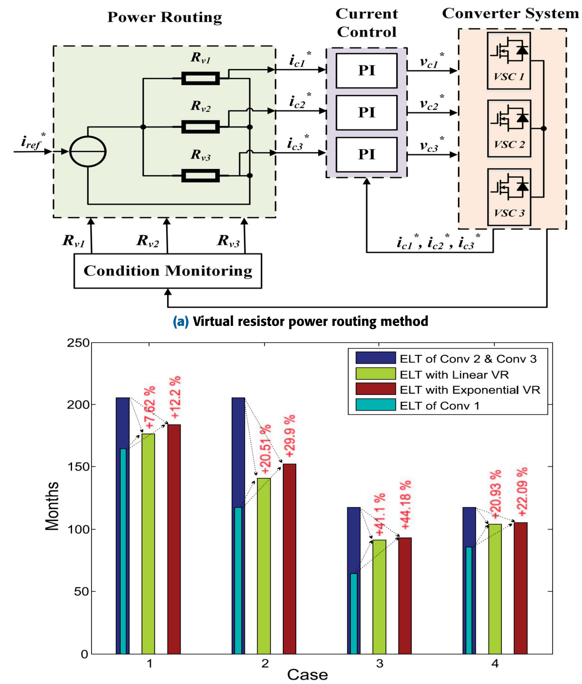

(a) Virtual resistor power routing method

(b) The ELT of parallel converters with and without power routing

FIGURE 26. A virtual resistor based power routing technique for parallel converters in an ST [69].

accumulated damage of the converters, comparing scenarios with and without the power routing algorithm. In the absence of any lifetime control method, the cells wear out at a different rate. However, when active lifetime control through the power routing algorithm is implemented, the accumulated damages of the converters start to converge towards a common point, as demonstrated in Figure 28b. This convergence signifies that the power routing algorithm effectively equalizes the wear and tear on the converters, resulting in a more balanced and extended operational life for the entire system.

A study conducted in [72] examined how power routing influences the aging of a set of 10 parallel-connected DAB cells within a smart transformer. Another study conducted by Liserre et al. [66] demonstrated the efficacy of power routing in mitigating the thermal cycling effects on the most deteriorated cells within the low-voltage conversion stage of a smart transformer (ST). A further study conducted in [73] assessed the efficiency of the power routing approach based on virtual resistors in alleviating thermal stress within a modular DC/DC converter featuring multiple Quadruple Active Bridge (QAB) converters. The outcomes of this research demonstrate the effectiveness of the control algorithm in prolonging the system's operational lifespan.

Modified modulation strategies offer the flexibility to effectively implement power routing by allowing thermal stress control in each converter. A specific approach called Discontinuous PWM (DPWM) for power routing in Cascaded H-Bridge (CHB) converters is introduced in [74]. The DPWM strategy minimizes switching losses

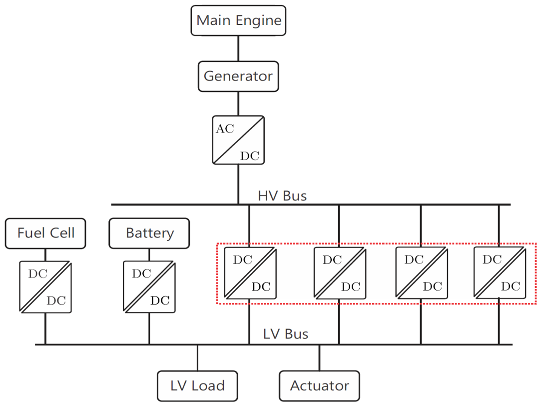

(a) Proposed MEA architecture

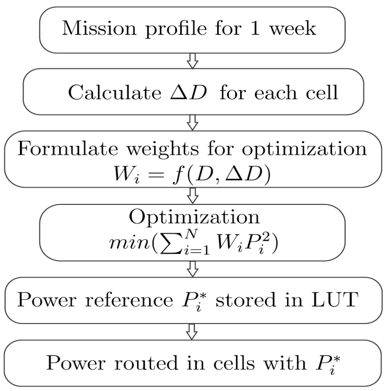

(b) Control algorithm

FIGURE 27. Power routing for an MEA [71].

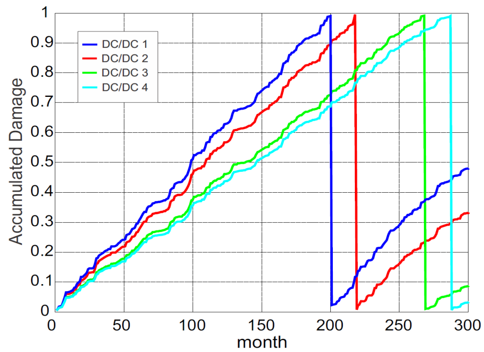

(a) Power routing disabled

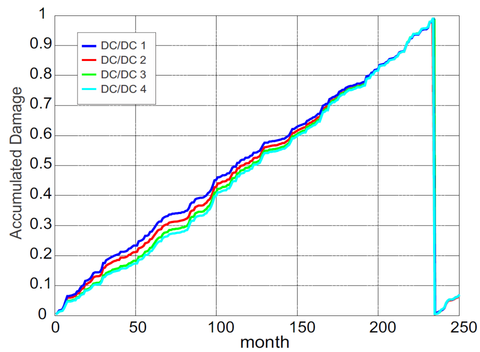

(b) Power routing enabled

FIGURE 28. Impact of power routing on the accumulated damage [71].

by clamping the output voltage at either the positive or negative DC-link voltage. This loss reduction is substantial compared to continuous PWM techniques because it prevents semiconductor devices from switching within the clamping region. As depicted in Figure 29a, the proposed method employs two types of modulation signals. First, a positive offset voltage $V_{off,p}$ is added to the fundamental reference voltage $V_{ref,fund}$ to generate the modulation signal $V_{ref,ns}$, which includes a clamping zone. This modulation signal is applied to the most vulnerable converters since the clamping region helps reduce the generation of losses. On the other hand, the second modulation signal $V_{ref,s}$ lacks a clamping region and incorporates a negative offset voltage $V_{off,n}$. This signal is utilized for the less vulnerable converters, serving to compensate for the clamping that occurs in the other converters. The ultimate objective of this modulation strategy is to delay the failure of the most vulnerable converters by optimizing the control of thermal stress.

The application of the modulation strategy, as illustrated in Figure 29b, depends on the condition of the converters. Specifically, the choice of modulation signal depends on the Remaining Useful Life (RUL) of each converter. When a converter has a shorter RUL, it is modulated with the signal $V_{ref,ns}$ to mitigate thermal stress effectively. In contrast, converters with a longer RUL are modulated with the signal $V_{ref,s}$, which helps offset the positive offset voltage and maintain their optimal operation. The ATC concept, initially introduced in [74], is further developed and extended in [75]. This extended concept employs a discontinuous modulation technique within the Medium Voltage Alternating Current (MVAC) to Low Voltage Direct Current (LVDC) building block of an ST to effectively achieve thermal management. After applying the proposed modulation technique, the estimated junction temperature of a CHB cell and a DAB cell with a fixed clamping angle of 60° is shown in Figures 30a and 30b, respectively. For the CHB cell, the junction temperature rises to 82°C with the non-clamped signal, while for the clamped signal, the junction temperature reaches around 43.5°C. For the DAB cells, the maximum junction temperature reaches 99.8°C with the clamped signal and 78.7°C for the non-clamped signal. A power routing technique for STs is presented in [76], which introduces an advanced discontinuous modulation technique for power routing. This technique is designed to handle thermal stress within the Cascaded H-Bridge (CHB) converters and the isolated DC/DC converters, enhancing the overall system's thermal performance. Another approach, proposed in [77], focuses on improving the thermal performance of CHB converters. This method employs a non-conventional phase-shifted Pulse Width Modulation (PWM) technique, resulting in an extended lifespan for the most vulnerable cells while simultaneously reducing harmonic distortion in the cells. A multi-frequency modulation-based power routing

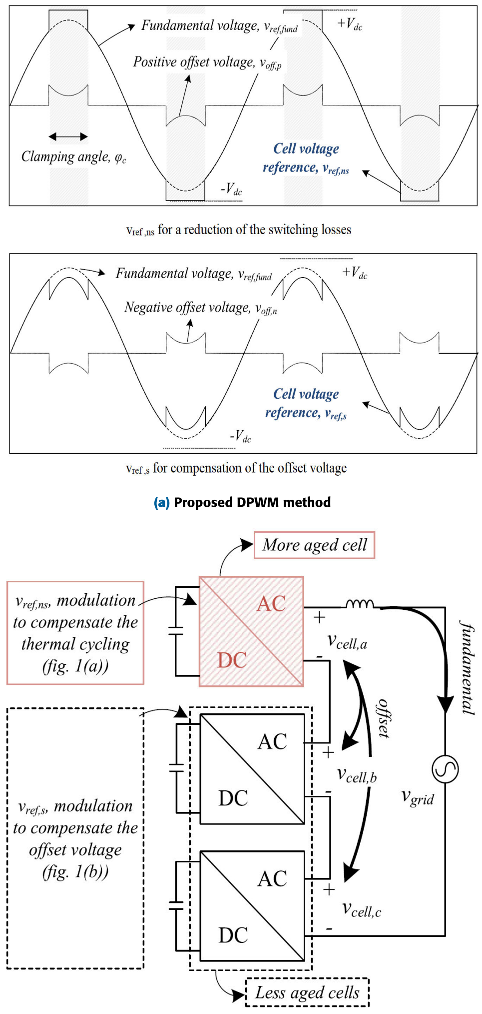

(a) Proposed DPWM method

(b) Proposed modulation strategy

FIGURE 29. Power routing with DPWM method [74].

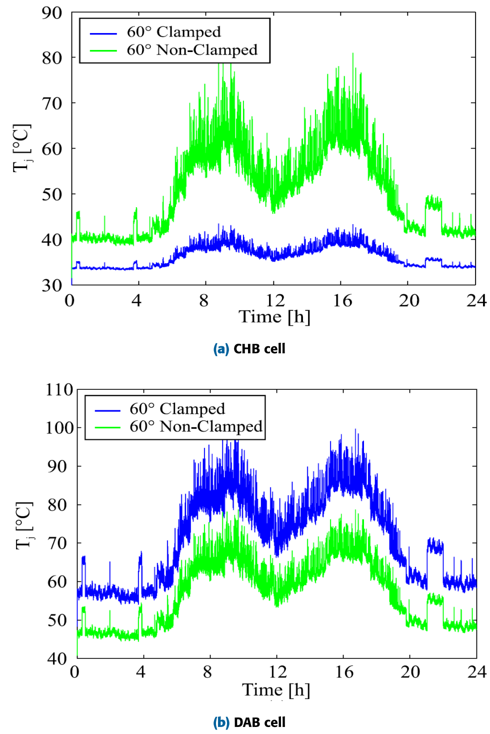

(a) CHB cell

(b) DAB cell

FIGURE 30. Junction temperature of CHB and DAB cells with and without clamping signal [75].

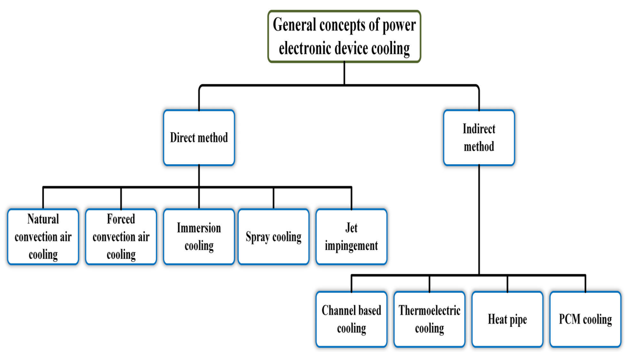

FIGURE 31. Concepts of power electronic device cooling.

technique is introduced in another study, presented in [78]. This technique involves injecting a third harmonic component into the duty cycle of CHB converters. This injection of the third harmonic component optimizes the utilization of DC-link voltage, similar to the Third Harmonic Injected PWM (THIPWM) method. It contributes to improved power routing within the system. These innovative power routing techniques collectively contribute to the efficient management of thermal stress and enhanced performance in smart transformers.

III. CONTROL OF HEAT DISSIPATION

The second approach for controlling the temperature of semiconductor modules is to apply passive or active cooling techniques. Passive cooling systems are normally based on natural convection and utilize capillary or gravitational buoyancy forces to circulate the working fluid. In contrast, external energy must be supplied to active cooling systems for higher cooling capacity and improved performance [79]. Usually, a pump or compressor drives the coolant in an active cooling system. Commonly used cooling techniques for PSDs can be classified depending on whether there is direct contact between the coolant and the electronic device. Based on this classification, cooling techniques can be of two types: direct and indirect cooling, as shown in Figure 31. Natural convection is an economical and straightforward passive cooling mechanism where conductive surfaces are attached to the heat-dissipating component. The generated heat from the component is accumulated in the conductive surfaces and released to the environment through natural convection [80]. This method only applies to low-power electronic devices due to low heat flux density and is unsuitable for modern power electronic devices [81]. From Figure 32, it can be seen that the natural convection technique has the lowest capacity for heat removal.

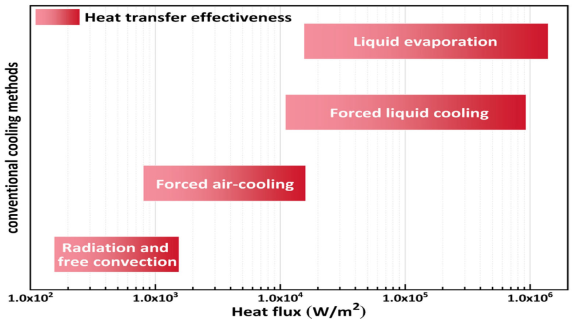

FIGURE 32. Comparison of heat removal rate from conventional methods [82].

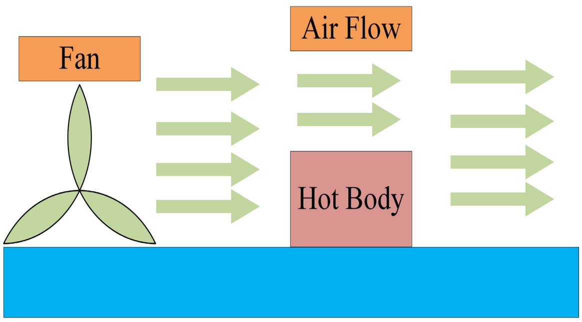

FIGURE 33. Forced air cooling method.

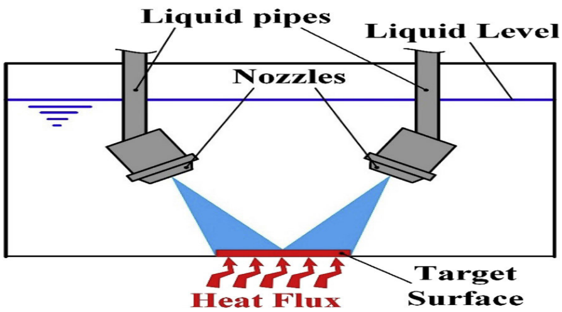

FIGURE 34. Immersed spray cooling [83].

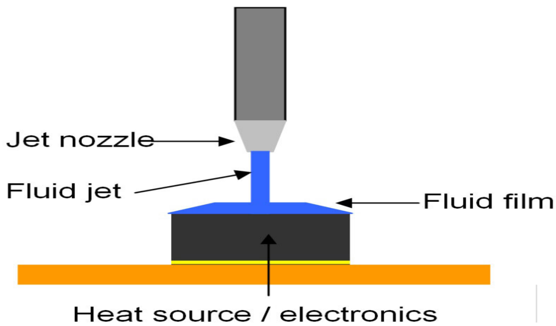

FIGURE 35. Jet-impingement cooler [89].

An active method for heat removal is forced convection-based air cooling, which provides improved cooling performance by forcing air using a fan. This method is suitable for high-power electronic devices [82]. A schematic of forced air cooling is shown in Figure 33.

Another highly effective method to achieve significant cooling performance is liquid cooling, which is compatible with high-power density applications [20]. There are several emerging technologies for implementing liquid cooling, which include cold plates, microchannel, jet impingement, spray cooling, and immersion cooling-based designs [83], [84], [85]. A spray cooling-based technique is depicted in Figure 34, where a pressurized coolant is sprayed from a nozzle that fragments the coolant into liquid droplets and then cools the hot surface. This method maintains uniform heat flux and temperature across a hot surface. Moreover, this method reduces the effect of the thermal boundary layer acting as a thermally insulating medium, as a result of which it is suitable for compact designs that require high cooling capacity [86]. Nevertheless, spray cooling requires a significant pressure drop in the nozzle, which impedes its performance [87].

Figure 35 shows the main components of a jet-impingement based cooling system. A jet nozzle forces a continuous flow of coolant to a heated surface with adequate pressure. This cooling method can provide a superior localized HTC (HTC) than spray cooling. This concept is suited for compact designs as it can provide a fine thermal boundary layer and a preferable HTC [88]. However, the design and manufacturing process is considerably more complicated than channel-based cooling.

Microchannel systems have become popular for high heat flux generating applications. Figure 36 shows the main components of a microchannel cooler. The coolant passes through the microchannel, transferring heat from the electronic device to the coolant. By incorporating numerous small channels in parallel, microchannel-based designs can substantially enhance heat transfer capabilities. Microchannel-based designs offer the advantage of flexibility, particularly in terms of reducing the channel diameter. This flexibility allows for the development of more compact TMSs [90]. However, further scaling down can be limited due to an increase in pressure drop [91]. Immersion cooling is a direct cooling method where the electronic device is submerged in a coolant or dielectric fluid [92]. However, the prerequisite of fluid suitable for electronic devices limits the utilization of this cooling technique.

Liquid evaporation technology provides the highest heat removal rate. This method converts the coolant liquid to vapor when heat is transferred from the heat-dissipating component [93]. The application of evaporation techniques has emerged in heat-pipe and phase change material (PCM) based designs [94], [95]. Heat sinks combined with PCM have significantly high latent heat absorption compared to sensible heat absorption designs. Nevertheless, this technique faces challenges due to the low thermal conductivity of the

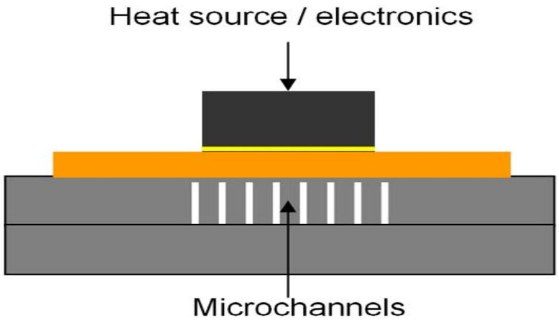

FIGURE 36. **Microchannel cooler [89].**

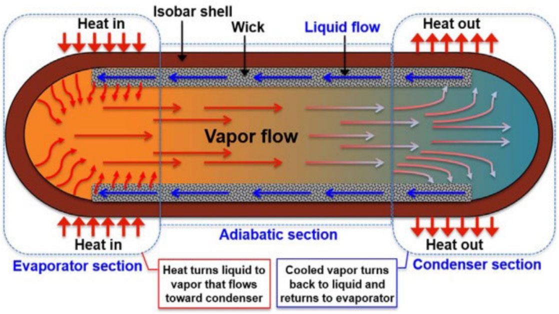

FIGURE 37. **Heat pipe structure [93].**

materials used as PCM. Accordingly, improving the thermal conductivity of PCM-based cooling systems has attracted significant interest from researchers [96], [97]. Additionally, heat pipes take advantage of the liquid-vapor phase change process and reach very high thermal conductivity, which is reasonable for TMSs [98]. Figure 37 shows the basic structure of a heat pipe that consists of a pipe, wick, and working fluid. Any external heat source would evaporate the fluid in the evaporation section, and the vapor moves from the evaporator to the condenser, where it releases the heat and turns back into liquid. The wick allows the condensed liquid to flow back to the evaporator through capillary pumping, and the cycle starts again.

Thermoelectric (TE) cooling is an emerging technology where cooling is accomplished based on the Peltier effect [99]. A thermoelectric module employs thermoelectric materials to create a temperature gradient between two sides of the module by consuming electrical energy. Then heat is transferred from one side of the device to the other, resulting in a cooling effect [100]. Thermoelectric coolers can be combined with microchannels, heat pipes, and additional heat sinks to enhance thermal performance. A thermoelectric cooling scheme is depicted in Figure 38.

A comparison of the general cooling techniques is provided in Table 1.

The next segment provides a detailed overview of several core TMSs

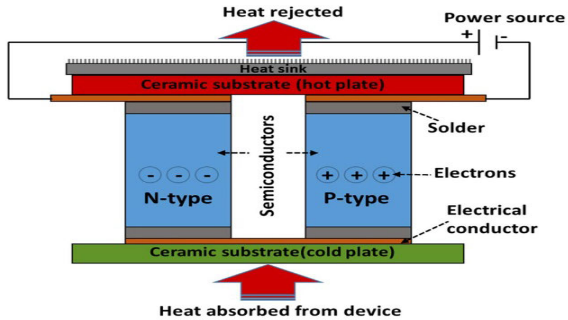

FIGURE 38. **Thermoelectric cooling concept [93].**

TABLE 1. **Comparison of cooling techniques [82], [93].**

Cooling Technique	Cooling system type	Advantages	Disadvantages
Natural convection	Passive Cooling	• Simple design • Low Cost • High reliability • Noise-free	• Lowest heat removal rate • Requires large heat transfer area
Forced convection based air cooling	Active Cooling	• Well established cooling method • Very reliable • Low maintenance • Simple design • Easy installation	• Low HTC • Need additional means such as a fan which generates noise
Forced convection based Liquid cooling	Active Cooling	• Higher cooling capacity compared to air cooling • Suitable for high power density applications	• Difficult to use with small devices • Generates noise from fan or pump
Liquid evaporation	Passive Cooling	• Highest heat removal rate • Good for barren climates	• Performs poorly in cold and highly humid weather conditions • Not suitable for small electronic devices
Thermoelectric cooling	Active cooling	• Compact Design • Can cool below ambient temperature • Noise-free • No moving parts	• Compared to passive cooling, performance is poor with existing thermoelectric materials

A. CHANNEL COOLING

This section reviews different channel- and microchannel-based cooling system designs that have gained significant attention in the design of TMSs. Tuckerman and Pease introduced the idea of microchannel for the first time in 1981 [101]. Microchannels have demonstrated high cooling performance that can dissipate heat efficiently from a small surface area. The hydraulic diameter of the microchannels can be in the range of 10 to 200 μm and 1 to 100 μm according to Kandlikar et al. [102] and Mehendale et al. [103], respectively. The characteristic parameters for channel-based cooling strategies can be described using the following equations [104].

$$D_h = \frac{4A}{p} \tag{6}$$

Here D_h, A, and P represent hydraulic diameter, flow cross-section, and wetted perimeter, respectively.

$$R_e = \frac{\rho v D}{\mu} \tag{7}$$

where R_e, ρ, v, D, and μ are the Reynolds number, fluid density, velocity, length, and dynamic viscosity, respectively.

$$P_r = \frac{c_p \mu}{k} \tag{8}$$

Here, P_r, C_p, μ, and k represent the Prandtl number, specific heat, dynamic viscosity, and thermal conductivity, respectively.

$$S_t = \frac{vL}{U} \tag{9}$$

Here, S_t, v, L, and U represent the Strouhal number, vortex shedding frequency, length, and flow velocity, respectively.

$$R_{th} = \frac{T_h - T_c}{P_t} \tag{10}$$

Here, R_{th}, T_h, T_c, and P_t are total thermal resistance, power loss, hot spot temperature, and inflow bulk temperature, respectively.

$$h = \frac{q}{T_w - T_b} \tag{11}$$

where h, q, T_w, and T_b are convective coefficients, heat flux, channel wall temperature, and average coolant temperature, respectively.

$$N_u = \frac{hD}{k} \tag{12}$$

Here, N_u, h, D, and K represent the Nusselt number, convective coefficient, length, and thermal conductivity, respectively.

$$P.P = Q\Delta P \tag{13}$$

Here, P.P is pumping power, Q is volumetric flow rate, and ΔP is pressure drop.

$$f = \frac{2\Delta P D_h}{\rho \mu^2 L} \tag{14}$$

where f, u, and L represent friction factor, average flow velocity, and channel length, respectively.

$$n_i = \frac{N_u}{f^{1/3}} \tag{15}$$

where n_i, n_u, and f represent the thermal efficiency index, Nusselt number, and friction factor, respectively.

$$\eta = \frac{\frac{N_u}{N_{up}}}{\frac{f}{f_p}} \tag{16}$$

Here, η is the thermal performance factor, N_u is the Nusselt number, and f is the friction factor. The subscript p indicates a plain channel without any enhancement. Several ideas for enhancing channel cooling are discussed in the next section.

1) EMPLOYING APPROPRIATE MATERIAL

The material employed for microchannel-based heat sinks significantly affects thermal performance. The performance of heat sinks with different materials such as Si, Cu, Steel, Glass, Quartz, and Polyimide was investigated using numerical simulation in [85], and it was determined that the Nusselt number reduces with materials of lower thermal conductivity. Moreover, a numerical analysis comparing the cooling performance with materials like Cu alloy, Al, tungsten, and Si was performed in [105], and it was concluded that materials with higher thermal conductivity provide superior thermal performance. Muhammad et al. [106] came to the same conclusion while conducting a numerical investigation on microchannel heat sink materials such as copper, aluminum, steel, and titanium. A numerical analysis employing the finite volume method was conducted in [107] that investigated the heat transfer performance of ZrB2, TiB2, and HfB2, which are ultra-high temperature ceramic (UHTC) materials. It was found that all three materials provide optimum performance, while HfB2 offers the maximum HTC.

2) MODIFYING CHANNEL CONFIGURATION

An investigation of conventional and novel microchannel configurations was conducted in [108], which showed that the proposed configuration accomplished homogeneous temperature distribution with minimized pressure drop and pumping power due to balanced flow distribution. The proposed heat sink configuration in this study is shown in Figure 39. Another study by Zeng et al. [109] proposed an air-cooled heat sink using topology optimization to achieve better thermal performance and minimize pressure drop. Gunnasegaran et al. [110] investigated the heat transfer performance of microchannels with different shapes as depicted in Figure 40. It was determined that superior uniformity in HTC is obtained in heat sinks with minimum hydraulic diameter, and rectangular microchannel provided the best heat transfer capability out of the shapes investigated in these studies.

However, few studies [111], [112] have reported that circular microchannels provide better thermal and hydraulic performance than other shapes. Dewan et al. [113] reported that flow disruption strategies such as modifying the shape of the channel, dimpled surfaces, pin-fins, ribs, cavities, groove structures, porous medium, etc., can minimize the disadvantage of rising pressure drop while providing efficient

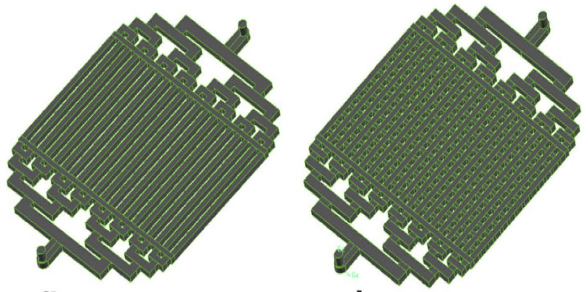

FIGURE 39. Proposed heat sink configurations for uniform temperature distribution [108].

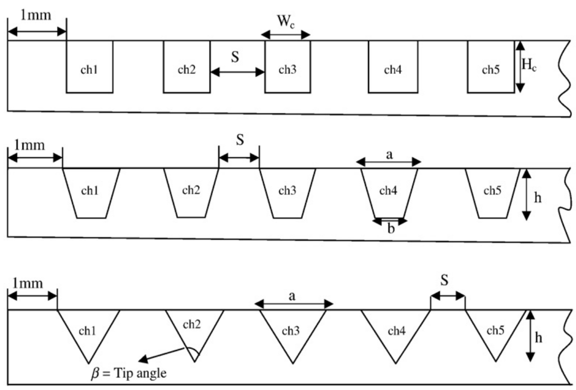

FIGURE 40. Schematic of microchannels with different shapes: Rectangular, trapezoidal, and triangular [110].

heat transfer. An efficient method using simulated annealing for improving microchannel surface roughness was proposed in [114]. The presented method can optimize the roughness of the wall for improved heat transfer while maintaining a specified constraint on the pressure drop. The effect of surface roughness on the heat transfer performance was also reported in [115]. Researchers have also explored the application of bionic structure to enhance microchannel performance, as shown in Figure 41 [116].

Bionic structures based on the wing arrangement of dragon louse [117] and shark skin [116] have demonstrated evidence of friction loss reduction. The inlet channel geometry also plays a crucial role in temperature distribution and hydraulic performance, according to studies conducted in [118] and [119]. The impact of manifold design on the hydrothermal performance of microchannels has been investigated in [120] and [121]. These studies have reported that optimizing manifold design facilitated uniform flow distribution and thus provided better thermal performance. Figure 42 shows different types of arrangements of these manifolds.

Numerous studies [122], [123], [124], [125] have investigated the effect of geometrical design on the heat transfer performance of microchannels. Some commonly used microchannel structures for enhancing heat transfer are depicted in Figure 43. Moreover, the insertion of metal

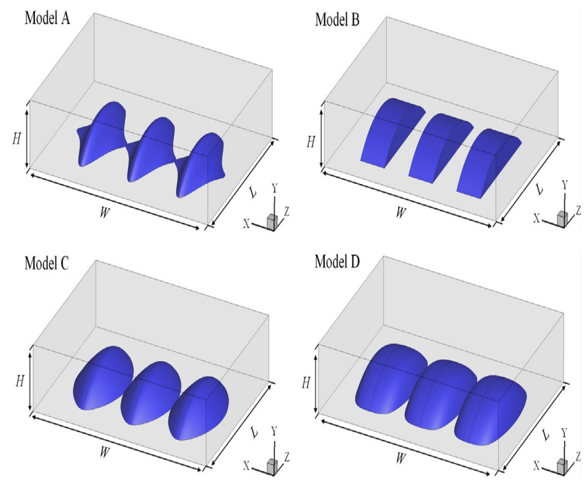

FIGURE 41. Microchannel heat sink design based on bionic structure [116].

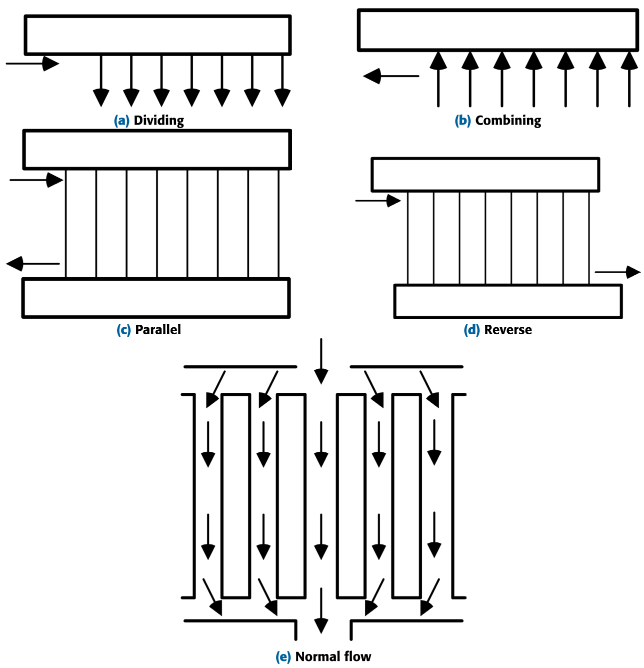

FIGURE 42. Different types of manifold layout [120].

foam [126], porous structure [127], and lattice structure [128] also showed desirable improvement in thermal performance.

3) EMPLOYING APPROPRIATE COOLANT

The use of nanofluids as coolant has garnered interest from researchers as well. Kumar et al. [132] used a hybrid nanofluid with 0.01 % concentration of Al_2O_3 and multi-walled carbon nanotube particles with various mixing ratios for improving the hydrothermal performance of mini channel heatsinks. The application of nanofluids for the performance improvement of microchannels has been investigated in [133], [134], [135], and [136]. It is experimentally demonstrated in [137] that the HTC of

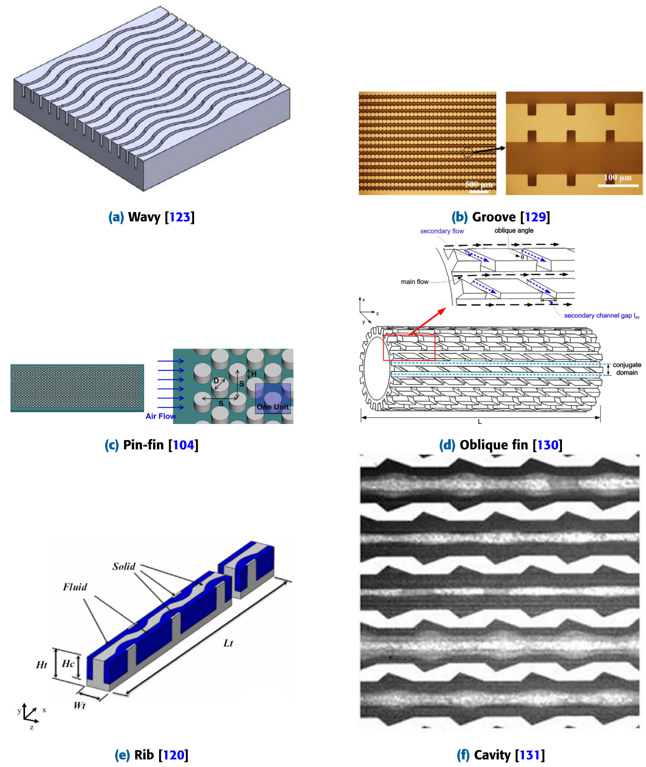

FIGURE 43. Commonly used structure in microchannel.

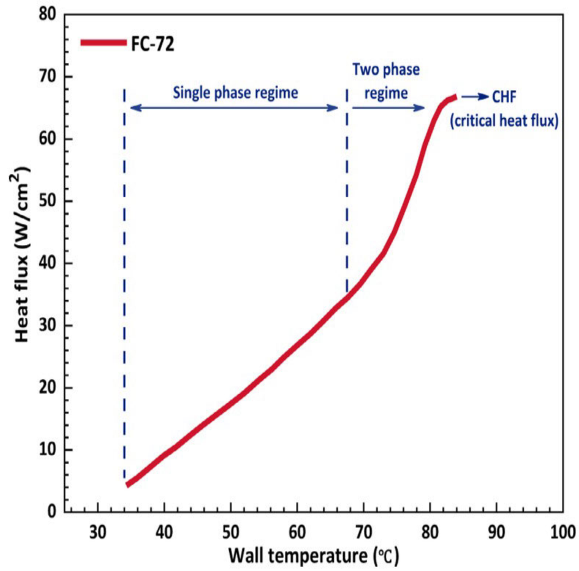

FIGURE 44. Typical spray cooling curve [153].

a microchannel increased by 73% when carbon-acetone nanofluid is used. The performance of single-walled and multi-walled carbon nanotubes with water and kerosene as base fluid was investigated in [138]. This study concluded that using single-walled carbon nanotubes increased Nusselt (Nu) number, and water as base fluid provided better hydrothermal performance. Researchers still need to find solutions for some challenges associated with nanofluids, such as erosion, corrosion, high cost, clogging, waste management, thermal conductivity, pressure drop, pumping power, etc. [139]. Liquid metals such as $Ga_{68}In_{20}Sn_{12}$ have also generated interest from researchers due to high thermal conductivity [140]. The thermal performance of mini channel heat sinks with four gallium alloys (EGaInSn, EGaIn, GaIn and GaSn) was investigated in [141], and it was determined that GaIn is the most suitable liquid metal coolant. Further studies about the suitability of liquid metal for channel cooling have been reported in [142] and [105]. Although compared to water and nanofluid, liquid metal provides better thermal performance, it also requires higher pumping power. Moreover it can be the source of corrosion, which necessitates further investigation regarding the choice of material and flow arrangement [82].

4) TWO PHASE COOLING

Further improvement in thermal performance can be achieved by replacing single-phase cooling with processes such as flow boiling that undergoes phase change while cooling [143], [144], [145]. Numerous techniques, such as channel modification and coolant alteration, have been suggested by researchers to improve the HTC while employing the flow boiling process. Raj et al. [146] proposed a stepped microchannel employing a flow boiling process, which resulted in a 98% improvement in HTC and 77% reduction in pressure drop compared to a rectangular microchannel. It also mitigated instability due to flow boiling. A method for reducing flow boiling instability and improving hydrothermal performance using inlet restrictors was presented in [147]. Furthermore, Ren et al. [148] proposed fabricating parallel microgrooves on the bottom surface of microchannels to enhance the flow boiling process. The impact of nanofluid on the flow boiling process was presented in [149] and [150] and provided no evidence of HTC improvement. Hence, the use of nanofluid for microchannel flow boiling requires further research. Moreover, further research is needed to improve the fabrication methods of microchannels and reduce manufacturing costs. Channel layout, microstructure positioning, and nanofluid application must be carefully studied to improve the heat transfer performance of microchannels.

B. SPRAY COOLING

One of the highly efficient approaches for thermal management is spray cooling, which has excellent heat dissipation capacity, increased cooling area, and provides more uniformly distributed heat removal [151], [152]. The spray cooling mechanism can be split into three segments with separate wall temperatures, as depicted in Figure 44.

The spray cooling curve is almost linear when the wall temperature is low, and the cooling fluid does not change its phase. Moreover, sufficient fluid supply prevents nucleation, and agitation of liquid due to droplet impact increases heat transfer performance. With the increase in wall temperature, the process enters two phase segment, and the slope of the curve increases. At this stage, the heater starts to dry out beyond the impact area of droplets. With further increases in wall temperature, the process enters the critical heat flux (CHF) stage when the heat supplied just offsets the heat removal capacity. Numerous performance-enhancing concepts for spray cooling have been discussed in literature, including the configuration and arrangement of nozzles, flow behavior, coolant properties, heating surface characteristics, and the effect of droplets on liquid film. Some characteristic parameters for analyzing spray cooling performance are CHF, surface and junction temperature, HTC, thermal resistance, and spray angle droplet diameter and velocity. Some well-known dimensionless parameters for determining spray cooling performance are Reynolds number(R_e), Weber number(W_e), capillary number(C_a), Ohnesorge number(O_h), Froude number(F_r), Nusselt number (N_u), and Prandtl number (P_r) expressed as follows [154], [155]:

$$R_e = \frac{U_0 D_0}{v} \tag{17}$$

$$W_e = \frac{\rho D_0 {U_0}^2}{\sigma} \tag{18}$$

$$C_a = \frac{W_e}{R_e} \tag{19}$$

$$O_h = \frac{\sqrt{W_e}}{R_e} \tag{20}$$

$$F_r = \frac{\rho g D_0}{\sigma} \tag{21}$$

$$N_u = \frac{h_{film} \dot{q}}{\lambda \Delta T} \tag{22}$$

$$P_r = \frac{v}{a} \tag{23}$$

Here, U_0 and D_0 are the impact velocity and drop diameter, respectively. ρ, σ, and v are the liquid's density, surface tension, and kinematic viscosity, respectively. $h_f ilm$, $\dot{q}$, λ, ΔT, and a represent the convective HTC, heat flux, thermal conductivity, and temperature difference between substrate and liquid, and thermal diffusivity, respectively. Several concepts for implementing spray cooling systems are reviewed in the next section.

1) HEATING SURFACE AUGMENTATION

The attributes of the heating surface play a crucial role in the performance of spray cooling-based concepts. Several researchers have studied the influence of surface roughness on spray cooling performance improvement [156], [157], [158], [159], [160]. Zhou et al. [161] studied the impact of surface modification on heat transfer enhancement of R410A based spray cooled scheme. The assessed surfaces included pyramid/square macrostructures and nano-porous surfaces with various pore structures, as depicted in Figure 45. It was concluded that even though pyramid fins showed a smaller rise in the wetted area, they provided superior CHF and HTC compared to square fins. Moreover, due to increased nucleation sites and wettability, nano-porous surfaces showed

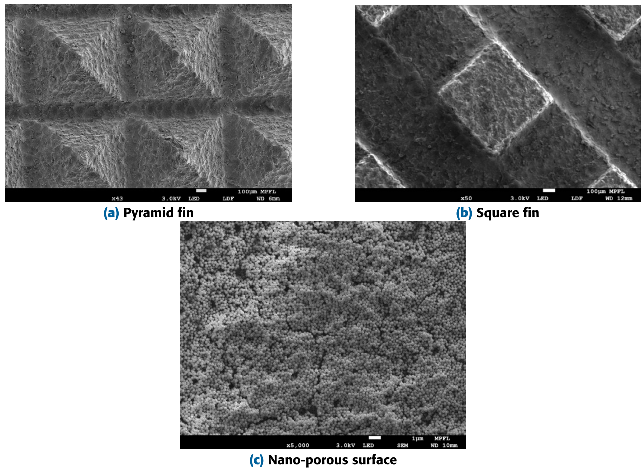

FIGURE 45. Scanning electron microscope (SEM) images of tested surfaces [161].

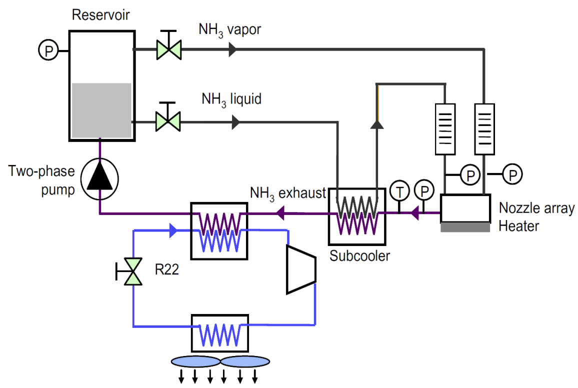

FIGURE 46. Spray cooling setup [162].

improved heat transfer performance. However, the CHF was lower than microstructures. Another experimental study by Bostanci et al. [162] reported that a multi-scale framework combining macro-scale protrusions and indentations with micro-scale structures with different pin fin shapes achieved high HTC. The experiments were carried out in a closed-loop system employing ammonia as the coolant, as shown in Figure 46. An experimental study carried out by Zhao et al. [163] reported that surface alignment (vertical, upward, and downward) has no significant impact on heat transfer effectiveness in single and two-phase regions. Additional investigation into the effects of surface structure on spray cooling was conducted in [164], [165], and [166].

2) ADJUSTING NOZZLE CHARACTERISTIC

Nozzle characteristics such as placement and structure, subcooling, surface heat flux, injection pressure, and nozzle-to-surface height, are important parameters that affect spray cooling performance [167]. Liu et al. [168] reported that as inlet pressure increases, the HTC rises gradually due to the accelerated atomization effect. However, power consumption also rises at an increased rate. Moreover, HTC has a

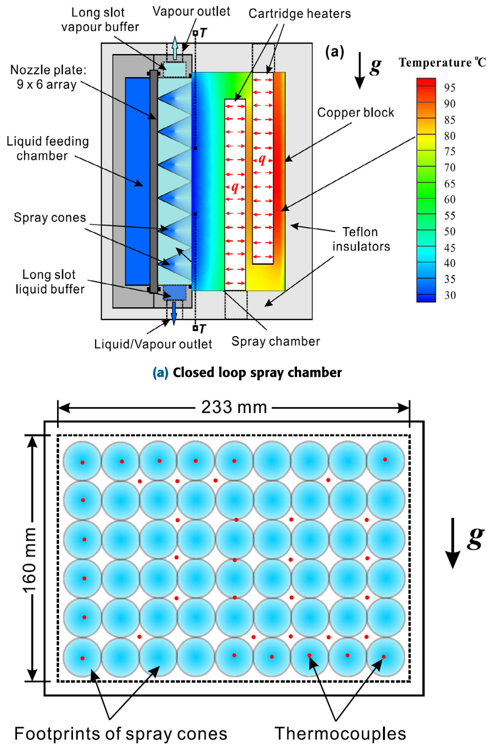

(a) Closed loop spray chamber

(b) Multi nozzle array

FIGURE 47. Schematic of multi nozzle spray chamber [171].

pressure-dependent ideal spray height at which it can be optimized. Similar studies were conducted in [169] and [170], which reported that higher injection pressure improves heat transfer effectiveness. Xie et al. [171] presented a closed-loop spray cooling system with 54 nozzles and R134a as the coolant to investigate cooling performance on high-power electronic devices with a big area. The arrangement of the designed spray chamber is depicted in Figure 47. The obtained results showed that increased nozzle pressure drop and flow rate improved the HTC and provided excellent uniformity in surface temperature. A compact spray cooling module with a micro nozzle applicable to high heat flux generating multi-heat source was presented in [172] and depicted in Figure 48. The experimental results showed that the heat flux could reach a maximum value of 304.7 W/m^2, and the maximum temperature difference was less than 6.5°C, which implied the suitability of this method in multi-heat source applications. A similar study was conducted in [173] that demonstrated increasing the nozzle number resulted in greater heat flux. However, an optimum number of nozzles must be selected considering manufacturing complexity and cost. Another study conducted by Zhang et al. [174] investigated the effect of spray flow rate, pressure, and inlet temperature on the performance of flash spray cooling. The obtained experimental results demonstrated that increased inlet temperature resulted in high HTC. Particle Image Velocimetry (PIV) was used in [175] to study the arrangement of flow patterns for various nozzle sprays. It was determined

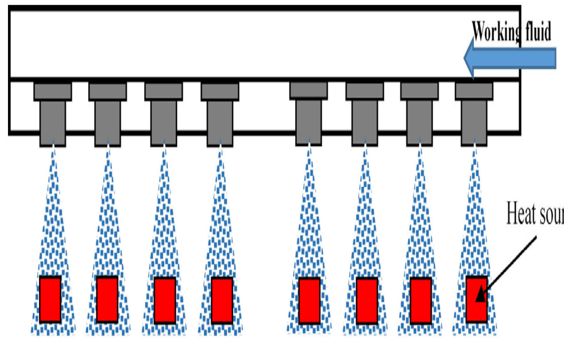

FIGURE 48. Proposed spray cooling module [172].

that with an increase in nozzle diameter, droplet velocity and outlet pressure decreased, which resulted in uniformly distributed droplet velocity and high HTC.

3) MODIFYING WORKING FLUID CHARACTERISTIC

Thermal characteristics of working fluid also affect the performance of spray cooling. Performance-enhancing ideas for spray cooling utilizing cooling fluids such as nanofluid [176], [177], alcoholic liquid [170], [178], and surfactants solution [179] have been investigated by researchers. Liu et al. [180] examined the cooling efficiency of alcohol-water mixtures and pure water and concluded that the addition of alcohols (n-propanol, iso-propanol, and ethanol) to water significantly improves heat dissipation due to increased wettability. Moreover, Chapman et al. [181] investigated electrospray (ES) phase change cooling for enhancing heat transfer from the target surface with methanol as the working fluid. Spray cooling is an exciting option for thermal management, but more research needs to be conducted to overcome the challenges and improve efficiency and reliability.

C. JET IMPINGEMENT COOLING

Jet impingement is a widely used cooling method for PEC, similar to the spray cooling process, excluding droplet atomization. The favorable features of the jet impingement method include improved temperature uniformity, lower thermal resistance, convenience for reducing hot spots, and higher local thermal absorption [82], [182]. Important characteristic parameters for analyzing the performance of jet impingement cooling are CHF, HTC, jet dimension, jet-to-wall distance, Reynolds number, Nusselt number, pressure drop, pressure coefficient, steady state temperature, outlet temperature, coolant flow rate, and pumping power. The equation for the pressure coefficient is as follows [183].

$$C_p = \frac{2P_x - P_{atm}}{\rho_f {u_{in,ave}}^2} \tag{24}$$

Here, P_x, P_{atm}, ρ_f, and ${u_{in,ave}}^2$ are the local pressure on the target surface, atmospheric pressure, cooling fluid density, and jet inlet velocity, respectively.

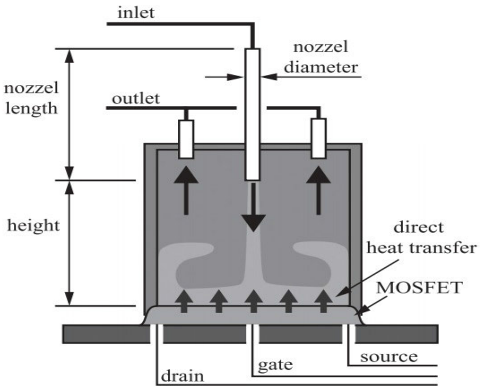

FIGURE 49. Proposed injection chamber for direct impingement cooling [184].

1) ADJUSTING NOZZLE ARRANGEMENT

Nozzle configurations such as nozzle diameter to surface ratio and single or multi-jet arrangement play an important role in jet impingement cooling. A method of liquid impingement cooling of a MOSFET module with a single micro water jet was proposed in [184]. This method was successful in removing hot spots and minimizing thermal resistance. Moreover, HTC increased with the increase in Reynolds number in the high flow regime (1000 < Re < 4000) and low flow regime (Re < 1000). The investigated injection chamber for the proposed method is depicted in Figure 49. An additively manufactured (AM) jet nozzle for cooling GaN transistors, with comparable cooling performance to jet nozzles manufactured from alternative materials, was presented in [185]. AM provides design flexibility and facilitates complex designs. Moreover, multiple components, such as the nozzle, flow distributor, and fluid delivery structure, can be combined in a single compact part. The schematic of AM nozzles working on a PCB is illustrated in Figure 50.

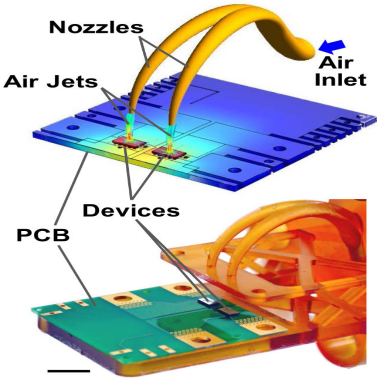

FIGURE 50. Additively manufactured jet nozzle working on GaN devices [185].

Tepe et al. [84] reported that prolonged jet holes improved the thermal performance of jet impingement systems with in-line array configuration. The obtained result demonstrated that decreasing the nozzle space to jet diameter ratio resulted in improved HTC on the target surface. Gao et al. [186] examined the effects of varying nozzle positions (changing spray height and/or tilting the nozzle) on a sputter-coated thin-film heater situated on a silicon wafer. Figure 51 shows different spray nozzle positioning. The authors reported that the height that provided the greatest rise in cooling was not the same as the height required to cover the target surface fully. Furthermore, increasing the flow rate led to a decrease in optimum nozzle height. Further studies conducted by Sabato et al. [187] and Wu et al. [188] reported that decreasing the nozzle diameter led to increased HTC. Many researchers have also studied the impact of arrays of two or more jet nozzles on the cooling performance. The introduction of multiple jets allows sprayed liquid to cover a bigger surface, improving heat transfer capacity. Nadda et al. [189] and Wei et al. [190] reported that increasing the number of jet nozzles provided better thermal performance than a single jet system. The image of the jet cooler and the cross-sectional view presented in [190] is depicted in Figure 52.

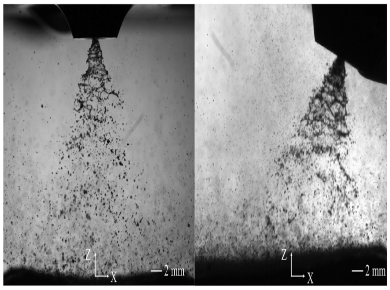

FIGURE 51. Normal and inclined impact of spray cooling [186].

San et al. [191] investigated the Nusselt number variation for an array of five circular air jets with one jet in the center and the other four arranged in a square around the middle one. They reported that the proportion of jet-to-jet distance to jet diameter influences the non-uniformity of heat transfer. Singh et al. [192] reported that the thermal performance of a square channel with aluminum metal foam can be increased by 6 - 10% using an array (5 × 5) of impingement jets. Godi et al. [193] investigated the heat transfer performance of three-dimensional wall jets coming from a series of circular nozzle outlets over a flat surface. They reported that a reduced number of jets provided better performance for a specific diameter compared to closely situated jets when the mass flow rate was fixed.

2) MODIFYING WORKING FLUID CHARACTERISTICS

The nature of working fluid plays a crucial role in jet impingement cooling performance. The use of molten salt as the cooling fluid was investigated by Gao et al. [194]. This study reported favorable thermal behavior of molten salt comparable to water at stagnation area, but the Nusselt number decreased more quickly compared to water at radial

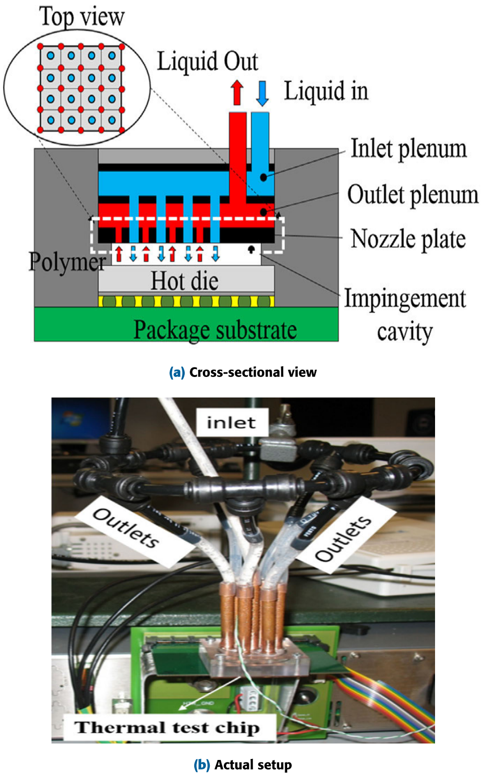

(a) Cross-sectional view

(b) Actual setup

FIGURE 52. Proposed jet cooler [190].

flow. The addition of paraffin in particulate form (nano PCM) to water was suggested by Wu et al. [195] to improve the HTC of jet impingement. Moreover, Rehman et al. [196] showed that adding PCM slurry and nanofluid improves heat transfer capacity but increases the pressure drop. Employing PCM exclusively resulted in reduced pressure drop compared to employing nanofluid only. The impact of the shape of nanoparticles on jet cooling was reported by Selimefendigil et al. [197] and Ekiciler et al. [198]. Naphon et al. [199] reported that the addition of T_iO_2 nanofluids (at 15% concentration) with water in a jet impingement system enhanced the convective heat transfer by 18.56%. Moreover, the HTC increased when the nozzle-to-surface ratio decreased. Amjadian et al. [200] conducted experiments investigating the effect of Cu_2O nanofluid-based jet impingement intended for cooling an aluminum disk. Obtained results show that compared to base fluid, there is a 45% increase in heat transfer while using nanofluid 0.07 wt% concentration. Further studies on nanofluids include investigating the effect of Ag/ZnO hybrid nanofluid on heated copper surface [201], achieving maximum heat transfer using Al_2O_3/water nanofluid [202], cooling a flat plate using a combination of Al_2O_3 and MgO nanoparticles [203], and investigating a numerical model of impingement jet with boehmite alumina nanofluid in water and ethylene glycol mixture [204]. Moreover, Wu et al. [205] investigated the effect of HFE7100 dielectric liquid used with a PCM material for jet impingement cooling and reported significant improvement in heat transfer compared to water.

3) SURFACE CHARACTERISTIC AUGMENTATION

Recently, researchers have also studied the impact of surface material and characteristics on jet impingement technique. Bhansali et al. [206] investigated the effect of pin-fin structure on a rotating surface and reported that the average Nusselt number considerably improved compared to a surface with no pin-fins. The maximum improvement was determined to be 3.9 times more than a plain surface with a Reynolds number of 5000. Wiriyasart et al. [207] studied heat spreading of heat sinks with circular, rectangular, and conical fin shapes while applying jet impingement cooling. The results indicated circular fins provide better thermal performance by reducing the thermal resistance by 25% and 12% compared to conical and rectangular fins, respectively. Another study on pin fin shape conducted by Ravanji et al. [208] reported favorable thermal performance of elliptical pin-fins on a concave surface. Further analysis of the impact of pin-fin structure on impingement cooling was conducted in [190] and [209]. Zhang et al. [210] conducted an experiment on the performance of an impingement jet on a protruded surface and reported heat transfer enhancement compared to a smooth surface. Moreover, the Nusselt number increased with an increase in protrusion depth. Investigation of air impingement system on a curved surface [211] and rough surface [212] reported the impact of surface curvature and roughness on the cooling performance. Further information on impingement cooling can be found in review articles published by Plant et al. [213] and Ekkad et al. [214]. So, jet impingement is also an exciting option for power electronics cooling due to its great heat transfer performance and ease of application.

D. IMMERSION COOLING

Immersion cooling is a promising thermal management technique that requires dielectric fluid or coolant with excellent heat conduction and poor electrical conductivity. In this approach, the heated device is submerged in coolant. Some commonly used coolants for this cooling approach are ethanol, water-ethylene glycol, mineral oil, novec 649 and 7000, FC 3283, 43, and 72. Data centers [215], servers [216], EV battery thermal management [217], power transformers [296], and solar PV [218] are some common application areas for immersion cooling.

A modified cooling method blending spray cooling and immersed cooling is proposed by Wang et al. [83], which resulted in a maximum 65.6% increase in heat flux compared to regular spray cooling with a surface temperature of 205°C. The enhanced performance is attributed to vapor layer removal and the chaotic effect surrounding the surface. The experimental setup for this study is depicted in Figure 53. This setup contains an ejector for controlling the fluid level in the cooling compartment.

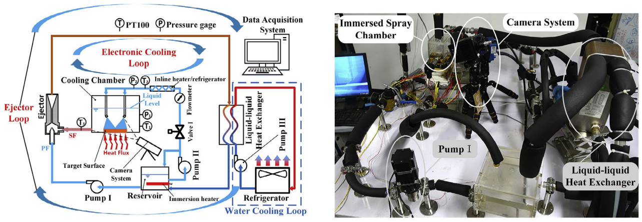

(a) Schematic view (b) Actual view

FIGURE 53. Proposed immersed spray cooling system [83].

It was reported by Patil et al. [219] that immersion cooling with dielectric coolant improved cooling performance with a 46.3% reduction in temperature compared to conventional natural cooling. Approaches for using immersion cooling with water have also been proposed in literature [220]. Figure 54 depicts an immersion cooling system from [220] where the PCB is insulated from water by Parylene C coatings. This cooling system was effectively tested on a 2 kW PEC with 97.2% efficiency.

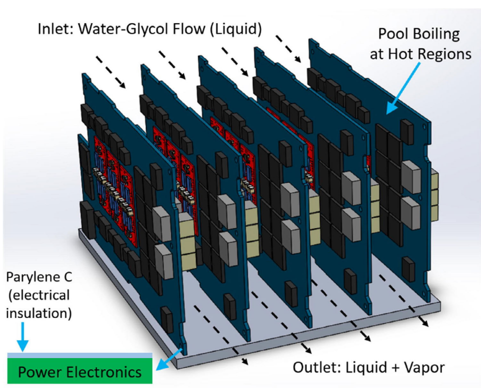

FIGURE 54. Schematic diagram of power electronics cooling with immersion technique [220].

Kuncoro et al. [221] applied the Taguchi method to determine the factors influencing cooling performance with mineral oil. It was reported that the decrease in CPU temperature and electric power was significantly affected by the cooling fan arrangement, with contribution reaching over 70%. Further performance-enhancing ideas using heat spreaders [222], ethanol phase-change coolant [223], and nanofluid [224] have been reported in literature. Hsu et al. [225] applied three array structures (Si nanowire (SiNW), Si micropillar (SiMP), and Si nanowires on a Si micropillar (SiNW/MP)) to improve the cooling performance of Novec 649. They reported SiNW/MP is the most effective surface for immersion cooling with CHF and HTC enhancement of 30% and 455%, respectively, compared to plain SiO_2 surface.

E. PCM BASED COOLING

Thermal management involving PCM includes materials that can absorb or release heat via the phase transition process within a particular temperature setting [226], [227]. Solid-to-liquid and liquid-to-gas are the commonly employed phase-changing processes. One major advantage of PCM is that when there is cyclic fluctuation in heating power, it can absorb and release heat when the power is at peak and minimum, respectively. Moreover, it provides a high density of heat storage due to the high latent heat of fusion. The major shortcoming of PCM is very low thermal conductivity. PCM is usually combined with another cooling mechanism, such as a pin-fin heat sink, heat pipe, and TE module. A significant number of studies have been conducted to enhance PCM performance. Typical parameters for evaluating the performance of PCM-based cooling include melting fraction, phase change time, heat source temperature, operation time, input power, solid insert efficiency, filling ratio, total thermal resistance, condenser/evaporator temperature and stored energy. The thermal resistances are calculated using the following equations [179].

$$R_{th,e} = \frac{T_e - t_a}{p_h} \tag{25}$$

$$R_{th,c} = \frac{T_a - T_c}{P_h} \tag{26}$$

$$R_{th,t} = R_{th,e} + R_{th,c} \tag{27}$$

Here, P_h is the heat load, and T_a, T_e, and T_c represent the temperature at the adiabatic section, evaporator, and condenser. The heat transfer capacity can be calculated using the following equation [182].

$$Q_{capacity} = \frac{Q_{transferred}}{Q_{input}} \tag{28}$$

The following section reviews several thermal management techniques using PCM.

1) IMPROVING PCM THERMAL CHARACTERISTICS

Yang et al. [228] investigated a new PCM named low melting point metal (LMPM), which was applied to a finned heat sink. The obtained results show LMPM has high thermal conductivity and good latent heat properties. Another study conducted by Krishna et al. [229] compared Water, Tricosane, and nano-enhanced Tricosane and reported that nano-enhanced PCM can improve thermal conductivity by 32% compared to pure Triscosane. Farzanehnia et al. [230] conducted experiments on the thermal performance of nano PCM on an electronic chipset. Paraffin wax was used as PCM in this study and was combined with multiwall carbon nanotubes (MWCNT) for improved performance. Experimental results showed that nano-PCM reduces the cooling time by 6% compared to regular PCM. Some common materials employed for improving PCM performance are shown in Figure 55.

2) COMBINING PCM WITH HEAT SINKS

PCM can be combined with pin-fin heat sinks for performance improvement. Some commonly used pin-fin structure found in literature is depicted in Figure 56.

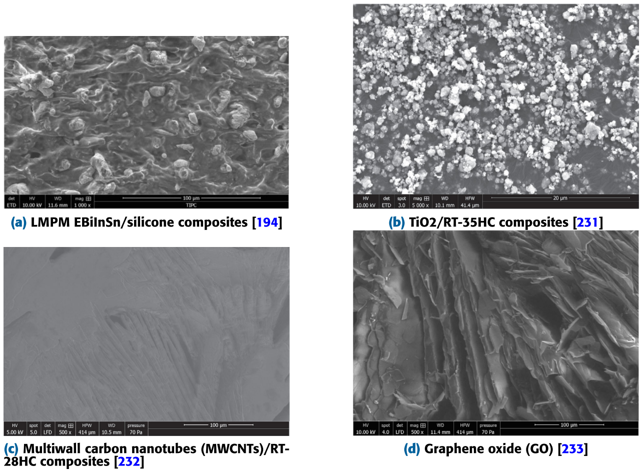
(a) LMPM EBiInSn/silicone composites [194]
(b) TiO2/RT-35HC composites [231]
(c) Multiwall carbon nanotubes (MWCNTs)/RT-28HC composites [232]
(d) Graphene oxide (GO) [233]

FIGURE 55. Microstructural features of different PCM materials.

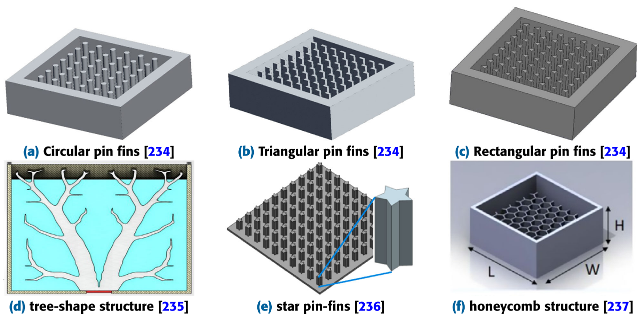
(a) Circular pin fins [234]
(b) Triangular pin fins [234]
(c) Rectangular pin fins [234]
(d) tree-shape structure [235]
(e) star pin-fins [236]
(f) honeycomb structure [237]

FIGURE 56. Commonly used pin-fin structure.

Desai et al. [96] developed multiple pin fin shapes (circular, rectangular, pyramid, and triangular) for PCM and reported that the triangular structure provided optimum cooling. Another study by Bondareva et al. [238] reported that the heat transfer rate decreases when the width of the PCM-based pin-fin is increased. However, increasing the pin-fin length beyond the limit would decrease the energy storage capacity of the heat sink. So, the pin-fin parameter must be designed appropriately. Other studies also reported that pin-fin parameters might affect the PCM-based heat sinks performance both positively (improved thermal conductivity) and negatively (reduced phase change enthalpy) [239], [240].

3) COMBINING PCM WITH OTHER COOLING METHODS

PCM can also be combined with a TE cooler, heat pipe, and vapor chamber for performance improvement. Krishna et al. [229] observed a 25.75% decrease in the temperature of the heat pipe evaporator when PCM is added. Another favorable result was presented in [241] where it was reported that 86.7% contribution of the cooling performance can be expected from PCM in a PCM-heat pipe arrangement.

IV. DISCUSSION, CHALLENGES AND FUTURE WORK

A. MULTILEVEL INVERTER FRAMEWORK

Several multilevel converters (MLC) topologies have been presented in literature to improve the power rating, thermal performance, reliability, efficiency and THD of PECs. Some of the Traditional MLC configurations discussed in literature are neutral point clamped (NPC), active neutral point clamped (ANPC), flying capacitor converter (FCC), cascaded H-bridge (CHB), and modular multilevel converters (MMC). 3-level NPC converters have widespread application in high power and high voltage applications such as motor drives and renewable energy conversion. However, increasing the number of levels in NPC configuration results in many clamping diodes and increased unbalanced loss distribution. The authors in [41], [52], and [242] have presented approaches for thermal management of 3-level NPC converters in EV and wind power applications. A four-level ANPC converter with switching cell arrays is presented in [243] that achieves thermal management utilizing the available redundancies in the converter configuration. However, the control algorithm becomes more complex, and the overall cost increases due to the increased number of PSDs. FCCs are suitable for high-level applications, although system reliability might be decreased due to the presence of many flying capacitors. The thermal design of a Sic-based FCC is presented in [244] that achieves optimal thermal performance. CHBs and MMCs have modular structures and good fault-tolerant capabilities. However, they require numerous capacitors and have reduced power density. The authors in [74], [76], and [77] have discussed thermal management techniques for CHB-based smart transformers. Moreover, references [63], [64], and [65] have presented thermal management techniques for MMCs. Recently, hybrid MLC topologies such as T-type NPC [245], stacked multicell (SM) converter [246], hybrid CHB (HCHB) [247], switched series/parallel sources (SSPS) based MLC [248], nest NPC (NNPC) [249] have been developed for industrial applications. A summary of commonly used MLC configurations along with their advantages, disadvantages and applications are summarized in Table 2.

B. THERMAL MANAGEMENT DURING FAULT CONDITION

Methods for employing thermal management under fault conditions must also be investigated to enhance the reliability of PECs. The influence of various grid faults such as single-phase, two-phase connected and three-phase grounded faults on the thermal behavior of a 3-level NPC converter is investigated in [251]. The authors reported that single-phase and two-phase connected faults lead to uneven thermal loading in the three phases. However, for three-phase grounded faults, the thermal loading pattern in the three phases is the same. Furthermore, during fault conditions, the junction temperature of some specific power devices will be higher than the junction temperature of the power device with the highest thermal stress during regular operation. The thermal performance of an MMC with ATC during single line to ground fault is presented in [252]. A foster-based thermal model of the MMC has been developed in this study to establish a proportional relationship between

TABLE 2. Summary of multilevel converter performance [31], [247], [250].

Topology	Advantages	Disadvantages	Applications
NPC	* Simple structure * Fault tolerance capability * Superior dynamic response * Lower number of required DC sources * Uniform blocking voltage in switches * Cost effective in three-level configuration	* Uneven distribution of power loss * Limited to three-level configuration * Higher voltage level leads to an increase in the number of clamping diodes * Higher number of diodes results in low reliability	* Static VAR compensation (SVC) * Variable speed motor drives * High voltage system interconnections
ANPC	* Simple structure * Uniform distribution of losses across switches * Satisfactory dynamic response * Floating capacitor not required for three-level structure	* Floating capacitor required for structures higher than three-level * Complexity in control circuit * Requirement of switches of different voltage ratings for high voltage applications	* Motor drives * Solar inverters
FCC	* Modular structure * Good fault tolerance capability * Balanced loss distribution * Lower number of required DC sources * No requirement of clamping diodes * Availability of redundant states	* Higher voltage level leads to an increase in the number of clamping diodes * Increased cost due to increased number of capacitors * Reduced reliability due to high number of flying capacitors * Complexity in voltage balancing * Presence of ripple at low switching frequencies	* Static VAR generation * AC motor drives * Active filters * Switched converters
CHB	* Modular and simple structure * Higher reliability * No requirement of floating capacitors or clamping diodes * Fault tolerant capability * Simple control circuit * Reduced current harmonics * Low requirement of output filter	* Requirement of multiple DC voltage sources * Requirement of numerous DC link voltage regulators * Implementation is expensive * Greater number of power switches is required * Comparatively lower level of output voltage	* Motor drives * Power factor compensators * Flexible alternating current transmission system (FACTS)
MMC	* Modular structure * Good fault tolerance capability * Voltage scalability by cascading cells * Fault tolerant capability * No requirement for filters * High reliability and efficiency * Negligible losses * Low switching frequency	* Complex control circuit needed for capacitor voltage balancing (CVB) and circulating current suppression (CCS) * Requirement of complex data collection and communication system * Large number of power electronic interfaces is required * Greater number of capacitors is required	* Motor drives * Electric vehicles * FACTS * HVDC systems * Active power filters

MMC DC current and thermal imbalance in the submodules. Afterward, an ATC technique based on the neutral-point-shift (NPS) method is proposed to reshape the MMC AC voltage to balance the MMC DC current. This causes a balanced thermal stress distribution among the three phases. Another NPS-based approach for thermal management of a half-bridge-based MMC during unbalanced grid conditions is investigated in [253]. The MMC under consideration in this study is depicted in Figure 57. Here, every phase of the MMC has two arms, each consisting of an arm inductor, S number of active submodules, and R number of redundant submodules. The surplus submodules and the NPS are employed to achieve thermal management.

Deng et al. [254] proposed a variable frequency (VF) based control strategy for balancing the temperature among the three phases of an MMC during unbalanced grid voltages. Each phase of an MMC experiences unbalanced arm currents due to unbalanced voltages, which result in unequal temperature distribution and power losses. The VF strategy adjusts the carrier frequency of each phase to regulate the temperature distribution. The proposed VF control for phase

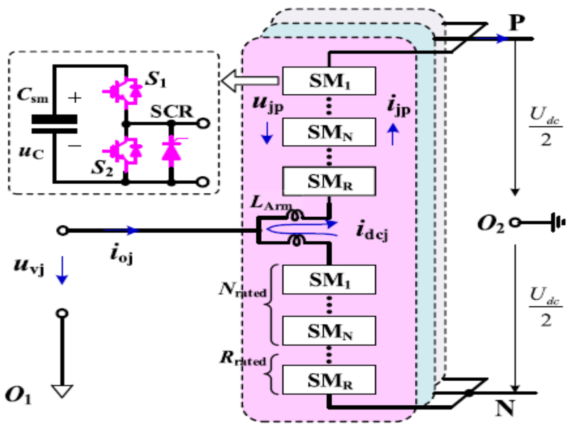

FIGURE 57. MMC circuit configuration [253].

a is depicted in Figure 58. Here, the PI controller regulates the carrier frequency f_{w_a} by generating a compensating frequency f_a. If the average temperature is greater than the reference temperature, then the PI controller reduces the

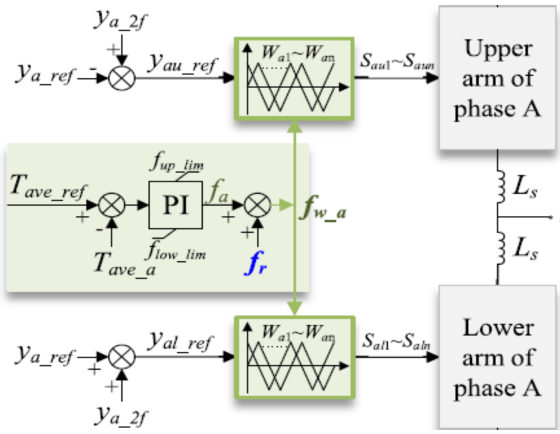

FIGURE 58. Proposed VF control for a single phase [254].

compensating component f_a, and the opposite happens if the average temperature becomes lesser than the reference value.

A space vector modulation (SVM) based ATC approach is presented in [242] that optimizes the thermal performance of a 3-level Neutral point clamped (NPC) connected wind turbine under low voltage ride through (LVRT) conditions. The space vector diagram for the converter is shown in Figure 59. There is switching redundancy for all state vectors at the inner part of sector 1, which is exploited to generate a suitable modulation sequence for reducing conduction losses in the semiconductor device. This reduces the junction temperature of the devices under thermal stress, as shown in Figure 60.

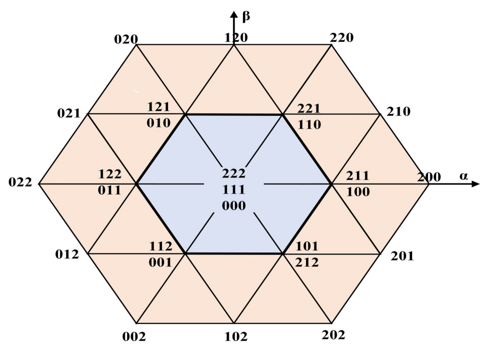

FIGURE 59. Space vector diagram for 3-level NPC converter.

Another thermal management technique focusing on the fault-resilient design of an integrated gate-commutated thyristor (IGCT) based 3-level NPC converter is discussed in [255]. The results showed that through the optimized design of busbars and temperature regulation, the IGCTs could withstand converter shoot-through situations even if there is a failure in the circuit breakers. This is achieved by adding extra resilience impedance to the NPC's clamping diodes that ensures the diodes will reach the thermal limit before the IGCTs.

The authors in [256] presented a model-based technique for fault detection and diagnosis of the TMS of the central

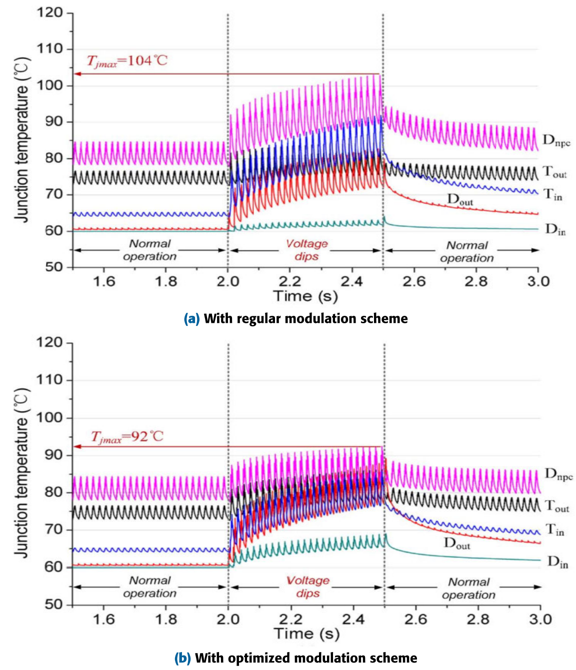

FIGURE 60. Junction temperature reduction of 3-level NPC [242].

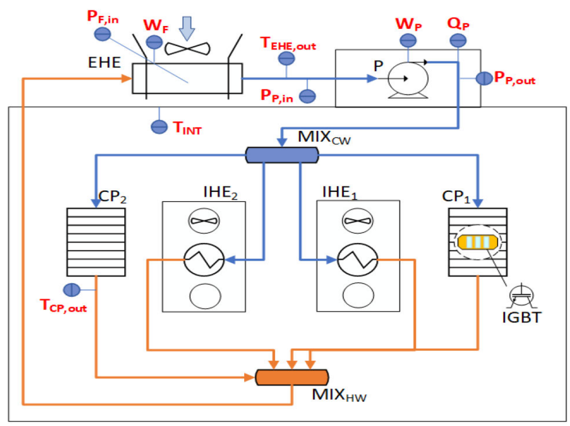

FIGURE 61. PV central inverter TMS [256].

inverter in a PV system. The investigated TMS is based on liquid cooling and includes cold plates (CP), internal and external heat exchangers (HE), recirculating pump (P), and water collectors (WC), as shown in Figure 61. Fault tree analysis (FTA) was applied to identify the faults occurring in any of the components of the TMS. Faults in the heat exchanger were identified as the most impactful as they resulted in a 7.5% rise in the junction temperature of the investigated IGBTs.

C. IMPACT OF AMBIENT ENVIRONMENT ON PEC THERMAL MANAGEMENT

The ambient environment significantly influences the thermal management of PECs, and overlooking certain considerations related to environmental adaptability can lead to severe performance issues and reduced reliability. Some key factors to consider are temperature variations, humidity and moisture, dust and contaminants, corrosive atmospheres and solar radiation.

Temperature variations in the ambient environment affect the cooling efficiency of TMSs employed in PECs. High temperatures can reduce the converter's overall efficiency and lifespan. So, the PECs must be designed in a way that operates within specified temperature ranges, and advanced thermal management techniques, such as liquid cooling or heat sinks, must be applied to dissipate heat effectively. Wang et al. [257] proposed an innovative thermal modeling method for power electronic components, addressing the shortcomings of existing analytical methods that depend on steady ambient temperatures. This method takes into account the thermal dynamics caused by variations in ambient temperature and self-heating before calculating the thermal coefficients based on frequency-domain modeling. The accuracy of the model was validated by experimental results obtained after considering a 10°C variation in local ambient temperature caused by both the environment and loading profile. Figure 62 shows the obtained results from this study, demonstrating the proposed method's accuracy.

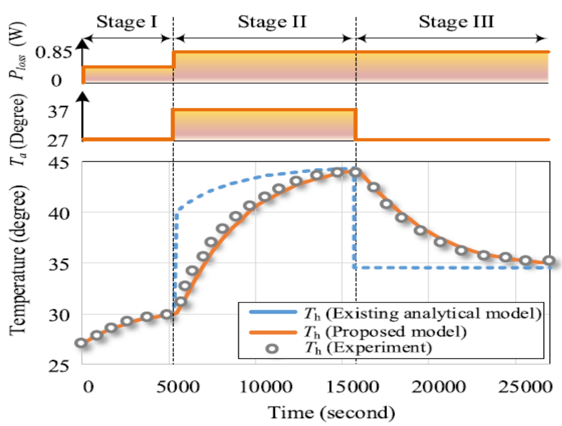

FIGURE 62. Comparison of hot-spot temperature between the proposed and existing thermal model [257].

Wei et al. [258] proposed another thermal modeling approach considering convection thermal coupling for accurately estimating the junction temperature under varying ambient temperatures. This study developed a FEM-based model for establishing a relationship between junction temperature and variation in ambient temperature. This relationship can be utilized to gain a better understanding of the influence of the environment on junction temperature variations and assist in developing improved TMS for converters.

Another key environmental parameter that influences the PECs is humidity, which can lead to electrical leakage, corrosion and insulation breakdown in power electronic components. Therefore, TMSs must include sufficient protective measures to safeguard the converter against moisture and ensure the system accounts for potential condensation. Hazardous condensation may occur in offshore wind power converters equipped with water cooling due to a rapid drop in active power production. Zhang et al. [259] addressed this issue by proposing an ATC-based anti-condensation technique that keeps the temperature of potential cold spots in a 3-MW real-scale wind power converter above the dew point. The proposed method employs the reactive circulating current control strategy inherent in parallel PECs to develop the anti-condensation technique. Moreover, Yu et al. [260] investigated the influence of relative humidity on the reliability of wind power converters and proposed a reliability evaluation framework to identify the effect of relative humidity on the reliability evaluation of these converters.

Accumulation of dust and contaminants on the converter surfaces can also hinder heat dissipation and reduce the efficiency of the TMS. Regular maintenance and cleaning protocols should be implemented to address this issue. Furthermore, the thermal design of enclosures for outdoor power electronics becomes challenging due to the need to isolate the system from moisture, dust, and other environmental contaminants. Owens et al. [261] proposed the design of a breathable enclosure using computational fluid dynamics (CFD) for the thermal management of outdoor power electronics. The study revealed that certain water-resistant textiles used in sportswear possess sufficient air permeability to offer major cooling benefits when combined with internal fans. Also, typically used membrane materials such as polytetrafluoroethylene (PTFE) do not provide substantial cooling advantage due to being too air-impermeable.

Altitude also affects TMS performance as higher altitude leads to lower air density, which influences the cooling efficiency and thermal performance of the converter. The cooling mechanism must be adaptable to compensate for reduced heat dissipation efficiency. In [262] an investigation on the impact of altitude on forced air convective cooling in high-power electronics used in MEA was conducted. To investigate this, the convective HTC at altitudes ranging from 0 to 52,000 feet above sea level, with a constant room temperature of 24°C, was measured and the test results indicated that the Nusselt number and pressure loss coefficient remain independent of altitude. This finding would facilitate the optimization of thermal management solutions for flight control systems. Chang et al. [263] proposed a TMS for a 200-kW high-density inverter used in MEA which is designed for an altitude of 25,000 feet. In high altitudes, it is challenging to cool power devices with high heat flux using air cooling methods. So, a liquid cooling method using a microchannel was proposed, which has a high cooling capacity in addition to low cost and weight. Moreover, this study also addressed the issue of localized hotspot generation in areas such as busbars, gate-driver boards, and terminals of the drive system when operating in high altitudes. The proposed solution to this issue involved adding a localized forced cooling air duct with optimized internal and external airflow that reduced the hotspot temperature by 37%. The air ducts minimized the effect of hotspots without adding extra weight to the system. Moreover, it was demonstrated that the hotspot temperature of the inverter inside a sealed enclosure can be maintained below 130°C with an ambient temperature of 75°C and at an altitude of 7620 m. Another study conducted by Elsayed et al. [264] assessed the thermal performance of an air-cooling-based TMS operating across various altitudes ranging from sea level to 12,000m. The cooling mechanism included a parallel plate-fin heat sink (PPFHS) with a guide plate for optimizing performance at high altitudes. Performance analysis carried out using ANSYS indicated that heat sink configuration without any guide plate is not suitable for high altitude operation. Figure 63 shows the heat sink design with the guide plate.

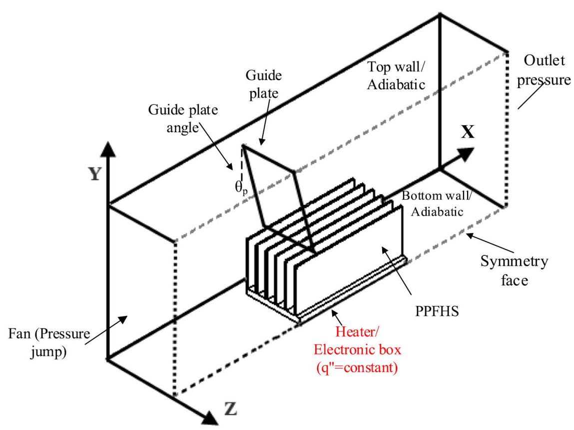

FIGURE 63. **Heat sink with guide plate [264].**

Li et al. [265] addressed the challenges of electronic cooling at high altitudes, revealing that solar radiation can cause a temperature deviation of 4.1°C for electronic devices operating at 20 km altitude. To mitigate this issue, an optimized heat sink design validated by a 3D model was proposed. The consideration of solar radiation in heat sink design led to a change in the heat transfer area ratio that ultimately resulted in a 5.7% increase in heat sink weight. Considering these environmental factors, incorporating robust design strategies for thermal management is crucial for ensuring the long-term reliability and performance of PECs in diverse operating conditions. It is essential to conduct thorough environmental testing and analysis during the design phase to identify and address potential issues proactively.

D. IMPACT OF HARSH ENVIRONMENT ON PEC THERMAL MANAGEMENT

Operating converters in harsh conditions, especially under extreme temperatures and high humidity, presents several challenges. PECs in electric aircraft function within challenging conditions with temperature fluctuations ranging from -55°C to -70°C [266]. Considering this challenging environment, forced liquid cooling continues to be the preferred choice in PECs designed for electrified transportation [267]. In high altitude applications, convective thermal resistance ($R_{th,conv}$) between a heat sink and its enclosure decreases due to decreased air density caused by a harsh environment [263]. So, the thermal model for such applications needs to be adjusted accordingly.

The high voltage high-power PECs used in EVs face a harsh environment due to the strict operating conditions [268]. The onboard cooling systems face significant challenges due to increased power density, high ambient temperature under the hood and high humidity. Moreover, sudden acceleration and deceleration lead to significant power cycling. To address these issues, advanced cooling techniques for EV converters have been presented in [41], [48], and [269].

Moreover, considering power converters in PV and wind systems are consistently subjected to harsh environments, it is essential to address this issue in TMSs to improve reliability [270]. Several thermal management techniques have been discussed for PV inverter thermal management [36], [256], [271] and wind converter thermal management [49], [259], [272].

Peng et al. [273] proposed a thermal management method to ensure the safe operation of high-power electronics in logging tools that are employed in high-temperature downhole environments for detecting underground oil and gas resources. This method integrates a heat sink, a heat storage module, and heat pipes within Phase Change Materials (PCMs). It was shown experimentally that the temperature of the electronic component can be maintained below 125°C, which significantly reduces thermal failures of high-power downhole electronic equipment.

E. THERMAL MANAGEMENT INTERACTION WITH CRITICAL CONVERTER FEATURE

ATC methods affect the power quality and harmonic performance of the PECs. Ozkan et al. [51] proposed an MPC-based ATC method for the PECs of a ship power system and discussed the tradeoff between thermal and electrical performance. Improving the thermal performance resulted in high THD, which can be mitigated by assigning an appropriate weighting factor to the MPC cost function. The impact of power routing-based ATC on the THD performance was discussed in [30]. The operation of modular converters becomes unbalanced due to the application of power routing, which results in high harmonic distortion. The harmonic performance can be improved by employing novel modulation techniques such as variable angle phase-shifted pulse-width modulation (PS-PWM). An ATC method for wind converters was presented in [272] that maintained the THD below 5%. Moreover, this study reported that a 1% increase in THD resulted in a 0.144-year increase in the lifetime of the IGBT modules in a wind power converter. Another ATC technique employing hybrid switching frequency is proposed in [274]

TABLE 3. Suggested cooling methods for thermal management of PECs.

Cooling method	Converter Configuration	Thermal management approach	Application	References
ATC	Interleaved DC/DC	Power routing	Wind power generation	[67] [68]
ATC	CHB	Power routing	Smart transformer	[75] [76] [277]
ATC	DAB	Power routing	More electric aircraft	[70] [71]
ATC	2-L Inverter	Gate driver parameter control	Solar power generation	[36]
ATC	3-L NPC inverter	Modified modulation	Wind power generation	[49] [54] [242]
ATC	2-L Inverter	Loss manipulation	Electric vehicle	[48] [43]
ATC	MMC	Balancing thermal stress	HVDC	[63] [64]
ATC	3-L NPC inverter	Optimized modulation	Electric vehicle	[278] [279]
Liquid cooling	3-L T-type propulsion inverter	Microchannel based cooling	More electric aircraft	[263]
Liquid cooling	PEBB	Cold plate	Ship power system	[280] [281]
Liquid cooling	3-L NPC inverter	Cold plate	Electric vehicle	[41]
Liquid cooling	Central inverter	Cold plate	Solar power generation	[256]
Air cooling	PEBB	Channel based heatsink	Ship power system	[282]

that improves the THD of line current in a 3-level NPC converter. Further ATC strategies that ensure optimum THD performance are presented in [242], [275], and [276].

F. SELECTION OF COOLING METHOD

The suggested area of application of some of the discussed thermal management methods is summarized in Table 3.

G. ECONOMIC ANALYSIS

The application of ATC gives rise to notable concern regarding the reliability of the PECs and their corresponding maintenance costs. These costs can be reduced through monitoring and controlling the lifespan of PSDs. Tackling these challenges requires a deep understanding of semiconductor physics, efficient management of electrical variables, and the creation of optimal maintenance plans and schedules. An optimized ATC method offers notable advantages. Firstly, it permits narrower safety margins, resulting in improved reliability, availability, and generally cooler systems. Secondly, it minimizes expenses occurring from unscheduled maintenance, which is a critical consideration as operational demands rise and financial resources become constrained. Hence, developing a cost-effective ATC method that incorporates the state of health (SOH) and degradation of power converters is beneficial for optimizing maintenance costs. Several literature have emphasized the cost reduction associated with ATC methods [30], [283] and power routing-based ATC was suggested for minimizing maintenance costs with minimal additional initial expenses [66], [67], [69].

Air-cooled systems are cost-effective but constrained by ambient temperature and low cooling capacity. On the other hand, liquid cooling, although more efficient, requires increased maintenance efforts and higher initial costs. A thorough investigation comparing air and liquid-cooled systems for automotive inverters was presented in [284]. The study concluded that liquid cooling is more suitable for automotive applications and justified the cost of implementation. Moreover, the cost analysis must also consider the associated manufacturing costs for the design procedure of heat sinks and cold plates. An optimized design of a cost-effective and environmentally friendly heat sink for PCM-based cooling was presented in [285]. The authors in [286] investigated a PCM-based heat sink with partially filled copper foam that had cost and weight benefits over fully filled copper foam. The design of a novel biporous spiral woven mesh wick for enhancing the thermal performance of an ultra-thin flattened heat pipe was presented in [287]. The optimal biporous wick had a 22% reduction in copper wires, leading to minimized production costs. An approach for optimizing pin fin heat sink design for semi-active configuration with an existing cooling fan was presented in [288]. This approach led to a 53% volume reduction compared to commercial heat sinks, which led to reduced production costs. From the perspective of coolant, hybrid nanofluids containing Al_2O_3 and multi-walled Carbon nanotube (MWCNT) were suggested for taking advantage of lost costs of Al_2O_3 nanoparticles in [132]. A comparison between jet impingement and microchannel-based design was conducted in [289] and concluded that jet impingement design would be more cost-effective as the simplicity of drilling holes led to reduced manufacturing costs. Further approaches for cost-effective thermal management design were presented in [290] and [291].

H. CHALLENGES AND FUTURE SCOPE

1) ATC CHALLENGES

A major challenge associated with thermal controllers is the accurate estimation of junction temperature with regard to the accuracy, bandwidth, and phase lag. Recent advancements in junction temperature sensing have seen the development of various technologies that provide higher accuracy and bandwidth [292], [293], [294]. Still, there are persistent challenges as many sensing approaches are costly, exhibit low signal-to-noise ratios and are sensitive to external influences and degradation.

Another challenge for thermal control lies in the assessment of health status and degradation prediction, as these factors are crucial for maintenance scheduling [26]. Effective thermal control cannot be applied without access to the RUL of power electronic components.

Minimizing the impact of thermal control methods on the operation of PECs is also a significant challenge. ATC methods involve changing the current or the PWM pattern by manipulating the switching frequency and losses to protect the PECs from thermal stress. These methods exert negligible impact on regular system operation but have a considerable impact when the converters are operating at their thermal limit [44]. So, all prevailing conditions must be considered for reducing the impact of these methods during operation at thermal limits.

The introduction of new semiconductor technologies and packaging also creates new challenges. The lifespan of WBG semiconductors is significantly more affected by thermal cycles compared to Si devices [26]. Another challenge in applying ATC with WBG devices is obtaining accurate and high-bandwidth junction temperature estimation. This difficulty arises due to the faster switching processes of WBG devices compared to Si devices and requires a more complex circuit for extracting temperature-related information [295].

2) TRADITIONAL COOLING TECHNIQUE CHALLENGES

Some of the challenges associated with channel cooling are pressure drop/pumping power penalty, limited heat transfer owing to the boundary layer, and uneven cooling due to unwanted temperature increases in the coolant [182]. To mitigate these problems, several researchers have carried out studies to decrease the thermal boundary layer and attain uniform cooling, considering minimum pressure loss. Modifying the channel configuration, changing the material type, attaching solid structures such as pin fin, using vortex generators, agitating the liquid flow, and improving the coolant type are some of the concepts applied to enhance the heat transfer process. Additionally, boiling fluid can provide improved heat transfer performance compared to single-phase cooling due to its superior cooling capacity.

Spray cooling is extremely suitable for high flux cooling, but several challenges are associated with this technique [82], [182]. The most significant of those is the considerable pumping power required for providing high-pressure drops to the nozzles. Moreover, there is an increased chance of clogging due to the narrow passages inside the nozzle. Furthermore, slight deviations in the fabrication process can lead to a significant alteration in the impact pattern of the nozzle.

Several challenging issues are associated with jet impingement cooling, such as considerable surface temperature fluctuation in single-phase cooling, large coolant delivery systems, complexity of pumping equipment, and flow obstruction between adjacent jets. Suggested performance-enhancing ideas for jet impingement cooling include nozzle configuration improvement, impingement surface modification, and improving cooling fluid properties.

Immersion cooling is an efficient technique for thermal management, but more research is needed to overcome issues such as floating fluff in the cooling fluid and aging of electronic devices with coolant. Establishing a balance between the electrical and thermal sides is also an exciting area of research for immersion cooling.

PCM has been commonly used for thermal management, although more detailed study is needed to enhance thermal performance. Nanofluid has been considered as a possible solution, but further studies are needed to optimize the concentration of nanofluid in PCM.

3) FUTURE SCOPE

Based on the investigated studies, the following suggestions are proposed as recommendations for future research.

- ATC methods need further research for enhancing junction temperature sensing by improving the accuracy and bandwidth of temperature monitoring systems. Additionally, research efforts should be directed to minimize the impact of ATC on PEC operations. Future research must explore scenarios where minor control actions are sufficient during transients, reserving more invasive actions only for worst-case situations.
- ATC methods focusing on increasing overload capacity need further improvement to guarantee the availability of rated power and ensure dynamic active thermal management.
- More research needs to be done to develop novel ATC methods acknowledging the trade-off between reliability, availability and lifetime of PSDs.
- ATC application in paralleled converters needs further research for improving PEC health status estimation and regulation of thermal loading across the PECs.
- Recently developed thermal management systems are vulnerable to cyber-physical threats, which must be addressed in future research. Major cybersecurity threats include unauthorized access, manipulation of data, and alteration of commands controlling critical thermal management features such as fan speed, pump speed,

valve position, coolant flow rate and pressure. Future research should look into measures such as encrypting data and commands transferred between TMS and the control unit or cloud to enhance resilience against cyberattacks. Moreover, designing diverse TMSs capable of independent operation or easy transition to a backup mode in case of a cyberattack needs more attention.

- The integration of AI methods such as expert systems, fuzzy logic, metaheuristic methods, and machine learning into the TMS is also an exciting area for future research.
- Research related to spray cooling and impingement cooling needs further investigation for developing ultra-compact design while preserving thermal performance. Moreover, heat pipe integrated cooling mechanism needs further improvement of the inner structure of the pipes. Attaining a compact heat sink design while preserving optimum thermal performance is also a recommended area for future work.
- Combining multiple cooling techniques considering potential synergies is also a promising topic for future study. These hybrid designs have exciting potential for future PECs.

V. CONCLUSION

Regulating the junction temperature of PSDs is greatly significant for improving the reliability of PECs. This paper has provided a detailed review of the state of the art of commonly employed methodologies for the thermal management of PECs. The main motivation was to provide an overview of frequently employed methods for ATC, direct and indirect cooling of electronic converters.

ATC is a technique used to improve the performance and reliability of a power converter by regulating its thermal behavior through control techniques. This paper has reviewed the ATC techniques considering different converter configurations and layers of thermal control. Moreover, the application of ATC with potential control objectives has been presented. The future scope of work for ATC includes improved junction temperature sensing, minimizing the influence of ATC on converter operation, health monitoring of PSDs, degradation forecasting, and experimental evaluation of ATC reduction.

This paper also provides a critical review of major techniques used for both direct and indirect cooling of power converters. The application, thermal performance, performance-enhancing ideas, and optimum configuration of these methods have been specifically highlighted. It can be inferred that liquid cooling is more suitable than air cooling for meeting the demands of modern power electronic systems with high heat flux. Cooling methods such as channel cooling, spray cooling, jet impingement cooling, immersion cooling, and PCM-based cooling show great potential in heat transfer performance and lowering of thermal resistance. Future work in this area includes improving structural design, employing novel materials with high thermal conductivity, advancement in surface design, and enhancement of cooling fluid.

This work has comprehensively reviewed typical methods for power electronics cooling. ATC implementation at different levels with applied control strategies has been thoroughly investigated. This study will serve as a reference for future research on thermal management systems.

ACKNOWLEDGMENT

This work was supported by Clemson University's Virtual Prototyping of Autonomy Enabled Ground Systems (VIPR-GS), under Cooperative Agreement W56HZV-21-2-0001 with the US Army DEVCOM Ground Vehicle Systems Center (GVSC).

DISTRIBUTION STATEMENT A. Approved for public release; distribution is unlimited. (OPSEC 7839)

The authors would like to acknowledge the Warren H. Owen Distinguished Professorship Endowment for its support of the research effort.

REFERENCES

[1] L. Timilsina, P. H. Hoang, A. Arsalan, B. R. Badr, G. Ozkan, B. Papari, and C. S. Edrington, "Degradation abatement in hybrid electric vehicles using data-driven technique," *Transp. Res. Proc.*, vol. 70, pp. 52–60, Jan. 2023, doi: 10.1016/j.trpro.2023.11.001.

[2] H. Wang, M. Liserre, and F. Blaabjerg, "Toward reliable power electronics: Challenges, design tools, and opportunities," *IEEE Ind. Electron. Mag.*, vol. 7, no. 2, pp. 17–26, Jun. 2013, doi: 10.1109/MIE.2013.2252958.

[3] M. Liserre, T. Sauter, and J. Y. Hung, "Future energy systems: Integrating renewable energy sources into the smart power grid through industrial electronics," *IEEE Ind. Electron. Mag.*, vol. 4, no. 1, pp. 18–37, Mar. 2010, doi: 10.1109/MIE.2010.935861.

[4] A. Arsalan, B. Papari, S. I. Rahman, L. Timilsina, A. Moghassemi, G. Muriithi, G. Ozkan, C. Edrington, and E. Buraimoh, "Machine learning approach for open circuit fault detection and localization in EV motor drive systems," SAE Int., Detroit, MI, USA, Tech. Paper 2024-01-2790, 2024.

[5] L. Timilsina, A. Moghassemi, S. I. Rahman, O. Ciftci, G. Ozkan, B. Papari, and C. Edrington, "A dual energy management for hybrid electric vehicles," in *Proc. IEEE Transp. Electrific. Conf. Expo (ITEC)*, Rosemont, IL, USA, Oct. 2024.

[6] A. Moghassemi, S. Padmanaban, V. K. Ramachandaramurthy, M. Mitolo, and M. Benbouzid, "A novel solar photovoltaic fed TransZSI-DVR for power quality improvement of grid-connected PV systems," *IEEE Access*, vol. 9, pp. 7263–7279, 2021, doi: 10.1109/ACCESS.2020.3048022.

[7] S. M. I. Rahman, M. R. Hazari, S. U. Hani, B. B. Pathik, M. A. Mannan, A. Mahfuz, M. K. Alam, and M. K. Hassan, "Primary frequency control of large-scale PV-connected multi-machine power system using battery energy storage system," *Int. J. Power Electron. Drive Syst. (IJPEDS)*, vol. 12, no. 3, p. 1862, Sep. 2021, doi: 10.11591/ijpeds.v12.i3.pp1862-1871.

[8] L. Timilsina, P. R. Badr, P. H. Hoang, G. Ozkan, B. Papari, and C. S. Edrington, "Battery degradation in electric and hybrid electric vehicles: A survey study," *IEEE Access*, vol. 11, pp. 42431–42462, 2023, doi: 10.1109/ACCESS.2023.3271287.

[9] E. Gumrukcu, A. Arsalan, G. Muriithi, C. Joglekar, A. Aboulebdeh, M. Alparslan Zehir, B. Papari, and A. Monti, "Impact of cyber-attacks on EV charging coordination: The case of single point of failure," in *Proc. 4th Global Power, Energy Commun. Conf. (GPECOM)*, Jun. 2022, pp. 506–511, doi: 10.1109/GPECOM55404.2022.9815727.

[10] G. Buticchi, S. Bozhko, M. Liserre, P. Wheeler, and K. Al-Haddad, "On-board microgrids for the more electric aircraft—Technology review," *IEEE Trans. Ind. Electron.*, vol. 66, no. 7, pp. 5588–5599, Jul. 2019, doi: 10.1109/TIE.2018.2881951.

[11] L. Timilsina, P. H. Hoang, A. Moghassemi, E. Buraimoh, P. K. Chamarthi, G. Ozkan, B. Papari, and C. S. Edrington, "A real-time prognostic-based control framework for hybrid electric vehicles," *IEEE Access*, vol. 11, pp. 127589–127607, 2023, doi: 10.1109/ACCESS.2023.3332689.

[12] P. H. Hoang, G. Ozkan, P. Badr, L. Timilsina, and C. Edrington, "A prognostic based control framework for hybrid electric vehicles," SAE Int., Detroit, MI, USA, Tech. Paper 2022-01-0352, 2022, doi: 10.4271/2022-01-0352.

[13] M. Andresen, K. Ma, G. Buticchi, J. Falck, F. Blaabjerg, and M. Liserre, "Junction temperature control for more reliable power electronics," *IEEE Trans. Power Electron.*, vol. 33, no. 1, pp. 765–776, Jan. 2018, doi: 10.1109/TPEL.2017.2665697.

[14] H. Wang, M. Liserre, F. Blaabjerg, P. D. P. Rimmen, J. B. Jacobsen, T. Kvisgaard, and J. Landkildehus, "Transitioning to physics-of-failure as a reliability driver in power electronics," *IEEE J. Emerg. Sel. Topics Power Electron.*, vol. 2, no. 1, pp. 97–114, Mar. 2014, doi: 10.1109/JESTPE.2013.2290282.

[15] A. Moghassemi, D. S. Vanaja, J. Olamaei, G. Ozkan, and C. S. Edrington, "A novel switching method in PV-fed quasi-ZSI-DVR for voltage quality enhancement of photovoltaic integrated networks," *IET Renew. Power Gener.*, Aug. 2022, doi: 10.1049/rpg2.12575.

[16] A. Moghassemi, S. Ebrahimi, and F. Ferdowsi, "A novel control scheme for TransZSI-DVR to enhance power quality in solar integrated networks," in *Proc. North Amer. Power Symp. (NAPS)*, Nov. 2021, pp. 1–6, doi: 10.1109/NAPS52732.2021.9654507.

[17] S. Yang, A. Bryant, P. Mawby, D. Xiang, L. Ran, and P. Tavner, "An industry-based survey of reliability in power electronic converters," *IEEE Trans. Ind. Appl.*, vol. 47, no. 3, pp. 1441–1451, May 2011, doi: 10.1109/TIA.2011.2124436.

[18] M. Andresen, M. Liserre, and G. Buticchi, "Review of active thermal and lifetime control techniques for power electronic modules," in *Proc. 16th Eur. Conf. Power Electron. Appl.*, Aug. 2014, pp. 1–10, doi: 10.1109/EPE.2014.6910822.

[19] I. Kovacevic, U. Drofenik, and J. W. Kolar, "New physical model for lifetime estimation of power modules," in *Proc. Int. Power Electron. Conf.*, 2010, pp. 2106–2114, doi: 10.1109/10.1109/IPEC.2010.5543755.

[20] M. Ciappa, "Selected failure mechanisms of modern power modules," *Microelectron. Rel.*, vol. 42, nos. 4–5, pp. 653–667, Apr. 2002, doi: 10.1016/s0026-2714(02)00042-2.

[21] A. Volke and M. Hornkamp, *IGBT Modules: Technologies, Driver and Application*. Munich, Germany: Infineon Technologies AG, 2017.

[22] A. Castellazzi, W. J. Choy, and P. Zanchetta, "Dynamic active cooling for improved power system reliability," *Microelectron. Rel.*, vol. 51, nos. 9–11, pp. 1964–1967, Sep. 2011, doi: 10.1016/j.microrel.2011.07.072.

[23] A. Wintrich, U. Nicolai, T. Reimann, and W. Tursky, *Application Manual Power Semiconductors*. Nuremberg, Germany: Semikron International GmbH, 2010.

[24] P. R. Wilson, "Thermal modeling and analysis of power electronic components and systems," in *Power Electronics Handbook*. Amsterdam, The Netherlands: Elsevier, 2018, pp. 1441–1450, doi: 10.1016/B978-0-12-811407-0.00052-0.

[25] J. Biela, M. Schweizer, S. Waffler, and J. W. Kolar, "SiC versus Si—Evaluation of potentials for performance improvement of inverter and DC–DC converter systems by SiC power semiconductors," *IEEE Trans. Ind. Electron.*, vol. 58, no. 7, pp. 2872–2882, Jul. 2011, doi: 10.1109/TIE.2010.2072896.

[26] J. Kuprat, C. H. van der Broeck, M. Andresen, S. Kalker, M. Liserre, and R. W. De Doncker, "Research on active thermal control: Actual status and future trends," *IEEE J. Emerg. Sel. Topics Power Electron.*, vol. 9, no. 6, pp. 6494–6506, Dec. 2021, doi: 10.1109/JESTPE.2021.3067782.

[27] M. Reynell, "Advanced thermal analysis of packaged electronic systems using computational fluid dynamics techniques," *Comput.-Aided Eng. J.*, vol. 7, no. 4, pp. 104–106, 1990, doi: 10.1049/cae.1990.0025.

[28] J. R. Black, "Electromigration—A brief survey and some recent results," *IEEE Trans. Electron Devices*, vol. ED-16, no. 4, pp. 338–347, Apr. 1969, doi: 10.1109/t-ed.1969.16754.

[29] A. Moghassemi, G. Ozkan, C. S. Edrington, G. Muriithi, and Z. Zhang, "Active thermal control of AC/DC power converter considering health monitoring of power modules," in *Proc. IEEE Electric Ship Technol. Symp. (ESTS)*, Aug. 2023, pp. 78–85, doi: 10.1109/ests56571.2023.10220528.

[30] M. Liserre, G. Buticchi, J. I. Leon, A. Marquez Alcaide, V. Raveendran, Y. Ko, M. Andresen, V. G. Monopoli, and L. Franquelo, "Power routing: A new paradigm for maintenance scheduling," *IEEE Ind. Electron. Mag.*, vol. 14, no. 3, pp. 33–45, Sep. 2020, doi: 10.1109/MIE.2020.2975049.

[31] A. Moghassemi, S. M. I. Rahman, G. Ozkan, C. S. Edrington, Z. Zhang, and P. K. Chamarthi, "Power converters coolant: Past, present, future, and a path toward active thermal control in electrified ship power systems," *IEEE Access*, vol. 11, pp. 91620–91659, 2023, doi: 10.1109/ACCESS.2023.3308523.

[32] J. Lemmens, P. Vanassche, and J. Driesen, "Optimal control of traction motor drives under electrothermal constraints," *IEEE J. Emerg. Sel. Topics Power Electron.*, vol. 2, no. 2, pp. 249–263, Jun. 2014, doi: 10.1109/JESTPE.2014.2299765.

[33] D. A. Murdock, J. E. R. Torres, J. J. Connors, and R. D. Lorenz, "Active thermal control of power electronic modules," *IEEE Trans. Ind. Appl.*, vol. 42, no. 2, pp. 552–558, Mar. 2006, doi: 10.1109/TIA.2005.863905.

[34] M. Weckert and J. Roth-Stielow, "Lifetime as a control variable in power electronic systems," in *Proc. Emobility-Elect. Power Train*, 2010, pp. 1–6, doi: 10.1109/EMOBILITY.2010.5668049.

[35] J. Lemmens, J. Driesen, and P. Vanassche, "Dynamic DC-link voltage adaptation for thermal management of traction drives," in *Proc. IEEE Energy Convers. Congr. Expo.*, Sep. 2013, pp. 180–187, doi: 10.1109/ECCE.2013.6646698.

[36] C. Sintamarean, H. Wang, F. Blaabjerg, and F. Iannuzzo, "The impact of gate-driver parameters variation and device degradation in the PV-inverter lifetime," in *Proc. IEEE Energy Convers. Congr. Expo. (ECCE)*, Sep. 2014, pp. 2257–2264, doi: 10.1109/ECCE.2014.6953704.

[37] K. Ma, M. Liserre, and F. Blaabjerg, "Reactive power influence on the thermal cycling of multi-MW wind power inverter," *IEEE Trans. Ind. Appl.*, vol. 49, no. 2, pp. 922–930, Mar. 2013, doi: 10.1109/TIA.2013.2240644.

[38] C. Qian, A. M. Gheitaghy, J. Fan, H. Tang, B. Sun, H. Ye, and G. Zhang, "Thermal management on IGBT power electronic devices and modules," *IEEE Access*, vol. 6, pp. 12868–12884, 2018, doi: 10.1109/ACCESS.2018.2793300.

[39] J. Liang, Y. Gan, Y. Li, M. Tan, and J. Wang, "Thermal and electrochemical performance of a serially connected battery module using a heat pipe-based thermal management system under different coolant temperatures," *Energy*, vol. 189, Dec. 2019, Art. no. 116233, doi: 10.1016/j.energy.2019.116233.

[40] H. M. Ali, "Recent advancements in PV cooling and efficiency enhancement integrating phase change materials based systems—A comprehensive review," *Sol. Energy*, vol. 197, pp. 163–198, Feb. 2020, doi: 10.1016/j.solener.2019.11.075.

[41] S. I. Rahman, G. Ozkan, A. Arsalan, P. K. Chamarthi, B. Papari, and C. S. Edrington, "Impact of active cooling on the thermal management of 3-level NPC converter for hybrid electric vehicle application," SAE Int., Greenville, SC, USA, Tech. Paper 2023-01-1684, 2023, doi: 10.4271/2023-01-1684.

[42] Y. Yoon, S. Hyeon, D. R. Kim, and K.-S. Lee, "Minimizing thermal interference effects of multiple heat sources for effective cooling of power conversion electronics," *Energy Convers. Manag.*, vol. 174, pp. 218–226, Oct. 2018, doi: 10.1016/j.enconman.2018.08.047.

[43] D. Kaczorowski, B. Michalak, and A. Mertens, "A novel thermal management algorithm for improved lifetime and overload capabilities of traction converters," in *Proc. 17th Eur. Conf. Power Electron. Appl. (EPE ECCE-Europe)*, Sep. 2015, pp. 1–10, doi: 10.1109/EPE.2015.7309262.

[44] C. H. van der Broeck and R. W. De Doncker, "Active thermal management for enhancing peak-current capability of three-phase inverters," in *Proc. IEEE Energy Convers. Congr. Expo. (ECCE)*, Oct. 2020, pp. 3312–3319, doi: 10.1109/ECCE44975.2020.9235387.

[45] C. H. van der Broeck, L. A. Ruppert, R. D. Lorenz, and R. W. De Doncker, "Methodology for active thermal cycle reduction of power electronic modules," *IEEE Trans. Power Electron.*, vol. 34, no. 8, pp. 8213–8229, Aug. 2019, doi: 10.1109/TPEL.2018.2882184.

[46] L. Wu and A. Castellazzi, "Temperature adaptive driving of power semiconductor devices," in *Proc. IEEE Int. Symp. Ind. Electron.*, Jul. 2010, pp. 1110–1114, doi: 10.1109/ISIE.2010.5636541.

[47] P. K. Prasobhu, G. Buticchi, S. Brueske, and M. Liserre, "Gate driver for the active thermal control of a DC/DC GaN-based converter," in *Proc. IEEE Energy Convers. Congr. Expo. (ECCE)*, Sep. 2016, pp. 1–8, doi: 10.1109/ECCE.2016.7855131.

[48] D. Kaczorowski and A. Mertens, "Reduction of the EV inverter chip size at constant reliability by active thermal control," in *Proc. IEEE Vehicle Power Propuls. Conf. (VPPC)*, Hangzhou, China, 2016, p. 1, doi: 10.1109/VPPC.2016.7791759.

[49] Y. Ko, M. Andresen, G. Buticchi, and M. Liserre, "Discontinuous-modulation-based active thermal control of power electronic modules in wind farms," *IEEE Trans. Power Electron.*, vol. 34, no. 1, pp. 301–310, Jan. 2019, doi: 10.1109/TPEL.2018.2819423.

[50] S. M. I. Rahman, Md. A. A. Samy, and S. Saha, "C-code implementation of a shunt active power filter based on finite set model predictive control," in *Proc. Int. Conf. Robotics, Electrical Signal Process. Techn. (ICREST)*, Jan. 2019, pp. 359–363, doi: 10.1109/ICREST.2019.8644287.

[51] G. Ozkan, P. H. Hoang, P. Ramezani Badr, C. S. Edrington, and B. Papari, "Real-time thermal management for two-level active rectifier with finite control set model predictive control," *Int. J. Electr. Power Energy Syst.*, vol. 131, Oct. 2021, Art. no. 107057, doi: 10.1016/j.ijepes.2021.107057.

[52] J. Falck, G. Buticchi, and M. Liserre, "Thermal stress based model predictive control of electric drives," *IEEE Trans. Ind. Appl.*, vol. 54, no. 2, pp. 1513–1522, Mar. 2018, doi: 10.1109/TIA.2017.2772198.

[53] M. Andresen, G. Buticchi, and M. Liserre, "Thermal stress analysis and MPPT optimization of photovoltaic systems," *IEEE Trans. Ind. Electron.*, vol. 63, no. 8, pp. 4889–4898, Aug. 2016, doi: 10.1109/TIE.2016.2549503.

[54] A. Isidori, F. M. Rossi, F. Blaabjerg, and K. Ma, "Thermal loading and reliability of 10-MW multilevel wind power converter at different wind roughness classes," *IEEE Trans. Ind. Appl.*, vol. 50, no. 1, pp. 484–494, Jan. 2014, doi: 10.1109/TIA.2013.2269311.

[55] B. P. McGrath and D. G. Holmes, "Multicarrier PWM strategies for multilevel inverters," *IEEE Trans. Ind. Electron.*, vol. 49, no. 4, pp. 858–867, Aug. 2002, doi: 10.1109/TIE.2002.801073.

[56] H. Wang, R. Zhao, Y. Deng, and X. He, "Novel carrier-based PWM methods for multilevel inverter," in *Proc. 29th Annu. Conf. IEEE Ind. Electron. Soc.*, Sep. 2003, pp. 2777–2782, doi: 10.1109/IECON.2003.1280687.

[57] *User Manual of Plecs Blockset Version 3.1*, Plexim, Zurich, Switzerland, 2011.

[58] T. Bruckner and D. G. Holmes, "Optimal pulse-width modulation for three-level inverters," *IEEE Trans. Power Electron.*, vol. 20, no. 1, pp. 82–89, Jan. 2005, doi: 10.1109/TPEL.2004.839831.

[59] C. J. Joseph, M. Zolghadri, A. Homaifar, F. Lee, and R. Lorenz, "Novel thermal based current sharing control of parallel converters," in *Proc. 26th Annu. Int. Telecommun. Energy Conf.*, 2004, pp. 647–653, doi: 10.1109/INTLEC.2004.1401539.

[60] V. Ferreira, M. Andresen, B. Cardoso, and M. Liserre, "Selective soft-switching for thermal balancing in IGBT-based multichip systems," *IEEE J. Emerg. Sel. Topics Power Electron.*, vol. 9, no. 4, pp. 3982–3991, Aug. 2021, doi: 10.1109/JESTPE.2020.3026782.

[61] V. Ferreira, M. Andresen, B. Cardoso, and M. Liserre, "Pulse-Shadowing-Based thermal balancing in multichip modules," *IEEE Trans. Ind. Appl.*, vol. 56, no. 4, pp. 4081–4088, Jul. 2020, doi: 10.1109/TIA.2020.2993526.

[62] J. Ewanchuk, J. Brandelero, and S. Mollov, "A gate driver based approach to improving the current density in a power module by equalizing the individual die temperatures," in *Proc. IEEE Energy Convers. Congr. Expo. (ECCE)*, Sep. 2018, pp. 4652–4658, doi: 10.1109/ECCE.2018.8557880.

[63] J. Sheng, H. Yang, C. Li, M. Chen, W. Li, X. He, and X. Gu, "Active thermal control for hybrid modular multilevel converter under overmodulation operation," *IEEE Trans. Power Electron.*, vol. 35, no. 4, pp. 4242–4255, Apr. 2020, doi: 10.1109/TPEL.2019.2936010.

[64] F. Hahn, M. Andresen, G. Buticchi, and M. Liserre, "Thermal analysis and balancing for modular multilevel converters in HVDC applications," *IEEE Trans. Power Electron.*, vol. 33, no. 3, pp. 1985–1996, Mar. 2018, doi: 10.1109/TPEL.2017.2691012.

[65] M. Aly, G. M. Dousoky, and M. Shoyama, "Lifetime-oriented SVPWM for thermally-overloaded power devices in three-level inverters," in *Proc. 41st Annu. Conf. IEEE Ind. Electron. Soc.*, Nov. 2015, pp. 003614–003619, doi: 10.1109/IECON.2015.7392662.

[66] M. Liserre, M. Andresen, L. Costa, and G. Buticchi, "Power routing in modular smart transformers: Active thermal control through uneven loading of cells," *IEEE Ind. Electron. Mag.*, vol. 10, no. 3, pp. 43–53, Sep. 2016, doi: 10.1109/MIE.2016.2588898.

[67] A. Marquez, J. I. Leon, S. Vazquez, and L. G. Franquelo, "Closed-loop active thermal control via power routing of parallel DC–DC converters," in *Proc. IEEE 12th Int. Conf. Compat., Power Electron. Power Eng.*, Apr. 2018, pp. 1–6, doi: 10.1109/CPE.2018.8372586.

[68] A. Marquez, J. I. Leon, S. Vazquez, L. G. Franquelo, G. Buticchi, and M. Liserre, "Power device lifetime extension of DC–DC interleaved converters via power routing," in *Proc. 44th Annu. Conf. IEEE Ind. Electron. Soc.*, Oct. 2018, pp. 5332–5337, doi: 10.1109/IECON.2018.8592912.

[69] M. Andresen, V. Raveendran, G. Buticchi, and M. Liserre, "Lifetime-based power routing in parallel converters for smart transformer application," *IEEE Trans. Ind. Electron.*, vol. 65, no. 2, pp. 1675–1684, Feb. 2018, doi: 10.1109/TIE.2017.2733426.

[70] V. Raveendran, M. Andresen, and M. Liserre, "Improving onboard converter reliability for more electric aircraft with lifetime-based control," *IEEE Trans. Ind. Electron.*, vol. 66, no. 7, pp. 5787–5796, Jul. 2019, doi: 10.1109/TIE.2018.2889626.

[71] V. Raveendran, M. Andresen, and M. Liserre, "Reliability oriented control of DC/DC converters for more electric aircraft," in *Proc. IEEE 27th Int. Symp. Ind. Electron. (ISIE)*, Jun. 2018, pp. 1352–1358, doi: 10.1109/ISIE.2018.8433853.

[72] M. Andresen, J. Kuprat, V. Raveendran, J. Falck, and M. Liserre, "Active thermal control for delaying maintenance of power electronics converters," *Chin. J. Electr. Eng.*, vol. 4, no. 3, pp. 13–20, Sep. 2018, doi: 10.23919/CJEE.2018.8471285.

[73] G. Buticchi, M. Andresen, M. Wutti, and M. Liserre, "Lifetime-based power routing of a quadruple active bridge DC/DC converter," *IEEE Trans. Power Electron.*, vol. 32, no. 11, pp. 8892–8903, Nov. 2017, doi: 10.1109/TPEL.2017.2650258.

[74] Y. Ko, M. Andresen, G. Buticchi, and M. Liserre, "Thermally compensated discontinuous modulation strategy for cascaded H-bridge converters," *IEEE Trans. Power Electron.*, vol. 33, no. 3, pp. 2704–2713, Mar. 2018, doi: 10.1109/TPEL.2017.2694455.

[75] Y. Ko, V. Raveendran, M. Andresen, and M. Liserre, "Thermally compensated discontinuous modulation for MVAC/LVDC building blocks of modular smart transformers," *IEEE Trans. Power Electron.*, vol. 35, no. 1, pp. 220–231, Jan. 2020, doi: 10.1109/TPEL.2019.2908853.

[76] Y. Ko, V. Raveendran, M. Andresen, and M. Liserre, "Advanced discontinuous modulation for thermally compensated modular smart transformers," *IEEE Trans. Power Electron.*, vol. 35, no. 3, pp. 2445–2457, Mar. 2020, doi: 10.1109/TPEL.2019.2931780.

[77] V. G. Monopoli, A. Marquez, J. I. Leon, Y. Ko, G. Buticchi, and M. Liserre, "Improved harmonic performance of cascaded H-bridge converters with thermal control," *IEEE Trans. Ind. Electron.*, vol. 66, no. 7, pp. 4982–4991, Jul. 2019, doi: 10.1109/TIE.2018.2868304.

[78] Y. Ko, M. Andresen, G. Buticchi, and M. Liserre, "Power routing for cascaded H-bridge converters," *IEEE Trans. Power Electron.*, vol. 32, no. 12, pp. 9435–9446, Dec. 2017, doi: 10.1109/TPEL.2017.2658182.

[79] S. S. Murshed, *Introductory Chapter: Electronics Cooling—An Overview*. London, U.K.: IntechOpen, 2016, pp. 1–11, doi: 10.5772/63321.

[80] M. J. Huang, P. C. Eames, B. Norton, and N. J. Hewitt, "Natural convection in an internally finned phase change material heat sink for the thermal management of photovoltaics," *Sol. Energy Mater. Sol. Cells*, vol. 95, no. 7, pp. 1598–1603, Jul. 2011, doi: 10.1016/j.solmat.2011.01.008.

[81] S. Pua, K. Ong, K. Lai, and M. Naghavi, "Natural and forced convection heat transfer coefficients of various finned heat sinks for miniature electronic systems," *Proc. Inst. Mech. Eng., A, J. Power Energy*, vol. 233, no. 2, pp. 249–261, Mar. 2019, doi: 10.1177/0957650918784420.

[82] Z. Zhang, X. Wang, and Y. Yan, "A review of the state-of-the-art in electronic cooling," *e-Prime-Adv. Electr. Eng., Electron. Energy*, vol. 1, 2021, Art. no. 100009, doi: 10.1016/j.prime.2021.100009.

[83] J.-X. Wang, Y.-Z. Li, J.-X. Li, C. Li, K. Xiong, and X.-W. Ning, "Enhanced heat transfer by an original immersed spray cooling system integrated with an ejector," *Energy*, vol. 158, pp. 512–523, Sep. 2018, doi: 10.1016/j.energy.2018.06.019.

[84] A. Ü. Tepe, Y. Yetisken, Ü. Uysal, and K. Arslan, "Experimental and numerical investigation of jet impingement cooling using extended jet holes," *Int. J. Heat Mass Transf.*, vol. 158, Sep. 2020, Art. no. 119945, doi: 10.1016/j.ijheatmasstransfer.2020.119945.

[85] A. Kosar, "Effect of substrate thickness and material on heat transfer in microchannel heat sinks," *Int. J. Thermal Sci.*, vol. 49, no. 4, pp. 635–642, Apr. 2010, doi: 10.1016/j.ijthermalsci.2009.11.004.

[86] P. Smakulski and S. Pietrowicz, "A review of the capabilities of high heat flux removal by porous materials, microchannels and spray cooling techniques," *Appl. Thermal Eng.*, vol. 104, pp. 636–646, Jul. 2016, doi: 10.1016/j.applthermaleng.2016.05.096.

[87] X. Gao and R. Li, "Spray impingement cooling: The state of the art," in *Advanced Cooling Technologies and Applications*. Rijeka, Croatia: IntechOpen, 2018, doi: 10.5772/intechopen.80256.

[88] P. Naphon and S. Wongwises, "Investigation on the jet liquid impingement heat transfer for the central processing unit of personal computers," *Int. Commun. Heat Mass Transf.*, vol. 37, no. 7, pp. 822–826, Aug. 2010, doi: 10.1016/j.icheatmasstransfer.2010.05.004.

[89] D. Sharar, N. R. Jankowski, and B. Morgan, *Review of Two-Phase Electronics Cooling for Army Vehicle Applications*. Adelphi, MD, USA: Army Research Laboratory, 2010.

[90] T. L. Bergman, *Fundamentals of Heat and Mass Transfer*. Hoboken, NJ, USA: Wiley, 2011.

[91] W. Duangthongsuk and S. Wongwises, "An experimental investigation on the heat transfer and pressure drop characteristics of nanofluid flowing in microchannel heat sink with multiple zigzag flow channel structures," *Experim. Thermal Fluid Sci.*, vol. 87, pp. 30–39, Oct. 2017, doi: 10.1016/j.expthermflusci.2017.04.013.

[92] M. Arik and A. Bar-Cohen, "Immersion cooling of high heat flux microelectronics with dielectric liquids," in *Proc. 4th Int. Symp. Adv. Packag. Mater. Processes, Properties Interfaces*, 1998, pp. 229–247, doi: 10.1109/ISAPM.1998.664464.

[93] S. M. Sohel Murshed and C. A. Nieto de Castro, "A critical review of traditional and emerging techniques and fluids for electronics cooling," *Renew. Sustain. Energy Rev.*, vol. 78, pp. 821–833, Oct. 2017, doi: 10.1016/j.rser.2017.04.112.

[94] M. I. Hasan and H. L. Tbena, "Using of phase change materials to enhance the thermal performance of micro channel heat sink," *Eng. Sci. Technol., Int. J.*, vol. 21, no. 3, pp. 517–526, Jun. 2018, doi: 10.1016/j.jestch.2018.03.017.

[95] A. A. El-Nasr and S. M. El-Haggar, "Effective thermal conductivity of heat pipes," *Heat Mass Transf.*, vol. 32, nos. 1–2, pp. 97–101, Nov. 1996, doi: 10.1007/s002310050097.

[96] A. N. Desai, A. Gunjal, and V. K. Singh, "Numerical investigations of fin efficacy for phase change material (PCM) based thermal control module," *Int. J. Heat Mass Transf.*, vol. 147, Feb. 2020, Art. no. 118855, doi: 10.1016/j.ijheatmasstransfer.2019.118855.

[97] X.-H. Yang, S.-C. Tan, Y.-J. Ding, L. Wang, J. Liu, and Y.-X. Zhou, "Experimental and numerical investigation of low melting point metal based PCM heat sink with internal fins," *Int. Commun. Heat Mass Transf.*, vol. 87, pp. 118–124, Oct. 2017, doi: 10.1016/j.icheatmasstransfer.2017.07.001.

[98] C. J. Lasance and R. E. Simons, "Advances in high-performance cooling for electronics," *Electron. Cooling*, vol. 11, no. 4, pp. 22–39, 2005.

[99] Y. Du, J. Xu, B. Paul, and P. Eklund, "Flexible thermoelectric materials and devices," *Appl. Mater. Today*, vol. 12, pp. 366–388, Sep. 2018, doi: 10.1016/j.apmt.2018.07.004.

[100] Y. Cai, Y. Wang, D. Liu, and F.-Y. Zhao, "Thermoelectric cooling technology applied in the field of electronic devices: Updated review on the parametric investigations and model developments," *Appl. Thermal Eng.*, vol. 148, pp. 238–255, Feb. 2019, doi: 10.1016/j.applthermaleng.2018.11.014.

[101] D. B. Tuckerman and R. F. W. Pease, "High-performance heat sinking for VLSI," *IEEE Electron Device Lett.*, vol. EDL-2, no. 5, pp. 126–129, May 1981, doi: 10.1109/EDL.1981.25367.

[102] S. Ashman and S. G. Kandlikar, "A review of manufacturing processes for microchannel heat exchanger fabrication," in *Proc. Int. Conf. Nanochannels, Microchannels, Minichannels*, vol. 47608, 2006, pp. 855–860, doi: 10.1115/ICNMM2006-96121.

[103] S. S. Mehendale, A. M. Jacobi, and R. K. Shah, "Fluid flow and heat transfer at micro- and meso-scales with application to heat exchanger design," *Appl. Mech. Rev.*, vol. 53, no. 7, pp. 175–193, Jul. 2000, doi: 10.1115/1.3097347.

[104] T. Yeom, T. Simon, T. Zhang, M. Zhang, M. North, and T. Cui, "Enhanced heat transfer of heat sink channels with micro pin fin roughened walls," *Int. J. Heat Mass Transf.*, vol. 92, pp. 617–627, Jan. 2016, doi: 10.1016/j.ijheatmasstransfer.2015.09.014.

[105] A. Muhammad, D. Selvakumar, A. Iranzo, Q. Sultan, and J. Wu, "Comparison of pressure drop and heat transfer performance for liquid metal cooled mini-channel with different coolants and heat sink materials," *J. Thermal Anal. Calorimetry*, vol. 141, no. 1, pp. 289–300, Jul. 2020, doi: 10.1007/s10973-020-09318-2.

[106] H. A. Mohammed, P. Gunnasegaran, and N. H. Shuaib, "Influence of various base nanofluids and substrate materials on heat transfer in trapezoidal microchannel heat sinks," *Int. Commun. Heat Mass Transf.*, vol. 38, no. 2, pp. 194–201, Feb. 2011, doi: 10.1016/j.icheatmasstransfer.2010.12.010.

[107] M. T. Sarowar, "Performance comparison of microchannel heat sink using boron-based ceramic materials," *Adv. Mater. Res.*, vol. 1163, pp. 73–88, Apr. 2021, doi: 10.4028/www.scientific.net/amr.1163.73.

[108] B. Ramos-Alvarado, P. Li, H. Liu, and A. Hernandez-Guerrero, "CFD study of liquid-cooled heat sinks with microchannel flow field configurations for electronics, fuel cells, and concentrated solar cells," *Appl. Thermal Eng.*, vol. 31, nos. 14–15, pp. 2494–2507, Oct. 2011, doi: 10.1016/j.applthermaleng.2011.04.015.

[109] S. Zeng, B. Kanargi, and P. S. Lee, "Experimental and numerical investigation of a mini channel forced air heat sink designed by topology optimization," *Int. J. Heat Mass Transf.*, vol. 121, pp. 663–679, Jun. 2018, doi: 10.1016/j.ijheatmasstransfer.2018.01.039.

[110] P. Gunnasegaran, H. A. Mohammed, N. H. Shuaib, and R. Saidur, "The effect of geometrical parameters on heat transfer characteristics of microchannels heat sink with different shapes," *Int. Commun. Heat Mass Transf.*, vol. 37, no. 8, pp. 1078–1086, Oct. 2010, doi: 10.1016/j.icheatmasstransfer.2010.06.014.

[111] N. A. F. Nik Mazlam, N. Mohd-Ghazali, T. Mare, P. Estelle, and S. Halelfadl, "Thermal and hydrodynamic performance of a microchannel heat sink cooled with carbon nanotubes nanofluid," *Jurnal Teknologi*, vol. 78, pp. 69–77, Oct. 2016, doi: 10.11113/jt.v78.9670.

[112] M. I. Hasan, A. A. Rageb, M. Yaghoubi, and H. Homayoni, "Influence of channel geometry on the performance of a counter flow microchannel heat exchanger," *Int. J. Thermal Sci.*, vol. 48, no. 8, pp. 1607–1618, Aug. 2009, doi: 10.1016/j.ijthermalsci.2009.01.004.

[113] A. Dewan and P. Srivastava, "A review of heat transfer enhancement through flow disruption in a microchannel," *J. Thermal Sci.*, vol. 24, no. 3, pp. 203–214, Jun. 2015, doi: 10.1007/s11630-015-0775-1.

[114] M. Kang, L. K. Hwang, and B. Kwon, "Computationally efficient optimization of wavy surface roughness in cooling channels using simulated annealing," *Int. J. Heat Mass Transf.*, vol. 150, Apr. 2020, Art. no. 119300, doi: 10.1016/j.ijheatmasstransfer.2019.119300.

[115] B. J. Jones and S. V. Garimella, "Surface roughness effects on flow boiling in microchannels," *J. Thermal Sci. Eng. Appl.*, vol. 1, no. 4, Jun. 2010, Art. no. 041007, doi: 10.1115/1.4001804.

[116] P. Li, D. Guo, and X. Huang, "Heat transfer enhancement, entropy generation and temperature uniformity analyses of shark-skin bionic modified microchannel heat sink," *Int. J. Heat Mass Transf.*, vol. 146, Jan. 2020, Art. no. 118846, doi: 10.1016/j.ijheatmasstransfer.2019.118846.

[117] J. Tang, C. Qi, Z. Ding, M. Afrand, and Y. Yan, "Thermo-hydraulic performance of nanofluids in a bionic heat sink," *Int. Commun. Heat Mass Transf.*, vol. 127, Oct. 2021, Art. no. 105492, doi: 10.1016/j.icheatmasstransfer.2021.105492.

[118] Y. Hadad, N. Fallahtafti, L. Choobineh, C. H. Hoang, V. Radmard, P. R. Chiarot, and B. Sammakia, "Performance analysis and shape optimization of an impingement microchannel cold plate," *IEEE Trans. Compon., Packag., Manuf. Technol.*, vol. 10, no. 8, pp. 1304–1319, Aug. 2020, doi: 10.1109/TCPMT.2020.3005824.

[119] X. Liu and J. Yu, "Numerical study on performances of mini-channel heat sinks with non-uniform inlets," *Appl. Thermal Eng.*, vol. 93, pp. 856–864, Jan. 2016, doi: 10.1016/j.applthermaleng.2015.09.032.

[120] I. A. Ghani, N. A. Che Sidik, N. Kamaruzzaman, W. Jazair Yahya, and O. Mahian, "The effect of manifold zone parameters on hydrothermal performance of micro-channel HeatSink: A review," *Int. J. Heat Mass Transf.*, vol. 109, pp. 1143–1161, Jun. 2017, doi: 10.1016/j.ijheatmasstransfer.2017.03.007.

[121] O. K. Siddiqui and S. M. Zubair, "Efficient energy utilization through proper design of microchannel heat exchanger manifolds: A comprehensive review," *Renew. Sustain. Energy Rev.*, vol. 74, pp. 969–1002, Jul. 2017, doi: 10.1016/j.rser.2017.01.074.

[122] N. A. C. Sidik, M. N. A. W. Muhamad, W. M. A. A. Japar, and Z. A. Rasid, "An overview of passive techniques for heat transfer augmentation in microchannel heat sink," *Int. Commun. Heat Mass Transf.*, vol. 88, pp. 74–83, Nov. 2017, doi: 10.1016/j.icheatmasstransfer.2017.08.009.

[123] N. H. Naqiuddin, L. H. Saw, M. C. Yew, F. Yusof, T. C. Ng, and M. K. Yew, "Overview of micro-channel design for high heat flux application," *Renew. Sustain. Energy Rev.*, vol. 82, pp. 901–914, Feb. 2018, doi: 10.1016/j.rser.2017.09.110.

[124] A. Datta, D. Sanyal, A. Agrawal, and A. K. Das, "A review of liquid flow and heat transfer in microchannels with emphasis to electronic cooling," *Sādhanā*, vol. 44, no. 12, pp. 1–32, Dec. 2019, doi: 10.1007/s12046-019-1201-2.

[125] Y. Alihosseini, M. Zabetian Targhi, M. M. Heyhat, and N. Ghorbani, "Effect of a micro heat sink geometric design on thermo-hydraulic performance: A review," *Appl. Thermal Eng.*, vol. 170, Apr. 2020, Art. no. 114974, doi: 10.1016/j.applthermaleng.2020.114974.

[126] B. Shen, H. Yan, B. Sunden, H. Xue, and G. Xie, "Forced convection and heat transfer of water-cooled microchannel heat sinks with various structured metal foams," *Int. J. Heat Mass Transf.*, vol. 113, pp. 1043–1053, Oct. 2017, doi: 10.1016/j.ijheatmasstransfer.2017.06.004.

[127] P.-H. Tseng, K.-T. Tsai, A.-L. Chen, and C.-C. Wang, "Performance of novel liquid-cooled porous heat sink via 3-D laser additive manufacturing," *Int. J. Heat Mass Transf.*, vol. 137, pp. 558–564, Jul. 2019, doi: 10.1016/j.ijheatmasstransfer.2019.03.116.

[128] J. Y. Ho, K. C. Leong, and T. N. Wong, "Experimental and numerical investigation of forced convection heat transfer in porous lattice structures produced by selective laser melting," *Int. J. Thermal Sci.*, vol. 137, pp. 276–287, Mar. 2019, doi: 10.1016/j.ijthermalsci.2018.11.022.

[129] X. Cheng and H. Wu, "Enhanced flow boiling performance in high-aspect-ratio groove-wall microchannels," *Int. J. Heat Mass Transf.*, vol. 164, Jan. 2021, Art. no. 120468, doi: 10.1016/j.ijheatmasstransfer.2020.120468.

[130] Y. Fan, P. S. Lee, L.-W. Jin, B. W. Chua, and D.-C. Zhang, "A parametric investigation of heat transfer and friction characteristics in cylindrical oblique fin minichannel heat sink," *Int. J. Heat Mass Transf.*, vol. 68, pp. 567–584, Jan. 2014, doi: 10.1016/j.ijheatmasstransfer.2013.09.027.

[131] Y. Li, G. Xia, Y. Jia, Y. Cheng, and J. Wang, "Experimental investigation of flow boiling performance in microchannels with and without triangular cavities—A comparative study," *Int. J. Heat Mass Transf.*, vol. 108, pp. 1511–1526, May 2017, doi: 10.1016/j.ijheatmasstransfer.2017.01.011.

[132] V. Kumar and J. Sarkar, "Experimental hydrothermal behavior of hybrid nanofluid for various particle ratios and comparison with other fluids in minichannel heat sink," *Int. Commun. Heat Mass Transf.*, vol. 110, Jan. 2020, Art. no. 104397, doi: 10.1016/j.icheatmasstransfer.2019.104397.

[133] S. Kumar, A. Kumar, A. D. Kothiyal, and M. S. Bisht, "A review of flow and heat transfer behaviour of nanofluids in micro channel heat sinks," *Thermal Sci. Eng. Prog.*, vol. 8, pp. 477–493, Dec. 2018, doi: 10.1016/j.tsep.2018.10.004.

[134] W. M. A. A. Japar, N. A. C. Sidik, S. R. Aid, Y. Asako, and T. L. Ken, "A comprehensive review on numerical and experimental study of nanofluid performance in microchannel heatsink (MCHS)," *J. Adv. Res. Fluid Mech. Thermal Sci.*, vol. 45, no. 1, pp. 165–176, 2018.

[135] G. Liang and I. Mudawar, "Review of single-phase and two-phase nanofluid heat transfer in macro-channels and micro-channels," *Int. J. Heat Mass Transf.*, vol. 136, pp. 324–354, Jun. 2019, doi: 10.1016/j.ijheatmasstransfer.2019.02.086.

[136] A. J. Chamkha, M. Molana, A. Rahnama, and F. Ghadami, "On the nanofluids applications in microchannels: A comprehensive review," *Powder Technol.*, vol. 332, pp. 287–322, Jun. 2018, doi: 10.1016/j.powtec.2018.03.044.

[137] Z. X. Li, U. Khaled, A. A. A. A. Al-Rashed, M. Goodarzi, M. M. Sarafraz, and R. Meer, "Heat transfer evaluation of a micro heat exchanger cooling with spherical carbon-acetone nanofluid," *Int. J. Heat Mass Transf.*, vol. 149, Mar. 2020, Art. no. 119124, doi: 10.1016/j.ijheatmasstransfer.2019.119124.

[138] Z. Lyu, F. Pourfattah, A. A. A. Arani, A. Asadi, and L. K. Foong, "On the thermal performance of a fractal microchannel subjected to water and kerosene carbon nanotube nanofluid," *Sci. Rep.*, vol. 10, no. 1, p. 7243, Apr. 2020, doi: 10.1038/s41598-020-64142-w.

[139] D. S. Saidina, M. Z. Abdullah, and M. Hussin, "Metal oxide nanofluids in electronic cooling: A review," *J. Mater. Sci., Mater. Electron.*, vol. 31, no. 6, pp. 4381–4398, Mar. 2020, doi: 10.1007/s10854-020-03020-7.

[140] A. Miner and U. Ghoshal, "Cooling of high-power-density microdevices using liquid metal coolants," *Appl. Phys. Lett.*, vol. 85, no. 3, pp. 506–508, Jul. 2004, doi: 10.1063/1.1772862.

[141] M. T. Sarowar, "Numerical analysis of a liquid metal cooled mini channel heat sink with five different ceramic substrates," *Ceram. Int.*, vol. 47, no. 1, pp. 214–225, Jan. 2021, doi: 10.1016/j.ceramint.2020.08.124.

[142] M. M. Sarafraz, J. Hart, E. Shrestha, H. Arya, and M. Arjomandi, "Experimental thermal energy assessment of a liquid metal eutectic in a microchannel heat exchanger equipped with a (10 Hz/50 Hz) resonator," *Appl. Thermal Eng.*, vol. 148, pp. 578–590, Feb. 2019, doi: 10.1016/j.applthermaleng.2018.11.073.

[143] S. G. Kandlikar, "History, advances, and challenges in liquid flow and flow boiling heat transfer in microchannels: A critical review," in *Proc. 14th Int. Heat Transfer Conf. 14th Int. Heat Transf. Conf.*, vol. 8. Washington, DC, USA: ASME, Aug. 2010, pp. 441–460, doi: 10.1115/IHTC14-23353.

[144] D. Deng, L. Zeng, and W. Sun, "A review on flow boiling enhancement and fabrication of enhanced microchannels of microchannel heat sinks," *Int. J. Heat Mass Transf.*, vol. 175, Aug. 2021, Art. no. 121332, doi: 10.1016/j.ijheatmasstransfer.2021.121332.

[145] N. Mao, J. Zhuang, T. He, and M. Song, "A critical review on measures to suppress flow boiling instabilities in microchannels," *Heat Mass Transf.*, vol. 57, no. 6, pp. 889–910, Jun. 2021, doi: 10.1007/s00231-020-03009-2.

[146] S. Raj, A. Shukla, M. Pathak, and M. K. Khan, "A novel stepped microchannel for performance enhancement in flow boiling," *Int. J. Heat Mass Transf.*, vol. 144, Dec. 2019, Art. no. 118611, doi: 10.1016/j.ijheatmasstransfer.2019.118611.

[147] S. K. Oudah, R. Fang, A. Tikadar, A. S. Salman, and J. A. Khan, "An experimental investigation of the effect of multiple inlet restrictors on the heat transfer and pressure drop in a flow boiling microchannel heat sink," *Int. J. Heat Mass Transf.*, vol. 153, Jun. 2020, Art. no. 119582, doi: 10.1016/j.ijheatmasstransfer.2020.119582.

[148] C. Ren, W. Li, J. Ma, G. Huang, and C. Li, "Flow boiling in microchannels enhanced by parallel microgrooves fabricated on the bottom surfaces," *Int. J. Heat Mass Transf.*, vol. 166, Feb. 2021, Art. no. 120756, doi: 10.1016/j.ijheatmasstransfer.2020.120756.

[149] A. Soleimani, A. Sattari, and P. Hanafizadeh, "Thermal analysis of a microchannel heat sink cooled by two-phase flow boiling of Al_2O_3 HFE-7100 nanofluid," *Thermal Sci. Eng. Prog.*, vol. 20, Dec. 2020, Art. no. 100693, doi: 10.1016/j.tsep.2020.100693.

[150] C. Zhang, L. Zhang, H. Xu, D. Wang, and B. Ye, "Investigation of flow boiling performance and the resulting surface deposition of graphene oxide nanofluid in microchannels," *Experim. Thermal Fluid Sci.*, vol. 86, pp. 1–10, Sep. 2017, doi: 10.1016/j.expthermflusci.2017.03.028.

[151] G. Liang and I. Mudawar, "Review of spray cooling—Part 1: Single-phase and nucleate boiling regimes, and critical heat flux," *Int. J. Heat Mass Transf.*, vol. 115, pp. 1174–1205, Dec. 2017, doi: 10.1016/j.ijheatmasstransfer.2017.06.029.

[152] G. Liang and I. Mudawar, "Review of spray cooling—Part 2: High temperature boiling regimes and quenching applications," *Int. J. Heat Mass Transf.*, vol. 115, pp. 1206–1222, Dec. 2017, doi: 10.1016/j.ijheatmasstransfer.2017.06.022.

[153] J. Kim, "Spray cooling heat transfer: The state of the art," *Int. J. Heat Fluid Flow*, vol. 28, no. 4, pp. 753–767, Aug. 2007, doi: 10.1016/j.ijheatfluidflow.2006.09.003.

[154] J. Breitenbach, I. V. Roisman, and C. Tropea, "From drop impact physics to spray cooling models: A critical review," *Experim. Fluids*, vol. 59, no. 3, pp. 1–21, Mar. 2018, doi: 10.1007/s00348-018-2514-3.

[155] J. D. Benther, J. D. Pelaez-Restrepo, C. Stanley, and G. Rosengarten, "Heat transfer during multiple droplet impingement and spray cooling: Review and prospects for enhanced surfaces," *Int. J. Heat Mass Transf.*, vol. 178, Oct. 2021, Art. no. 121587, doi: 10.1016/j.ijheatmasstransfer.2021.121587.

[156] M. R. Pais, L. C. Chow, and E. T. Mahefkey, "Surface roughness and its effects on the heat transfer mechanism in spray cooling," *J. Heat Transf.*, vol. 114, no. 1, pp. 211–219, Feb. 1992, doi: 10.1115/1.2911248.

[157] E. Martínez-Galván, R. Antón, J. C. Ramos, and R. Khodabandeh, "Influence of surface roughness on a spray cooling system with R134a. Part I: Heat transfer measurements," *Experim. Thermal Fluid Sci.*, vol. 46, pp. 183–190, Apr. 2013, doi: 10.1016/j.expthermflusci.2012.12.010.

[158] H. Fukuda, N. Nakata, H. Kijima, T. Kuroki, A. Fujibayashi, Y. Takata, and S. Hidaka, "Effects on surface conditions on spray cooling characteristics," *Tetsu-Hagane*, vol. 100, no. 12, pp. 1514–1522, 2014, doi: 10.2355/tetsutohagane.100.1514.

[159] K. Ali, R. Amna, M. Usman Rashid, M. I. Malik, and K. Kim, "An investigation of the influence of surface roughness, water quality and nozzle on spray cooling of aluminum alloy 6082," *Thermal Sci. Eng. Prog.*, vol. 10, pp. 280–286, May 2019, doi: 10.1016/j.tsep.2019.01.016.

[160] Y. Fang, H. Woche, and E. Specht, "Influence of surface roughness on heat transfer during quenching hot metals with different nozzles," *Heat Mass Transf.*, vol. 56, no. 8, pp. 2355–2365, Aug. 2020, doi: 10.1007/s00231-020-02864-3.

[161] Z.-F. Zhou, Y.-K. Lin, H.-L. Tang, Y. Fang, B. Chen, and Y.-C. Wang, ''Heat transfer enhancement due to surface modification in the close-loop R410A flash evaporation spray cooling,'' *Int. J. Heat Mass Transf.*, vol. 139, pp. 1047–1055, Aug. 2019, doi: 10.1016/j.ijheatmasstransfer.2019.05.063.

[162] H. Bostanci, D. P. Rini, J. P. Kizito, V. Singh, S. Seal, and L. C. Chow, ''High heat flux spray cooling with ammonia: Investigation of enhanced surfaces for HTC,'' *Int. J. Heat Mass Transf.*, vol. 75, pp. 718–725, Aug. 2014, doi: 10.1016/j.ijheatmasstransfer.2014.04.019.

[163] X. Zhao, B. Zhang, Z. Yang, and Y. Zhao, ''Surface orientation effects on heat transfer performance of spray cooling,'' *Int. J. Heat Mass Transf.*, vol. 147, Feb. 2020, Art. no. 118960, doi: 10.1016/j.ijheatmasstransfer.2019.118960.

[164] R.-N. Xu, L. Cao, G.-Y. Wang, J.-N. Chen, and P.-X. Jiang, ''Experimental investigation of closed loop spray cooling with micro- and hybrid micro-/nano-engineered surfaces,'' *Appl. Thermal Eng.*, vol. 180, Nov. 2020, Art. no. 115697, doi: 10.1016/j.applthermaleng.2020.115697.

[165] R. Xu, G. Wang, and P. Jiang, ''Spray cooling on enhanced surfaces: A review of the progress and mechanisms,'' *J. Electron. Packag.*, vol. 144, no. 1, Mar. 2022, Art. no. 010802, doi: 10.1115/1.4050046.

[166] B. H. Yang, H. Wang, X. Zhu, Q. Liao, Y. D. Ding, and R. Chen, ''Heat transfer enhancement of spray cooling with ammonia by microcavity surfaces,'' *Appl. Thermal Eng.*, vol. 50, no. 1, pp. 245–250, Jan. 2013, doi: 10.1016/j.applthermaleng.2012.06.029.

[167] X. Zhao, Z. Yin, B. Zhang, and Z. Yang, ''Experimental investigation of surface temperature non-uniformity in spray cooling,'' *Int. J. Heat Mass Transf.*, vol. 146, Jan. 2020, Art. no. 118819, doi: 10.1016/j.ijheatmasstransfer.2019.118819.

[168] L. Liu, X. Wang, M. Ge, and Y. Zhao, ''Experimental study on heat transfer and power consumption of low-pressure spray cooling,'' *Appl. Thermal Eng.*, vol. 184, Feb. 2021, Art. no. 116253, doi: 10.1016/j.applthermaleng.2020.116253.

[169] X. Liu, R. Xue, Y. Ruan, L. Chen, X. Zhang, and Y. Hou, ''Effects of injection pressure difference on droplet size distribution and spray cone angle in spray cooling of liquid nitrogen,'' *Cryogenics*, vol. 83, pp. 57–63, Apr. 2017, doi: 10.1016/j.cryogenics.2017.01.011.

[170] C. Cai, H. Liu, M. Jia, H. Yin, R. Xie, and P. Yan, ''Numerical investigation on heat transfer of water spray cooling from single-phase to nucleate boiling region,'' *Int. J. Thermal Sci.*, vol. 151, May 2020, Art. no. 106258, doi: 10.1016/j.ijthermalsci.2019.106258.

[171] J. L. Xie, Y. B. Tan, T. N. Wong, F. Duan, K. C. Toh, K. F. Choo, P. K. Chan, and Y. S. Chua, ''Multi-nozzle array spray cooling for large area high power devices in a closed loop system,'' *Int. J. Heat Mass Transf.*, vol. 78, pp. 1177–1186, Nov. 2014, doi: 10.1016/j.ijheatmasstransfer.2014.07.067.

[172] L.-J. Jiang, S.-L. Jiang, W.-L. Cheng, Y.-L. Nian, and R. Zhao, ''Experimental study on heat transfer performance of a novel compact spray cooling module,'' *Appl. Thermal Eng.*, vol. 154, pp. 150–156, May 2019, doi: 10.1016/j.applthermaleng.2019.03.078.

[173] Y. Hou, Y. Tao, X. Huai, Y. Zou, and D. Sun, ''Numerical simulation of multi-nozzle spray cooling heat transfer,'' *Int. J. Thermal Sci.*, vol. 125, pp. 81–88, Mar. 2018, doi: 10.1016/j.ijthermalsci.2017.11.011.

[174] Z. Zhang, Q. Li, and D. Hu, ''Experimental investigation on heat transfer characteristics of R1336mzz flash spray cooling,'' *Appl. Thermal Eng.*, vol. 174, Jun. 2020, Art. no. 115277, doi: 10.1016/j.applthermaleng.2020.115277.

[175] J. Bao, Y. Wang, X. Xu, X. Niu, J. Liu, and L. Qiu, *Analysis on the Influences of Atomization Characteristics on Heat Transfer Characteristics of Spray Cooling*. Amsterdam, The Netherlands: Elsevier, 2019, vol. 51, p. 101799, doi: 10.1007/978-981-13-9524-6_6.

[176] S.-S. Hsieh, H.-H. Liu, and Y.-F. Yeh, ''Nanofluids spray heat transfer enhancement,'' *Int. J. Heat Mass Transf.*, vol. 94, pp. 104–118, Mar. 2016, doi: 10.1016/j.ijheatmasstransfer.2015.11.061.

[177] M. Sanches, G. Marseglia, A. P. C. Ribeiro, A. L. N. Moreira, and A. S. Moita, ''Nanofluids characterization for spray cooling applications,'' *Symmetry*, vol. 13, no. 5, p. 788, May 2021, doi: 10.3390/sym13050788.

[178] A. R. Pati, A. Kumar, and S. S. Mohapatra, ''Upward and downward facing high mass flux spray cooling with additives: A novel technique to enhance the heat removal rate at high initial surface temperature,'' *Heat Mass Transf.*, vol. 54, no. 6, pp. 1669–1680, Jun. 2018, doi: 10.1007/s00231-017-2258-2.

[179] N. Liu, Z. Yu, T. Zhu, X. Yin, and H. Zhang, ''Effects of microstructured surface and mixed surfactants on the heat transfer performance of pulsed spray cooling,'' *Int. J. Thermal Sci.*, vol. 158, p. 106530, 2020, doi: 10.1016/j.ijthermalsci.2020.106530.

[180] H. Liu, C. Cai, M. Jia, J. Gao, H. Yin, and H. Chen, ''Experimental investigation on spray cooling with low-alcohol additives,'' *Appl. Thermal Eng.*, vol. 146, pp. 921–930, Jan. 2019, doi: 10.1016/j.applthermaleng.2018.10.054.

[181] J. D. Chapman, P. A. Kottke, and A. G. Fedorov, ''Enhanced thin film evaporation via impinging electrospray liquid jets with entrained air streaming,'' *Int. J. Heat Mass Transf.*, vol. 131, pp. 85–95, Mar. 2019, doi: 10.1016/j.ijheatmasstransfer.2018.11.049.

[182] S. Lohrasbi, R. Hammer, W. Essl, G. Reiss, S. Defregger, and W. Sanz, ''A comprehensive review on the core thermal management improvement concepts in power electronics,'' *IEEE Access*, vol. 8, pp. 166880–166906, 2020, doi: 10.1109/ACCESS.2020.3021946.

[183] Z. Tang, H. Li, F. Zhang, X. Min, and J. Cheng, ''Numerical study of liquid jet impingement flow and heat transfer of a cone heat sink,'' *Int. J. Numer. Methods Heat Fluid Flow*, vol. 29, no. 11, pp. 4074–4092, Nov. 2019, doi: 10.1108/hff-08-2018-0451.

[184] J. Jörg, S. Taraborrelli, G. Sarriegui, R. W. De Doncker, R. Kneer, and W. Rohlfs, ''Direct single impinging jet cooling of a MOSFET power electronic module,'' *IEEE Trans. Power Electron.*, vol. 33, no. 5, pp. 4224–4237, May 2018, doi: 10.1109/TPEL.2017.2720963.

[185] B. Kwon, T. Foulkes, T. Yang, N. Miljkovic, and W. P. King, ''Air jet impingement cooling of electronic devices using additively manufactured nozzles,'' *IEEE Trans. Compon., Packag., Manuf. Technol.*, vol. 10, no. 2, pp. 220–229, Feb. 2020, doi: 10.1109/TCPMT.2019.2936852.

[186] X. Gao and R. Li, ''Effects of nozzle positioning on single-phase spray cooling,'' *Int. J. Heat Mass Transf.*, vol. 115, pp. 1247–1257, Dec. 2017, doi: 10.1016/j.ijheatmasstransfer.2017.08.095.

[187] M. Sabato, A. Fregni, E. Stalio, F. Brusiani, M. Tranchero, and T. Baritaud, ''Numerical study of submerged impinging jets for power electronics cooling,'' *Int. J. Heat Mass Transf.*, vol. 141, pp. 707–718, Oct. 2019, doi: 10.1016/j.ijheatmasstransfer.2019.06.081.

[188] R. Wu, T. Hong, Q. Cheng, H. Zou, Y. Fan, and X. Luo, ''Thermal modeling and comparative analysis of jet impingement liquid cooling for high power electronics,'' *Int. J. Heat Mass Transf.*, vol. 137, pp. 42–51, Jul. 2019, doi: 10.1016/j.ijheatmasstransfer.2019.03.112.

[189] R. Nadda, A. Kumar, and R. Maithani, ''Efficiency improvement of solar photovoltaic/solar air collectors by using impingement jets: A review,'' *Renew. Sustain. Energy Rev.*, vol. 93, pp. 331–353, Oct. 2018, doi: 10.1016/j.rser.2018.05.025.

[190] T.-W. Wei, H. Oprins, V. Cherman, G. Van der Plas, I. De Wolf, E. Beyne, and M. Baelmans, ''Experimental characterization and model validation of liquid jet impingement cooling using a high spatial resolution and programmable thermal test chip,'' *Appl. Thermal Eng.*, vol. 152, pp. 308–318, Apr. 2019, doi: 10.1016/j.applthermaleng.2019.02.075.

[191] J.-Y. San and J.-J. Chen, ''Effects of jet-to-jet spacing and jet height on heat transfer characteristics of an impinging jet array,'' *Int. J. Heat Mass Transf.*, vol. 71, pp. 8–17, Apr. 2014, doi: 10.1016/j.ijheatmasstransfer.2013.11.079.

[192] P. Singh, K. Nithyanandam, and R. L. Mahajan, ''An experimental and numerical investigation of forced convection in high porosity aluminum foams subjected to jet array impingement in channel-flow,'' *Int. J. Heat Mass Transf.*, vol. 149, Mar. 2020, Art. no. 119107, doi: 10.1016/j.ijheatmasstransfer.2019.119107.

[193] S. C. Godi, A. Pattamatta, and C. Balaji, ''Heat transfer from a single and row of three dimensional wall jets—A combined experimental and numerical study,'' *Int. J. Heat Mass Transf.*, vol. 159, Oct. 2020, Art. no. 119801, doi: 10.1016/j.ijheatmasstransfer.2020.119801.

[194] F. Gao, Y. Chen, J. Cai, and C. Ma, ''Experimental study of free-surface jet impingement heat transfer with molten salt,'' *Int. J. Heat Mass Transf.*, vol. 149, Mar. 2020, Art. no. 119160, doi: 10.1016/j.ijheatmasstransfer.2019.119160.

[195] W. Wu, H. Bostanci, L. C. Chow, S. J. Ding, Y. Hong, M. Su, J. P. Kizito, L. Gschwender, and C. E. Snyder, ''Jet impingement and spray cooling using slurry of nanoencapsulated phase change materials,'' *Int. J. Heat Mass Transf.*, vol. 54, nos. 13–14, pp. 2715–2723, Jun. 2011, doi: 10.1016/j.ijheatmasstransfer.2011.03.022.

[196] M. M. U. Rehman, Z. G. Qu, R. P. Fu, and H. T. Xu, ''Numerical study on free-surface jet impingement cooling with nanoencapsulated phase-change material slurry and nanofluid,'' *Int. J. Heat Mass Transf.*, vol. 109, pp. 312–325, Jun. 2017, doi: 10.1016/j.ijheatmasstransfer.2017.01.094.

[197] F. Selimefendigil and H. F. Öztop, "Effects of nanoparticle shape on slot-jet impingement cooling of a corrugated surface with nanofluids," *J. Thermal Sci. Eng. Appl.*, vol. 9, no. 2, Jun. 2017, Art. no. 021016, doi: 10.1115/1.4035811.

[198] R. Ekiciler, M. S. A. Çetinkaya, and K. Arslan, "Effect of shape of nanoparticle on heat transfer and entropy generation of nanofluid-jet impingement cooling," *Int. J. Green Energy*, vol. 17, no. 10, pp. 555–567, Aug. 2020, doi: 10.1080/15435075.2020.1739692.

[199] P. Naphon, L. Nakharintr, and S. Wiriyasart, "Continuous nanofluids jet impingement heat transfer and flow in a micro-channel heat sink," *Int. J. Heat Mass Transf.*, vol. 126, pp. 924–932, Nov. 2018, doi: 10.1016/j.ijheatmasstransfer.2018.05.101.

[200] M. Amjadian, H. Safarzadeh, M. Bahiraei, S. Nazari, and B. Jaberi, "Heat transfer characteristics of impinging jet on a hot surface with constant heat flux using Cu_2O-water nanofluid: An experimental study," *Int. Commun. Heat Mass Transf.*, vol. 112, Mar. 2020, Art. no. 104509, doi: 10.1016/j.icheatmasstransfer.2020.104509.

[201] S. D. Barewar and S. S. Chougule, "Heat transfer characteristics and boiling heat transfer performance of novel Ag/ZnO hybrid nanofluid using free surface jet impingement," *Experim. Heat Transf.*, vol. 34, no. 6, pp. 531–546, Sep. 2021, doi: 10.1080/08916152.2020.1792587.

[202] P. A. K. Lam and K. A. Prakash, "Thermodynamic investigation and multi-objective optimization for jet impingement cooling system with Al_2O_3/water nanofluid," *Energy Convers. Manag.*, vol. 111, pp. 38–56, Mar. 2016, doi: 10.1016/j.enconman.2015.12.018.

[203] B. Boudraa and R. Bessaïh, "Numerical investigation of jet impingement cooling an isothermal surface using extended jet holes with various binary hybrid nanofluids," *Int. Commun. Heat Mass Transf.*, vol. 127, Oct. 2021, Art. no. 105560, doi: 10.1016/j.icheatmasstransfer.2021.105560.

[204] J. Sodagar-Abardeh, A. Edalati-nejad, K. Torkamani, and P. Nasery, "CFD modeling and analysis of effect of nanoparticle shape on heat transfer of confined slot-jet impingement with nanofluid," *Microfluidics Nanofluidics*, vol. 25, no. 6, p. 49, Jun. 2021, doi: 10.1007/s10404-021-02451-w.

[205] W. Wu, L. C. Chow, C. M. Wang, M. Su, and J. P. Kizito, "Jet impingement heat transfer using a Field's alloy nanoparticle—HFE7100 slurry," *Int. J. Heat Mass Transf.*, vol. 68, pp. 357–365, Jan. 2014, doi: 10.1016/j.ijheatmasstransfer.2013.09.029.

[206] P. S. Bhansali, K. R. Ramakrishnan, and S. V. Ekkad, "Effect of pin fins on jet impingement heat transfer over a rotating disk," *J. Heat Transf.*, vol. 144, no. 4, Apr. 2022, Art. no. 042303, doi: 10.1115/1.4053371.

[207] S. Wiriyasart and P. Naphon, "Heat spreading of liquid jet impingement cooling of cold plate heat sink with different fin shapes," *Case Stud. Thermal Eng.*, vol. 20, Aug. 2020, Art. no. 100638, doi: 10.1016/j.csite.2020.100638.

[208] A. Ravanji and M. R. Zargarabadi, "Effects of elliptical pin-fins on heat transfer characteristics of a single impinging jet on a concave surface," *Int. J. Heat Mass Transf.*, vol. 152, May 2020, Art. no. 119532, doi: 10.1016/j.ijheatmasstransfer.2020.119532.

[209] S. Ndao, Y. Peles, and M. K. Jensen, "Experimental investigation of flow boiling heat transfer of jet impingement on smooth and micro structured surfaces," *Int. J. Heat Mass Transf.*, vol. 55, nos. 19–20, pp. 5093–5101, Sep. 2012, doi: 10.1016/j.ijheatmasstransfer.2012.05.009.

[210] D. Zhang, H. Qu, J. Lan, J. Chen, and Y. Xie, "Flow and heat transfer characteristics of single jet impinging on protrusioned surface," *Int. J. Heat Mass Transf.*, vol. 58, nos. 1–2, pp. 18–28, Mar. 2013, doi: 10.1016/j.ijheatmasstransfer.2012.11.019.

[211] E. Öztekin, O. Aydin, and M. Avci, "Heat transfer in a turbulent slot jet flow impinging on concave surfaces," *Int. Commun. Heat Mass Transf.*, vol. 44, pp. 77–82, May 2013, doi: 10.1016/j.icheatmasstransfer.2013.03.006.

[212] P. Xu, A. P. Sasmito, S. Qiu, A. S. Mujumdar, L. Xu, and L. Geng, "Heat transfer and entropy generation in air jet impingement on a model rough surface," *Int. Commun. Heat Mass Transf.*, vol. 72, pp. 48–56, Mar. 2016, doi: 10.1016/j.icheatmasstransfer.2016.01.007.

[213] R. D. Plant, J. Friedman, and M. Z. Saghir, "A review of jet impingement cooling," *Int. J. Thermofluids*, vol. 17, Feb. 2023, Art. no. 100312, doi: 10.1016/j.ijft.2023.100312.

[214] S. V. Ekkad and P. Singh, "A modern review on jet impingement heat transfer methods," *J. Heat Transf.*, vol. 143, no. 6, Jun. 2021, Art. no. 064001, doi: 10.1115/1.4049496.

[215] I. W. Kuncoro, N. A. Pambudi, M. K. Biddinika, I. Widiastuti, M. Hijriawan, and K. M. Wibowo, "Immersion cooling as the next technology for data center cooling: A review," *J. Phys., Conf.*, vol. 1402, no. 4, Dec. 2019, Art. no. 044057, doi: 10.1088/1742-6596/1402/4/044057.

[216] N. A. Pambudi, A. Sarifudin, R. A. Firdaus, D. K. Ulfa, I. M. Gandidi, and R. Romadhon, "The immersion cooling technology: Current and future development in energy saving," *Alexandria Eng. J.*, vol. 61, no. 12, pp. 9509–9527, Dec. 2022, doi: 10.1016/j.aej.2022.02.059.

[217] C. Roe, X. Feng, G. White, R. Li, H. Wang, X. Rui, C. Li, F. Zhang, V. Null, M. Parkes, Y. Patel, Y. Wang, H. Wang, M. Ouyang, G. Offer, and B. Wu, "Immersion cooling for lithium-ion batteries—A review," *J. Power Sources*, vol. 525, Mar. 2022, Art. no. 231094, doi: 10.1016/j.jpowSources2022.231094.

[218] P. Dwivedi, K. Sudhakar, A. Soni, E. Solomin, and I. Kirpichnikova, "Advanced cooling techniques of PV modules: A state of art," *Case Stud. Thermal Eng.*, vol. 21, Oct. 2020, Art. no. 100674, doi: 10.1016/j.csite.2020.100674.

[219] M. Suresh Patil, J.-H. Seo, and M.-Y. Lee, "A novel dielectric fluid immersion cooling technology for Li-ion battery thermal management," *Energy Convers. Manag.*, vol. 229, Feb. 2021, Art. no. 113715, doi: 10.1016/j.enconman.2020.113715.

[220] P. Birbarah, T. Gebrael, T. Foulkes, A. Stillwell, A. Moore, R. Pilawa-Podgurski, and N. Miljkovic, "Water immersion cooling of high power density electronics," *Int. J. Heat Mass Transf.*, vol. 147, Feb. 2020, Art. no. 118918, doi: 10.1016/j.ijheatmasstransfer.2019.118918.

[221] I. W. Kuncoro, N. A. Pambudi, M. K. Biddinika, and C. W. Budiyanto, "Optimization of immersion cooling performance using the Taguchi method," *Case Stud. Thermal Eng.*, vol. 21, Oct. 2020, Art. no. 100729, doi: 10.1016/j.csite.2020.100729.

[222] A. Ali, "Thermal performance and stress analysis of heat spreaders for immersion cooling applications," *Appl. Thermal Eng.*, vol. 181, Nov. 2020, Art. no. 115984, doi: 10.1016/j.applthermaleng.2020.115984.

[223] X. Kang, Y. Wang, Q. Huang, Y. Cui, C. Wang, C. Wen, and J. Fan, "Phase-change immersion cooling high power light emitting diodes and heat transfer improvement," *Microelectron. Rel.*, vol. 79, pp. 257–264, Dec. 2017, doi: 10.1016/j.microrel.2017.05.033.

[224] A. Niazmand, P. Murthy, S. Saini, P. Shahi, P. Bansode, and D. Agonafer, "Numerical analysis of oil immersion cooling of a server using mineral oil and Al_2O_3 nanofluid," in *Proc. ASME Int. Tech. Conf. Exhib. Packag. Integr. Electron. Photonic Microsystems*, Oct. 2020, doi: 10.1115/ipack2020-2662.

[225] Y.-T. Hsu, J.-X. Li, and M.-C. Lu, "Enhanced immersion cooling using two-tier micro- and nano-structures," *Appl. Thermal Eng.*, vol. 131, pp. 864–873, Feb. 2018, doi: 10.1016/j.applthermaleng.2017.12.067.

[226] S. Zhang, D. Feng, L. Shi, L. Wang, Y. Jin, L. Tian, Z. Li, G. Wang, L. Zhao, and Y. Yan, "A review of phase change heat transfer in shape-stabilized phase change materials (ss-PCMs) based on porous supports for thermal energy storage," *Renew. Sustain. Energy Rev.*, vol. 135, Jan. 2021, Art. no. 110127, doi: 10.1016/j.rser.2020.110127.

[227] P. B. Salunkhe and P. S. Shembekar, "A review on effect of phase change material encapsulation on the thermal performance of a system," *Renew. Sustain. Energy Rev.*, vol. 16, no. 8, pp. 5603–5616, Oct. 2012, doi: 10.1016/j.rser.2012.05.037.

[228] X.-H. Yang, S.-C. Tan, Z.-Z. He, and J. Liu, "Finned heat pipe assisted low melting point metal PCM heat sink against extremely high power thermal shock," *Energy Convers. Manag.*, vol. 160, pp. 467–476, Mar. 2018, doi: 10.1016/j.enconman.2018.01.056.

[229] J. Krishna, P. S. Kishore, and A. B. Solomon, "Heat pipe with nano enhanced-PCM for electronic cooling application," *Experim. Thermal Fluid Sci.*, vol. 81, pp. 84–92, Feb. 2017, doi: 10.1016/j.expthermflusci.2016.10.014.

[230] A. Farzanehnia, M. Khatibi, M. Sardarabadi, and M. Passandideh-Fard, "Experimental investigation of multiwall carbon nanotube/paraffin based heat sink for electronic device thermal management," *Energy Convers. Manag.*, vol. 179, pp. 314–325, Jan. 2019, doi: 10.1016/j.enconman.2018.10.037.

[231] A. Arshad, M. Jabbal, L. Shi, J. Darkwa, N. J. Weston, and Y. Yan, "Development of TiO2/RT–35HC based nanocomposite phase change materials (NCPCMs) for thermal management applications," *Sustain. Energy Technol. Assessments*, vol. 43, Feb. 2021, Art. no. 100865, doi: 10.1016/j.seta.2020.100865.

[232] A. Arshad, M. Jabbal, and Y. Yan, "Preparation and characteristics evaluation of mono and hybrid nano-enhanced phase change materials (NePCMs) for thermal management of microelectronics," *Energy Convers. Manag.*, vol. 205, Feb. 2020, Art. no. 112444, doi: 10.1016/j.enconman.2019.112444.

[233] A. Arshad, M. Jabbal, L. Shi, and Y. Yan, "Thermophysical characteristics and enhancement analysis of carbon-additives phase change mono and hybrid materials for thermal management of electronic devices," *J. Energy Storage*, vol. 34, Feb. 2021, Art. no. 102231, doi: 10.1016/j.est.2020.102231.

[234] H. M. Ali, M. J. Ashraf, A. Giovannelli, M. Irfan, T. B. Irshad, H. M. Hamid, F. Hassan, and A. Arshad, "Thermal management of electronics: An experimental analysis of triangular, rectangular and circular pin-fin heat sinks for various PCMs," *Int. J. Heat Mass Transf.*, vol. 123, pp. 272–284, Aug. 2018, doi: 10.1016/j.ijheatmasstransfer.2018.02.044.

[235] J. Xie, K. F. Choo, J. Xiang, and H. M. Lee, "Characterization of natural convection in a PCM-based heat sink with novel conductive structures," *Int. Commun. Heat Mass Transf.*, vol. 108, Nov. 2019, Art. no. 104306, doi: 10.1016/j.icheatmasstransfer.2019.104306.

[236] A. N. Desai, H. Shah, and V. K. Singh, "Novel inverted fin configurations for enhancing the thermal performance of PCM based thermal control unit: A numerical study," *Appl. Thermal Eng.*, vol. 195, Aug. 2021, Art. no. 117155, doi: 10.1016/j.applthermaleng.2021.117155.

[237] S. Mahmoud, A. Tang, C. Toh, R. Al-Dadah, and S. L. Soo, "Experimental investigation of inserts configurations and PCM type on the thermal performance of PCM based heat sinks," *Appl. Energy*, vol. 112, pp. 1349–1356, Dec. 2013, doi: 10.1016/j.apenergy.2013.04.059.

[238] N. S. Bondareva and M. A. Sheremet, "Conjugate heat transfer in the PCM-based heat storage system with finned copper profile: Application in electronics cooling," *Int. J. Heat Mass Transf.*, vol. 124, pp. 1275–1284, Sep. 2018, doi: 10.1016/j.ijheatmasstransfer.2018.04.040.

[239] R. Kalbasi, M. Afrand, J. Alsarraf, and M.-D. Tran, "Studies on optimum fins number in PCM-based heat sinks," *Energy*, vol. 171, pp. 1088–1099, Mar. 2019, doi: 10.1016/j.energy.2019.01.070.

[240] A. Mosavi, H. Mehdizadeh, S. Abbasian-Naghneh, R. Kalbasi, A. Karimipour, and G. Cheraghian, "Incorporation of horizontal fins into a PCM-based heat sink to enhance the safe operation time: Applicable in electronic device cooling," *Appl. Sci.*, vol. 10, no. 18, p. 6308, Sep. 2020, doi: 10.3390/app10186308.

[241] H. Behi, M. Ghanbarpour, and M. Behi, "Investigation of PCM-assisted heat pipe for electronic cooling," *Appl. Thermal Eng.*, vol. 127, pp. 1132–1142, Dec. 2017, doi: 10.1016/j.applthermaleng.2017.08.109.

[242] K. Ma and F. Blaabjerg, "Modulation methods for neutral-point-clamped wind power converter achieving loss and thermal redistribution under low-voltage ride-through," *IEEE Trans. Ind. Electron.*, vol. 61, no. 2, pp. 835–845, Feb. 2014, doi: 10.1109/TIE.2013.2254099.

[243] S. Alepuz, J. Nicolás-Apruzzese, R. Rafiezadeh, S. Busquets-Monge, M. Raya, and À. Filba-Martínez, "Active thermal control in neutral-point-clamped multilevel converters based on switching-cell arrays," *Electronics*, vol. 12, no. 19, p. 4055, Sep. 2023, doi: 10.3390/electronics12194055.

[244] S. Mersche, R. Schreier, P. Himmelmann, and M. Hiller, "Medium voltage power electronic building block for quasi-two-level operation of a flying capacitor converter," in *Proc. 23rd Eur. Conf. Power Electron. Appl. (EPE ECCE Europe)*, Sep. 2021, pp. 1–10, doi: 10.23919/EPE21ECCEEurope50061.2021.9570590.

[245] S. Xu, J. Zhang, and J. Hang, "Investigation of a fault-tolerant three-level T-type inverter system," *IEEE Trans. Ind. Appl.*, vol. 53, no. 5, pp. 4613–4623, Sep. 2017, doi: 10.1109/TIA.2017.2697844.

[246] B. Fan, V. Blasko, R. Burgos, and D. Boroyevich, "A general carrier-based modulation and capacitor-voltage balancing method for multilevel matrix converters (AC-AC stacked multicell Converters)," in *Proc. IEEE Appl. Power Electron. Conf. Expo. (APEC)*, Mar. 2020, pp. 1230–1235, doi: 10.1109/APEC39645.2020.9124540.

[247] S. Choudhury, M. Bajaj, T. Dash, S. Kamel, and F. Jurado, "Multilevel inverter: A survey on classical and advanced topologies, control schemes, applications to power system and future prospects," *Energies*, vol. 14, no. 18, p. 5773, Sep. 2021, doi: 10.3390/en14185773.

[248] Y. Hinago and H. Koizumi, "A single-phase multilevel inverter using switched series/parallel DC voltage sources," *IEEE Trans. Ind. Electron.*, vol. 57, no. 8, pp. 2643–2650, Aug. 2010, doi: 10.1109/TIE.2009.2030204.

[249] M. Narimani, B. Wu, Z. Cheng, and N. R. Zargari, "A new nested neutral point-clamped (NNPC) converter for medium-voltage (MV) power conversion," *IEEE Trans. Power Electron.*, vol. 29, no. 12, pp. 6375–6382, Dec. 2014, doi: 10.1109/TPEL.2014.2306191.

[250] A. Moghassemi, L. Timilsina, S. I. Rahman, A. Arsalan, P. K. Chamarthi, G. Ozkan, B. Papari, C. Edrington, and Z. Zhang, "Nearest level control based modular multi-level converters for power electronics building blocks in electric ship system," in *Proc. IEEE Transp. Electrific. Conf. Expo (ITEC)*, Rosemont, IL, USA, Oct. 2024.

[251] K. Ma, F. Blaabjerg, and M. Liserre, "Operation and thermal loading of three-level neutral-point-clamped wind power converter under various grid faults," in *Proc. IEEE Energy Convers. Congr. Expo. (ECCE)*, Sep. 2012, pp. 2410–2418, doi: 10.1109/ECCE.2012.6342408.

[252] Y. Dong, H. Yang, W. Li, and X. He, "Neutral-point-shift-based active thermal control for a modular multilevel converter under a single-phase-to-ground fault," *IEEE Trans. Ind. Electron.*, vol. 66, no. 3, pp. 2474–2484, Mar. 2019, doi: 10.1109/TIE.2018.2833019.

[253] W. Li, H. Yang, J. Sheng, C. Li, M. Chen, X. He, and X. Gu, "Thermal optimization of modular multilevel converters with surplus submodule active-bypass plus neutral-point-shift scheme under unbalanced grid conditions," *IEEE J. Emerg. Sel. Topics Power Electron.*, vol. 7, no. 3, pp. 1777–1788, Sep. 2019, doi: 10.1109/JESTPE.2019.2921795.

[254] F. Deng, J. Zhao, C. Liu, Z. Wang, X. Cai, and F. Blaabjerg, "Temperature-balancing control for modular multilevel converters under unbalanced grid voltages," *IEEE Trans. Power Electron.*, vol. 37, no. 4, pp. 4614–4625, Apr. 2022, doi: 10.1109/TPEL.2021.3123634.

[255] A. V. Rocha, H. de Paula, M. E. dos Santos, and B. J. C. Filho, "A thermal management approach to fault-resilient design of three-level IGCT-based NPC converters," *IEEE Trans. Ind. Appl.*, vol. 49, no. 6, pp. 2684–2691, Nov. 2013, doi: 10.1109/TIA.2013.2265935.

[256] L. Cheli and C. Carcasci, "Model-based development of a diagnostic algorithm for central inverter thermal management system fault detection and isolation," in *Proc. 5th Int. Conf. Syst. Rel. Saf. (ICSRS)*, Nov. 2021, pp. 14–21, doi: 10.1109/ICSRS53853.2021.9660763.

[257] H. Wang, R. Zhu, H. Wang, M. Liserre, and F. Blaabjerg, "A thermal modeling method considering ambient temperature dynamics," *IEEE Trans. Power Electron.*, vol. 35, no. 1, pp. 6–9, Jan. 2020, doi: 10.1109/TPEL.2019.2924723.

[258] K. Wei, P. Shi, P. Bao, X. Gao, Y. Du, and Y. Qin, "Thermal analysis and junction temperature estimation under different ambient temperatures considering convection thermal coupling between power devices," *Appl. Sci.*, vol. 13, no. 8, p. 5209, Apr. 2023, doi: 10.3390/app13085209.

[259] J. Zhang, J. Wang, and X. Cai, "Active thermal control-based anticondensation strategy in paralleled wind power converters by adjusting reactive circulating current," *IEEE J. Emerg. Sel. Topics Power Electron.*, vol. 6, no. 1, pp. 277–291, Mar. 2018, doi: 10.1109/JESTPE.2017.2741447.

[260] X. Yu, X. Wang, Y. Hu, T. Niu, B. Hu, and K. Xie, "Effect of relative humidity on reliability of wind power converter and its application to wind farm reliability evaluation," in *Proc. 4th Int. Conf. Energy, Electr. Power Eng. (CEEPE)*, Apr. 2021, pp. 470–475, doi: 10.1109/CEEPE51765.2021.9475754.

[261] Z. Owens, L. Gilman, R. Dunne, J. McNulty, and A. Kemal, "Evaluation of breathable enclosures for thermal management of outdoor electronics," in *Proc. 16th IEEE Intersociety Conf. Thermal Thermomechanical Phenomena Electron. Syst. (ITherm)*, May 2017, pp. 6–12, doi: 10.1109/ITHERM.2017.7991850.

[262] E. M. Racine, "Experimental study-high altitude forced convective cooling of electromechanical actuation systems," M.S. thesis, Dept. Aerosp. Eng., Univ. Dayton, Dayton, OH, USA, 2015. [Online]. Available: http://rave.ohiolink.edu/etdc/view?acc_num=dayton1450286609

[263] C.-W. Chang, X. Zhao, R. Phukan, R. Burgos, S. Uicich, P. Asfaux, and D. Dong, "Thermal consideration and design for a 200-kW SiC-based high-density three-phase inverter in more electric aircraft," *IEEE J. Emerg. Sel. Topics Power Electron.*, vol. 11, no. 6, pp. 5910–5929, Dec. 2023, doi: 10.1109/JESTPE.2023.3308854.

[264] M. L. Elsayed, O. Mesalhy, J. P. Kizito, Q. H. Leland, and L. C. Chow, "Performance of a guided plate heat sink at high altitude," *Int. J. Heat Mass Transf.*, vol. 147, Feb. 2020, Art. no. 118926, doi: 10.1016/j.ijheatmasstransfer.2019.118926.

[265] X. Li, W. Song, Q. Wang, H. Li, X. Ding, and S. Liu, "Optimizing cooling electronic chips at high altitude with consideration of solar radiation," *Int. J. Thermal Sci.*, vol. 183, Jan. 2023, Art. no. 107879, doi: 10.1016/j.ijthermalsci.2022.107879.

[266] L. Dorn-Gomba, J. Ramoul, J. Reimers, and A. Emadi, "Power electronic converters in electric aircraft: Current status, challenges, and emerging technologies," *IEEE Trans. Transport. Electrific.*, vol. 6, no. 4, pp. 1648–1664, Dec. 2020, doi: 10.1109/TTE.2020.3006045.

[267] A. Sakanova, C. F. Tong, K. J. Tseng, R. Simanjorang, and A. K. Gupta, "Weight consideration of liquid metal cooling technology for power electronics converter in future aircraft," in *Proc. IEEE 2nd Annu. Southern Power Electron. Conf. (SPEC)*, Dec. 2016, pp. 1–5, doi: 10.1109/SPEC.2016.7846113.

[268] F. Blaabjerg, H. Wang, I. Vernica, B. Liu, and P. Davari, "Reliability of power electronic systems for EV/HEV applications," *Proc. IEEE*, vol. 109, no. 6, pp. 1060–1076, Jun. 2021, doi: 10.1109/JPROC.2020.3031041.

[269] Y. Wang, X. Dai, G. Liu, Y. Wu, Y. Li, and S. Jones, "Status and trend of power semiconductor module packaging for electric vehicles," in *Modeling and Simulation for Electric Vehicle Applications*. Rijeka, Croatia: IntechOpen, 2016, ch. 2, doi: 10.5772/64173.

[270] Z. Tang, Y. Yang, and F. Blaabjerg, "Power electronics: The enabling technology for renewable energy integration," *CSEE J. Power Energy Syst.*, vol. 8, no. 1, pp. 39–52, Jan. 2022, doi: 10.17775/CSEEJPES.2021.02850.

[271] Y. Yang, H. Wang, F. Blaabjerg, and T. Kerekes, "A hybrid power control concept for PV inverters with reduced thermal loading," *IEEE Trans. Power Electron.*, vol. 29, no. 12, pp. 6271–6275, Dec. 2014, doi: 10.1109/TPEL.2014.2332754.

[272] J. Zhang, X. Du, C. Qian, R. Du, X. Hu, and H.-M. Tai, "Thermal management of IGBT module in the wind power converter based on the ROI," *IEEE Trans. Ind. Electron.*, vol. 69, no. 8, pp. 8513–8523, Aug. 2022, doi: 10.1109/TIE.2021.3108729.

[273] J. Peng, W. Lan, Y. Wang, Y. Ma, and X. Luo, "Thermal management of the high-power electronics in high temperature downhole environment," in *Proc. IEEE 22nd Electron. Packag. Technol. Conf. (EPTC)*, Dec. 2020, pp. 369–375, doi: 10.1109/EPTC50525.2020.9315026.

[274] W. He, C. Ma, S. Zhang, H. Yue, Q. Xu, and W. Song, "An active thermal control scheme of three-level NPC inverters," in *Proc. IEEE 17th Conf. Ind. Electron. Appl. (ICIEA)*, Dec. 2022, pp. 540–544, doi: 10.1109/ICIEA54703.2022.10006222.

[275] M. Xia, Y. Xia, Y. Ding, S. Li, W. Mingyuan, J. Zhao, and S. Ding, "Active thermal control based on hybrid modulation strategy for MMCs," in *Proc. IEEE 18th Conf. Ind. Electron. Appl. (ICIEA)*, Aug. 2023, pp. 937–942, doi: 10.1109/ICIEA58696.2023.10241770.

[276] A. Tcai, T. Wijekoon, and M. Liserre, "Thermal control of quasi-2-level super-switch by power routing," *IEEE Trans. Ind. Electron.*, vol. 71, no. 1, pp. 360–368, Jan. 2024, doi: 10.1109/TIE.2023.3247765.

[277] V. Raveendran, M. Andresen, G. Buticchi, and M. Liserre, "Thermal stress based power routing of smart transformer with CHB and DAB converters," *IEEE Trans. Power Electron.*, vol. 35, no. 4, pp. 4205–4215, Apr. 2020, doi: 10.1109/TPEL.2019.2935249.

[278] P. R. Badr, G. Ozkan, P. Hoang, C. S. Edrington, and T. Parker, "Multi-objective finite control set model predictive control for interior permanent magnet motors in electric/hybrid-electric vehicles," SAE Int., Detroit, MI, USA, Tech. Paper 2022-01-0357, 2022, doi: 10.4271/2022-01-0357.

[279] S. I. Rahman, A. Moghassemi, L. Timilsina, P. Ramezani-Badr, Q. Zhu, R. Prucka, G. Ozkan, and C. Edrington, "Model-based active thermal management for neutral-point clamped power converter with adaptive weight," in *Proc. IEEE Transp. Electrific. Conf. Expo (ITEC)*, Rosemont, IL, USA, Oct. 2024.

[280] J. Padilla, J. S. Chalfant, C. Chryssostomidis, and C. M. Cooke, "Preliminary investigation into liquid-cooled PEBBs," in *Proc. IEEE Electric Ship Technol. Symp. (ESTS)*, Aug. 2021, pp. 1–9, doi: 10.1109/ESTS49166.2021.9512330.

[281] S. Yang, J. Chalfant, J. Ordonez, J. Khan, C. Li, I. Cvetkovic, J. Vargas, M. Chagas, Y. Xu, and R. Burgos, "Shipboard PEBB cooling strategies," in *Proc. IEEE Electric Ship Technol. Symp. (ESTS)*, Sep. 2019, pp. 24–31, doi: 10.1109/ESTS.2019.8847810.

[282] J. Stewart, J. Motwani, J. Yu, I. Cvetkovic, and R. Burgos, "Improved power density of a 6 kV, 1 mW power electronics building block through insulation coordination," in *Proc. IEEE 23rd Workshop Control Model. Power Electron. (COMPEL)*, Jun. 2022, pp. 1–7, doi: 10.1109/COMPEL53829.2022.9829968.

[283] A. M. Alcaide, G. Buticchi, A. Chub, and L. Dalessandro, "Design and control for high-reliability power electronics: State-of-the-art and future trends," *IEEE J. Emerg. Sel. Topics Ind. Electron.*, vol. 5, no. 1, pp. 50–61, Jan. 2024, doi: 10.1109/JESTIE.2023.3287513.

[284] E. Abramushkina, A. Zhaksylyk, T. Geury, M. El Baghdadi, and O. Hegazy, "A thorough review of cooling concepts and thermal management techniques for automotive WBG inverters: Topology, technology and integration level," *Energies*, vol. 14, no. 16, p. 4981, Aug. 2021, doi: 10.3390/en14164981.

[285] A. B. Solomon, A. K. Mahto, R. C. Joy, A. A. Rajan, D. A. Jayprakash, A. Dixit, and A. Sahay, "Application of bio-wick in compact loop heat pipe," *Appl. Thermal Eng.*, vol. 169, Mar. 2020, Art. no. 114927, doi: 10.1016/j.applthermaleng.2020.114927.

[286] Z.-Q. Zhu, Y.-K. Huang, N. Hu, Y. Zeng, and L.-W. Fan, "Transient performance of a PCM-based heat sink with a partially filled metal foam: Effects of the filling height ratio," *Appl. Thermal Eng.*, vol. 128, pp. 966–972, Jan. 2018, doi: 10.1016/j.applthermaleng.2017.09.047.

[287] W. Zhou, Y. Li, Z. Chen, L. Deng, and Y. Gan, "A novel ultra-thin flattened heat pipe with biporous spiral woven mesh wick for cooling electronic devices," *Energy Convers. Manag.*, vol. 180, pp. 769–783, Jan. 2019, doi: 10.1016/j.enconman.2018.11.031.

[288] L. Ventola, G. Curcuruto, M. Fasano, S. Fotia, V. Pugliese, E. Chiavazzo, and P. Asinari, "Unshrouded plate fin heat sinks for electronics cooling: Validation of a comprehensive thermal model and cost optimization in semi-active configuration," *Energies*, vol. 9, no. 8, p. 608, Aug. 2016, doi: 10.3390/en9080608.

[289] A. J. Robinson, "A thermal–hydraulic comparison of liquid microchannel and impinging liquid jet array heat sinks for high-power electronics cooling," *IEEE Trans. Compon. Packag. Technol.*, vol. 32, no. 2, pp. 347–357, Jun. 2009, doi: 10.1109/TCAPT.2008.2010408.

[290] G. Moreno, S. Narumanchi, X. Feng, P. Anschel, S. Myers, and P. Keller, "Electric-drive vehicle power electronics thermal management: Current status, challenges, and future directions," *J. Electron. Packag.*, vol. 144, no. 1, Mar. 2022, Art. no. 011004, doi: 10.1115/1.4049815.

[291] E. M. Dede, C. Zhang, Q. Wu, N. Seyedhassantehrani, M. Shattique, S. Roy, J. W. Palko, S. Narumanchi, B. Kekelia, S. Hazra, K. E. Goodson, R. Giglio, and M. Asheghi, "Techno-economic feasibility analysis of an extreme heat flux micro-cooler," *iScience*, vol. 26, no. 1, Jan. 2023, Art. no. 105812, doi: 10.1016/j.isci.2022.105812.

[292] C. H. van der Broeck, A. Gospodinov, and R. W. De Doncker, "IGBT junction temperature estimation via gate voltage Plateau sensing," *IEEE Trans. Ind. Appl.*, vol. 54, no. 5, pp. 4752–4763, Sep. 2018, doi: 10.1109/TIA.2018.2836362.

[293] J. Winkler, J. Homoth, and I. Kallfass, "Electroluminescence-based junction temperature measurement approach for SiC power MOSFETs," *IEEE Trans. Power Electron.*, vol. 35, no. 3, pp. 2990–2998, Mar. 2020, doi: 10.1109/TPEL.2019.2929426.

[294] H. Niu and R. D. Lorenz, "Evaluating different implementations of online junction temperature sensing for switching power semiconductors," *IEEE Trans. Ind. Appl.*, vol. 53, no. 1, pp. 391–401, Jan. 2017, doi: 10.1109/TIA.2016.2614773.

[295] S. Kalker, C. H. van der Broeck, and R. W. De Doncker, "Online junction-temperature sensing of SiC MOSFETs with minimal calibration effort," in *Proc. PCIM Eur. Digit. Int. Exhib. Conf. Power Electron., Intell. Motion, Renew. Energy Energy Manag.*, Jul. 2020, pp. 1–7. [Online]. Available: https://ieeexplore.ieee.org/document/9178165

[296] M. Daghrah, Z. Wang, Q. Liu, A. Hilker, and A. Gyore, "Experimental study of the influence of different liquids on the transformer cooling performance," *IEEE Trans. Power Del.*, vol. 34, no. 2, pp. 588–595, Apr. 2019, doi: 10.1109/TPWRD.2019.2895533.

S. M. IMRAT RAHMAN (Graduate Student Member, IEEE) received the B.Sc. degree in electrical and electronic engineering from the Islamic University of Technology, Bangladesh, in 2010, and the M.Sc. degree in power engineering from the Technical University of Munich, Germany, in 2015. He is currently pursuing the Ph.D. degree with the Holcombe Department of Electrical and Computer Engineering (ECE), Clemson University, under the supervision of Dr. Christopher S. Edrington and Dr. Gokhan Ozkan. He is a Graduate Research Assistant with the Real-Time COntrol and Optimization Laboratory (RT-COOL), Holcombe Department of ECE, Clemson University. His research interests include active thermal management of power electronic converters, distributed control, and thermal modeling of power electronic building blocks (PEBB) systems.

ALI MOGHASSEMI (Graduate Student Member, IEEE) received the B.S. and M.S. degrees in electrical engineering from Islamic Azad University, South Tehran Branch, Tehran, Iran, in 2012 and 2015, respectively. He is currently pursuing the Ph.D. degree with the Real-Time COntrol and Optimization Laboratory (RT-COOL), Holcombe Department of Electrical and Computer Engineering, Clemson University, Clemson, SC, USA, under the supervision of Dr. Christopher S. Edrington and Dr. Gokhan Ozkan. He is a Graduate Research Assistant. He is working on electro-thermal modeling, simulation, and control of power electronics building blocks (PEBBs) in all-electric ships (AESs). His research interests include modeling, simulation, and real-time modeling of power electronics and renewable energy systems.

ALI ARSALAN (Graduate Student Member, IEEE) received the bachelor's degree in electronics engineering from UCET, IUB, Pakistan, in 2015, and the master's degree in electrical engineering from UET, Lahore, Pakistan, in 2019. He is currently pursuing the Ph.D. degree in automotive engineering with Clemson University, SC, USA. After the bachelor's studies, he was a Laboratory Engineer with the Khwaja Fareed University of Engineering and Information Technology (KFUEIT), Pakistan, for five and a half years. He is a Graduate Research Assistant with the Secure Energy and Automation Laboratory (SEAL), International Center for Automotive Research (ICAR), Greenville, SC, USA. His research interests include optimization, microgrids, energy management, EV technologies, cyber security, and power system resiliency toward cyber threats.

LAXMAN TIMILSINA (Graduate Student Member, IEEE) received the B.E. degree in electrical engineering and the M.Sc. degree in distributed generation in electrical engineering from the Institute of Engineering, Tribhuvan University, Nepal, in 2016 and 2019, respectively. He is currently pursuing the Ph.D. degree in electrical engineering with Clemson University, under the supervision of Dr. Christopher S. Edrington. He is a Graduate Research Assistant with the Real-Time Control and Optimization Laboratory (RT-COOL), Holcombe Department of Electrical and Computer Engineering (ECE), Clemson University. His research interests include electric vehicles, the integration of renewable energy, and smart grids.

PHANI KUMAR CHAMARTHI (Member, IEEE) received the joint M.Tech. and Ph.D. degrees with a specialization in power electronics and power systems from the Department of Electrical and Electronics Engineering, Indian Institute of Technology Bombay, Mumbai, India, in 2018. He is currently a Postdoctoral Fellow with Clemson University, USA. His research interests include new single-stage transformerless inverter topologies, multilevel converter topologies, space vector control of multilevel converters, and new modulation and control strategies of multilevel converters with a focus on renewable energy applications.

BEHNAZ PAPARI (Senior Member, IEEE) received the B.S. degree in electrical engineering from the University of Bushehr, Iran, in 2008, the M.Sc. degree in electrical engineering from the K. N. Toosi University of Technology, Iran, in 2011, and the Ph.D. degree in electrical and computer engineering from Florida State University, USA, in 2018. Prior to joining the Department of Automotive Engineering and Electrical and Computer Engineering, Clemson University, in Spring 2022, she was an Assistant Professor with the Department of Marine Engineering Technology, Texas A&M University, and an Assistant Professor of practice with the Energy Production and Infrastructure Center (EPIC), UNC Charlotte, for three years, where she taught at undergraduate and graduate levels. Her background is in power systems controls with an emphasis on modeling, analysis, planning, and AI-based optimization. Her current research interests include distributed controls and secure control frameworks under uncertainty, applications on energy system modeling, and stochastic optimization, electric vehicles, including electric and hybrid-electric, and ESSs.

GOKHAN OZKAN (Senior Member, IEEE) received the first B.S. degree in teacher training (electrical field) from Marmara University, in 2006, the second B.S. and M.S. degrees in energy system engineering from Erciyes University, Turkey, in 2014 and 2015, respectively, and the Ph.D. degree in electrical and computer engineering from the FAMU-FSU College of Engineering. He was a Lecturer with Bozok University, Turkey. He was also a Graduate Research Assistant with the Center for Advanced Power Systems, FSU. He joined as a Postdoctoral Research Associate with the RT-COOL Group, Clemson University, where he is currently a Research Assistant Professor. His research interests include renewable energy sources, power and energy management, real-time modeling and simulation, power electronics, and control, distributed energy resources, and electrical vehicles.

CHRISTOPHER S. EDRINGTON (Senior Member, IEEE) received the B.S. degree in engineering from Arkansas State University, in 1999, and the M.S. and Ph.D. degrees in electrical engineering from Missouri University of Science and Technology, in 2001 and 2004, respectively. He was a DoE GAANN Fellow, NSF IGERT Fellow, and a Grainger Foundation Fellow with Missouri University of Science and Technology. He is currently the Warren H. Owen Distinguished Professor of Electrical and Computer Engineering with Clemson University; the Lead of the Real-Time COntrol and Optimization Laboratory (RT-COOL), Clemson University; and the Co-Director of the Smart Energy and Propulsion Focus Area in the new VIrtual PRototyping for Ground Vehicle Systems (VIPR-GS) Center. He has published more than 170 papers (including two IEEE Prize Awards and multiple conference paper awards). He has graduated 23 M.S. students and 16 Ph.D. students (with three in the process), and eight patents (in real-time stability and complexity metrics, insulation breakdown, and linear machines). His research interests include modeling, simulation, and control of electromechanical drive systems; applied power electronics; distributed control; and integration of renewable energy, storage, and pulse power loads.